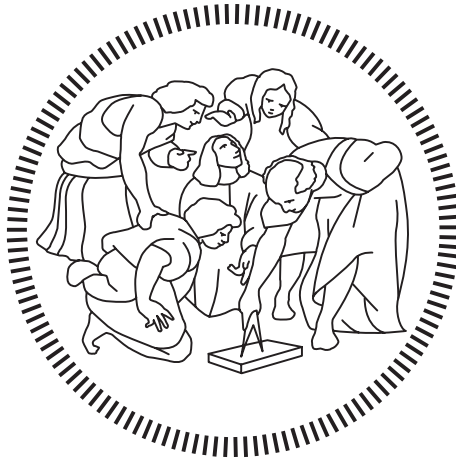


Politecnico di Milano

SCHOOL OF INDUSTRIAL AND INFORMATION ENGINEERING

DEPARTMENT OF ELECTRONICS, INFORMATION AND BIOENGINEERING

Master of Science – Biomedical Engineering



**Modeling of an *in vitro* testing device for simulating
tubular biological tissue manipulation**

Supervisor

Professor Sara MANTERO

Co-Supervisor

Federica POTERE

Candidate

Antonio IEZZI – 919262

Academic Year 2019 – 2020

Acknowledgments

First of all, I would like to thank my supervisor, the gentle Professor Sara Mantero, for the opportunity and the trust she gave me for working in her Laboratory, and Ph.D. students Federica Potere and Beatrice Belgio, for the help and the guidance they gave me, especially while learning about new technologies, such as the 3D printers and bioreactors.

Secondly, I want to express my gratefulness to my parents and my sister, as they always followed me through the years of my studies, showing me their availability and support: I am here thanks to what they have done for me.

Moreover, I need to thank Professor Brenda Russell and Ph.D. student Kyle Dittloff, as I have worked with them at the University of Illinois at Chicago for my thesis there and they taught me how to work and think in the research field, along with technical skills, allowing me to perform the work presented in this thesis at the best of my potential.

Finally, I want to thank my girlfriend, Giulia, for always being next to me.

Summary

During the last years, the demand for transplants has grown vertiginously, unmatched by the availability of donors, indispensable for such procedure. Indeed, new solutions to the problem have been investigated by a huge number of groups all over the world, meeting the characteristics of tissue engineering and, more recently, of 3D printing. Indeed, the development of tissue engineering has offered an alternative to the widely used traditional organs and prostheses transplant techniques in order to restore the functionalities of an unhealthy tissue. The main aim of this discipline is the creation of a vital construct able to adapt, grow and regenerate once implanted. The innovative idea is to develop the construct starting from the cells of the patients.

In this discipline, the three fundamental key elements are the cells, the scaffold and the bioreactor. The cells are the smallest element of life and, according to their type and source, they have more or less capability to form new cells and mature in one or more particular phenotypes: for this reason, it is crucial to select the most suitable for each tissue engineering application. The scaffold is the structure which has the function to host and furnish to the cells the right tridimensional environment for them to multiply and spread; the material, the texture and the shape are aspects that must be tuned by the tissue engineer. Finally, the bioreactor is the dynamic system which stimulates and conditions correctly the artificial tissue, keeping it sterile and controlled, while allowing a higher nutrient and gas diffusion with respect to the traditional bidimensional static culture.

This thesis is focused on one of the aspects of this topic, that is the development, through the means of 3D printing, of the dynamic system able to host certain engineered constructs and to meet the requirements for their growth and maturation, according to their shape and properties. In addition to this, the design of a 3D-printed hollow, tubular construct will also be presented, specifically designed for the regeneration of the trachea. In this way, it will be possible to provide an example of the suitable scaffold for the developed bioreactor.

In the first part of this thesis and in the introduction chapter a brief description of tissue engineering approaches will be given, followed by cues about the anatomy of the main organs that will be discussed. Following, the state of the art and the innovations brought by 3D-printed bioreactors for these applications will be listed and discussed, along with the issues and limitations that have been met in the last few years.

In the materials and methods chapter, the evolution and the steps which led to the development of the final bioreactor for tubular constructs will be explained, pointing out the reasons behind the crucial choices for its design. This will be followed by the description of an ideal scaffold suitable for the bioreactor, particularly thought for the regeneration and study of the trachea.

In the discussion and conclusion chapters, different experiments performed on the developed system will be presented, discussing about their outcomes and the occurred difficulties. Finally, possible future developments of this study will be listed and briefly explained.

Sommario

Durante gli ultimi anni, la richiesta per i trapianti è cresciuta vertiginosamente, non equiparata dalla disponibilità di donatori, indispensabili per tale procedura. Infatti, nuove soluzioni per il problema sono state oggetto di ricerca per un gran numero di gruppi in tutto il mondo, incontrando le caratteristiche dell'ingegneria dei tessuti e, più di recente, della stampa 3D. Infatti, lo sviluppo dell'ingegneria dei tessuti ha offerto un'alternativa alle tradizionali e largamente utilizzate tecniche di trapianto di organi e protesi col fine di ripristinare le funzionalità di un tessuto non sano. Il principale obiettivo di questa disciplina è la creazione di un costrutto vitale, partendo dalle cellule del paziente, capaci di adattarsi, crescere e rigenerarsi una volta impiantate.

In questa disciplina, i tre elementi chiave fondamentali sono le cellule, lo scaffold e il bioreattore. Le cellule sono l'elemento più piccolo della vita e, a seconda del loro tipo e sorgente, hanno più o meno capacità di formare nuove cellule e maturare in uno o più particolari fenotipi: per questa ragione, selezionare il più adatto per ogni applicazione dell'ingegneria dei tessuti è cruciale. Lo scaffold è la struttura che ha la funzione di ospitare e fornire alle cellule il giusto ambiente tridimensionale per la loro moltiplicazione e diffusione; il materiale, la texture e la forma sono aspetti che devono essere modificati dall'ingegnere dei tessuti. Infine, il bioreattore è il sistema dinamico che stimola e condiziona correttamente il tessuto artificiale, tenendolo sterile e controllato, mentre permette una diffusione dei nutrienti e dei gas migliorata rispetto alla tradizionale coltura statica.

Questa tesi è incentrata su uno degli aspetti di questo argomento, ossia lo sviluppo del sistema dinamico capace di ospitare certi costrutti ingegnerizzati e di rispettare i requisiti per la loro crescita e maturazione, a seconda della loro forma e proprietà. In aggiunta a ciò, il design di un costrutto tubulare cavo, da stampare in 3D, verrà presentato, specificatamente progettato per la rigenerazione della trachea. In tal modo, sarà possibile fornire un esempio di uno scaffold adatto al bioreattore sviluppato.

All'inizio e nel paragrafo introduttivo, una breve descrizione degli approcci dell'ingegneria dei tessuti sarà presentata, seguita da dettagli riguardo l'anatomia dei principali organi che verranno trattati. In seguito, lo stato dell'arte e le innovazioni portate dai bioreattori stampati in 3D per queste

applicazioni verranno elencati e discussi, insieme ai problemi che sono stati incontrati negli ultimi anni.

Nel capitolo di materiali e metodi, l'evoluzione e i passi che hanno condotto allo sviluppo del bioreattore finale per costrutti tubulati saranno spiegati, evidenziando le ragioni dietro le scelte cruciali per il suo design. Questo sarà seguito da una descrizione dei dettagli per uno scaffold ideale adatto al bioreattore, particolarmente pensato per la rigenerazione e lo studio della trachea.

Nei capitoli della discussione e conclusioni saranno presentati diversi esperimenti fatti sul sistema sviluppato, discutendo riguardo i loro risultati e le difficoltà incontrate. Infine, possibili sviluppi futuri per questo studio saranno elencati e spiegati brevemente.

Abstract

The latest findings in the biomedical and technology field have led physicians and researchers to focus on the application of artificially developed constructs to be implanted in patients needing tissues or organ replacement. This approach opens new pathways for the solution to problems related to the shortage of donors and both physiological and ethical concerns about allogeneic transplantations. The key to effectively being able to use an artificially designed construct for a transplant on man is to find a way to allow the construct to grow enough and reach the maturity required from the body to install a strong bond between the host tissue and the transplanted one, consisting of both vascularization and cell migration into the site. In order to obtain this, bioreactors are used. These devices allow to cultivate different types of cells separately, each with their own biochemical and physical stimuli, overcoming the static culture issues related mainly to nutrient diffusion. The cells and the materials can interact in a controlled and sensorized environment, designed for a particular application in a specific shape, driving the tridimensional maturation of the tissue. In this way, the optimal maturation of the tissue can be granted before implantation, allowing improved results in field.

In this thesis, the steps for the development of a dynamic system for the culture of tissue-engineered hollow organs will be presented, starting from the state of the art at the moment of the beginning of the study, then listing the choices made and their reasons, ending with the results obtained and the limitations met, while in the end the future directions of the project will be discussed.

Specifically, 3D print technology has been used to produce through fused deposition modeling the components to assemble the bioreactor. The material used was polylactic acid. These components have been designed and produced according to the dimensions of the culture chamber that was wanted to be used and to the desired interaction with the artificial tissue.

Once produced, the components were assembled with the polysulfone-made culture chamber. The assembled system was studied, focusing on its capability to respect the requirements for a bioreactor. Mainly the hydraulic seal and the sterility maintenance were assessed. In order to do this, the components were manipulated, adjusted and then studied. In conclusion, both these requirements were satisfied by the designed system.

Nevertheless, the system met some limitations, that will be discussed deeply in the last chapter of this thesis. Some of these concerned the CAD design of the components, while other their assembly. However, solutions to these problems will be presented, along with possible future developments to improve the quality of the system.

Acronyms

ABS	Acrylonitrile butadiene styrene
BBB	Blood brain barrier
CAD	Computer-aided drafted
DLP	Digital light processing
DMLS	Direct metal laser sintering
ECM	Extracellular matrix
EtOH	Ethanol
FDM	Fused deposition modeling
FFF	Fused filament fabrication
IR	Infrared
OOC	Organ-on-a-chip
PBS	Phosphate buffer saline
PC	Polycarbonate
PCL	Polycaprolactone
PDMS	Polydimethylsiloxane
PGA	Polyglycolic acid
PLA	Polylactic acid
PMMA	Polymethylmethacrylate
PSU	Polysulfone

Acronyms (cont.)

PVC	Polyvinyl chloride
SLA	Stereolithography
SLM	Selective laser melting
UV	Ultraviolet

Table of Contents

Acknowledgments	III
Summary	IV
Sommario	VI
Abstract	VIII
Acronyms	X
Table of Contents	XII
List of Figures	XIV
List of Tables	XVIII
Chapter 1 Introduction	1
1.1 Key elements of tissue engineering	1
1.1.1 The cell sources	3
1.1.2 The scaffold	4
1.1.3 The bioreactor	5
1.2 The tubular tissues	7
1.2.1 Anatomy and pathophysiology of the trachea	7
1.2.2 Anatomy and pathophysiology of aorta and vessels	8
1.2.3 Anatomy and pathophysiology of the esophagus	10
1.2.4 Anatomy and pathophysiology of the ureter	11
1.2.5 Anatomy and pathophysiology of the small intestine	12
1.3 Clinical significance of the work	13
1.4 3D printed bioreactors and bioreactors for tubular constructs	14
1.4.1 3D printed bioreactors	15
1.4.2 Bioreactors for tubular constructs	19

Chapter 2	Materials and Methods	21
2.1	Evolution of the bioreactor design	21
2.1.1	The first model	21
2.1.2	The second model	25
2.1.3	The third model	28
2.2	Final design of the bioreactor	34
2.2.1	The culture chamber	34
2.2.2	The lid	37
2.2.3	Inlets and outlets	38
	2.2.3.1 Perfusion inlet	38
	2.2.3.2 Assembly inlet	41
2.2.4	Inner perfusion axis	43
2.2.5	Scaffold grips	45
2.2.6	Assembled chamber	47
2.3	Steps for the production of a 3D printed object	49
2.4	Production of the bioreactor 3D printed components	52
2.4.1	The choice of the printing technique	53
2.4.2	The choice of the material	57
2.4.3	Choice of the printing parameters in Ultimaker Cura	58
2.5	Design of a tubular scaffold suitable for the bioreactor	67
Chapter 3	Results	71
3.1	Study of the functionality of the developed components	71
3.1.1	Assessment of the hydraulic seal of the bioreactor	71
3.1.2	Sterilization of the bioreactor components	73
3.1.3	Sterility maintenance of the bioreactor	75
Chapter 4	Conclusions and future developments	77
4.1	Conclusions on the system performance	77
4.2	Future developments and possible improvements	80
Bibliography		83

List of Figures

Figure 1.1 *Flowchart for the development and use of a tissue-engineered construct.*

Figure 2.1 *Views of the first model: top view (top left), side view (top right), front view (bottom left), isometric view (bottom right). Measures in mm.*

Figure 2.2 *The lid of the second model bioreactor, with the grips fixed on it. Fixed grip (left), mobile grip (right). Magnets shown in black.*

Figure 2.3 *Global views (left), exploded views (middle) and details (right) of the fixed grip (top row) and the mobile grip (bottom row).*

Figure 2.4 *The chamber and the lid create a tortuous path of Pasteur thanks to the extrusion on the corners of the structure (circled in red).*

Figure 2.5 *The chamber with the assembled inlets. Perfusion inlet (right), assembly inlet (left).*

Figure 2.6 *Details of the components of the assembly inlet.*

Figure 2.7 *Top panel. Assembling of the system. Middle panel. Detail of the threads on the axis and the mobile grip. Bottom panel. Detail of the hole in the axis reaching the perfusion inlet.*

Figure 2.8 *The assembled bioreactor, without the lid.*

Figure 2.9 *Photo of the culture chamber.*

Figure 2.10 *Views of the final culture chamber: front view (top left), side view (top right), top view (bottom left), isometric view (bottom right). Measures in mm.*

Figure 2.11 *The lid of the final model. Note that it is now flat.*

Figure 2.12 *The components which form the perfusion inlet. Top left. Ring. Bottom left. Perfusion screw. Top right and bottom right. Supplementary components to connect the various components.*

Figure 2.13 *The perfusion inlet fully assembled with the chamber.*

Figure 2.14 *Top and bottom views of the perfusion inlet (left) and assembly inlet (right).*

Figure 2.15 *The assembly inlet fully assembled with the chamber.*

Figure 2.16 *Assembly of the bioreactor with the components listed until now: perfusion inlet, assembly inlet, inner perfusion axis, three-way stopcock. Note the addition of smaller components to improve feasibility of 3D printing.*

Figure 2.17 *The inner axis. Note the holes and the grooves on its sides.*

Figure 2.18 *Detail of the holes and grooves on the inner axis.*

Figure 2.19 *Single scaffold grip. The fixed and the mobile grip have the same shape and dimensions, hence only one is shown here.*

Figure 2.20 *The two 3D printed scaffold grips.*

Figure 2.21 *Additional 3D printed components required for the full assembly of the system.*

Figure 2.22 *Assembled chamber with three-way stopcock (without lid).*

Figure 2.23 *Assembled chamber with three-way stopcock (without lid). Section view.*

Figure 2.24 *CAD model of the scaffold grip shown in SolidWorks.*

Figure 2.25 *STL file of the mobile grip shown in the Windows 10 built-in 3D viewer program.*

Figure 2.26 *Interface of Ultimaker Cura, the slicing software used in this thesis. The sliced object is the scaffold grip.*

Figure 2.27 *Diagram of the workflow for the production of a 3D printed object.*

Figure 2.28 *The Kentstrapper Verve 3D printer used for all the 3D prints in this thesis.*

Figure 2.29 *Underextrusion was observed in the first 3D printed components (left), but enhancing some parameters allowed to obtain satisfying first layers (right). As it is possible to see, underextrusion causes rough and unflat first layers, in which the extruded material often detaches.*

Figure 2.30 *For the ring components, presenting an internal thread, it was necessary to print the inner walls before the outer ones to avoid large overhangs.*

Figure 2.31 *Enabling ironing allows to obtain smoother and more defined top surfaces (left) with respect to unironed parts (right), in which it is possible to see the extruded PLA lines and the presence of small holes.*

Figure 2.32 *Main interface of Ultimaker Cura. Note the list of parameters to be set on the right and the material chosen on the top, in the middle.*

Figure 2.33 *Isometric (top left), side (top right), front (bottom left) and top (bottom right) views of the designed tracheal scaffold. Tracheal rings in green, inner surface in gray, flat rear portion in red.*

Figure 3.1 *The PDMS caps formed from the larger parts (left) using a set of punchers (right).*

Figure 3.2 *The PTFE tape (left) and the PVC caps (right) used.*

Figure 3.3 *The bioreactor perfusion and assembly inlet were mounted and closed with PVC caps and Teflon tape. The system showed water seal capacity for one hour when filled with cold water.*

Figure 3.4 *The 3D printed components were left in a 70% EtOH bath inside the chamber for 5 hours to provide sterility.*

Figure 3.5 *The sterilized 3D printed components and the chamber had to be left to dry in the sterile hood overnight (left). The used sterile hood (right).*

Figure 3.6 *The incubator used for the sterility maintenance experiment (left). Note the values of temperature, relative humidity and CO₂ partial pressure. The sterilized PBS-filled bioreactor inside the incubator (right).*

Figure 3.7 *The sterilized PBS-filled bioreactor showed no sign of contamination after one day of culture in incubator.*

Figure 4.1 *The 3D printed inner perfusion axis did not present a suitable structure for a successful 3D print.*

Figure 4.2 *The fully assembled bioreactor from different perspectives. It is possible to appreciate the two inlets fully assembled along with the fixed grip. It was not possible to place the mobile grip due to the absence of the perfusion axis.*

Figure 4.3 *Rupture of the components often happen on the plane of linkage between volumes of different width.*

Figure 4.4 *The O-rings used to enhance the sterility maintenance and the water seal were too thick to be fully compatible with the etches on the 3D printed rings components.*

List of Tables

Table 1 *Summary table of the different 3D printing techniques properties.*

Table 2 *Important properties of the main printing materials. Color-code for positive and negative values. Note how the color-code for Cost is in reverse.*

Table 3 *A summary table of the most relevant printing parameters.*

Chapter 1

Introduction

Starting from the last decade of the XX century, tissue engineering started to attract the interest of researchers and physicians, as it showed the potential to be a valid alternative, and a solution, to the older technique of organ transplant and prostheses development, not free from any kind of issue, both ethical and practical. The final aim of tissue engineering is the development of a construct with the capability to integrate with the host organism and regenerate damaged or unhealthy tissue, both from the point of view of the aesthetic appearance and the functionality. The advantage with respect to the introduction of a donor implant or a prosthesis is the fact that with this new approach it is possible to use the cells from the patient itself. The exploitation of this source, referred as autologous source, reduces drastically and partially avoids all the issues related to the inflammatory response that the body undergoes after an implant of non-self material ¹. On the other hand, the findings in this field and the subsequent development of *in vitro* systems able to recapitulate more faithfully the phenoms that happen *in vivo* allow researchers to study and perform tests with higher clinical significance. Indeed, thanks to the latest findings in the fields of developmental biology, chemistry, and materials science, it is possible to recreate *in vitro* most of the phenoms that are of major interest in the context of medicine and pathophysiology. Starting from the observation and the study of certain anatomic cues and events in the body, the tissue engineer can aim to recreate them, selecting the exact chemical and physical elements and parameters. However, for higher biological fidelity, new study platforms need to be developed, as the response of a living tissue is not completely realistic in a traditional bidimensional culture with respect to how it would be *in vivo*.

1.1 Key elements of tissue engineering

The phases required for the production of a tissue-engineered construct include the choices of the materials and cells, passing through the development of the design of the culture system, and the ways to allow their interaction.

First of all, a tridimensional construct must be obtained in biodegradable material. Once implanted, this can be degraded after that the cells have created the sufficient extracellular matrix (ECM) to support the newformed tissue. In case of a premature degradation, the risk is that the cells have not

yet created an environment sufficiently strong to withstand the stresses. However, the cells must be extracted from the patient and cultured to amplify their number. In fact, even a reasonably large biopsy cannot contain a sufficient number of cells for a tissue engineering application, hence the cell number expansion is needed. Once grown and proliferated, the cells can be seeded onto the scaffold: many different seeding techniques and approaches exist, depending on the shape of the scaffold, the material and the purpose of use of the construct itself. After a brief period of static culture, required by the necessity of cells to form strong bonds with the tridimensional structure, the scaffold can undergo dynamic stimulation inside a dynamic system called bioreactor. The latter has the duty of both providing adequate stimuli to the construct but also giving the possibility to the operator to monitor the parameters to evaluate cell viability and health. The most common monitored parameters are oxygen and carbon dioxide concentration, pH and temperature. At least after several weeks, once the construct is fully developed and mature, it is implanted in the patient in the required site. Then, according to the material degradation kinetics, it will slowly degrade, allowing cells to migrate in the rest of the host tissue and gain functionality while integrating with the biological environment.

From this first description of the steps included in a tissue engineering application, it is easy to evince that there are three main components in this kind of study: the cells, the scaffold and the bioreactor (Figure 1.1).

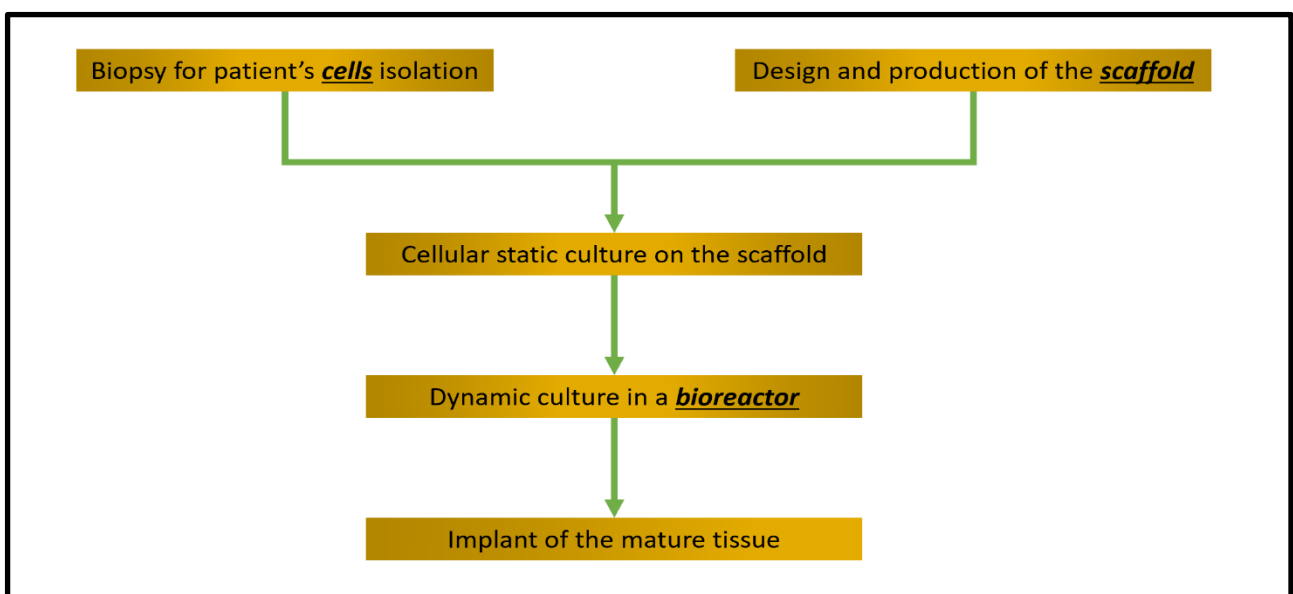


Figure 1.1 Flowchart for the development and use of a tissue-engineered construct.

1.1.1 The cell sources

The first step for the development of an engineered tissue is undoubtedly the choice of the cell source. Despite the possibility of involving autologous mature cells is one of the biggest innovations of this field, sometimes it is not possible to use them. In fact the tissue of the patient could be pathological, hence compromising the possibility to simply obtain the cells from a biopsy. For this reason, the choice of the cellular source can vary and bring benefits or drawbacks to the final product. Several parameters influence the choice of the source. Some of these are related to practical advantages that some cell types present, such as high availability and high proliferative capability, which make it easier for the operator to obtain the cells and treat them. Other characteristics are more technical: these can regard the capability of cells to express and keep their phenotype *in vitro* and to avoid the insurgence of an immunogenic response.

In addition, cells can be classified according to their state of maturation, so they can be undifferentiated or differentiated. As for the latter, these are the cells that mainly constitute the tissues in the body, in which they carry out their activity, while they replicate until a certain number of times and then die. These cells are not able to produce cells different from themselves: when they proliferate, or duplicate, they produce two daughter cells identical to the mother. If differentiated, or mature, cells tend to lose their phenotype when plated outside of the body. One way to avoid this is to provide biochemical and physical stimuli in order to mimic their natural environment. In the worst scenario, the cells reach the fibroblastic phenotype, characterized by a sparse population and a spindle shape ². In addition to what has been just said, there are different drawbacks in the use of mature cells: first of all, a pathologic tissue will not be able to produce a sufficient number of healthy cells for a tissue engineering application, and also the procedure related to the biopsy can be harmful to the tissue itself. Then, even if the cells can be isolated, they usually do not last long enough to be useful for an implant, as they undergo senescence after a few days or weeks, and die.

Stem cells are what have been previously called undifferentiated cells, which are cells still capable of undergoing a theoretically infinite series of duplications and to produce one or more different phenotypes. When a stem cell duplicates itself, it creates a cell that is identical to the mother (self-replication capability) and a cell that will differentiate in a particular phenotype (potency). According to the number of phenotypes that a stem cell can reach, they can be classified as unipotent, pluripotent or totipotent. Unipotent stem cells can only differentiate in a single phenotype: these are often precursors of fully mature cells. Pluripotent stem cells are able to differentiate into a whole family of cells, for example belonging to the same tissue, so they have a

much higher potency. Totipotent stem cells, finally, are cells able to generate all the cells in the organism and these play a fundamental role during the development of the embryo. In fact, stem cells can also be classified as embryonic and adult stem cells. Embryonic stem cells are present in the organism from a few days post fertilization until the birth, so during its development from the embryonic phase. In the fully developed organism, instead, adult stem cells are present, presenting the tendency to decrease in number with age ³.

Thanks to the ability to proliferate and differentiate into several phenotypes, stem cells have revolutionized tissue engineering approaches. In fact, stem cells are the best choice according to their potential. However, the use of these cells is not free from difficulties and issues. First of all, their availability is low with respect to the differentiated cells one: embryonic stem cells can only be obtained from blastocysts, which can be generated *in vitro* with techniques of therapeutic cloning, causing heated ethics debates; adult stem cells can be obtained from several human body districts, which however tend to produce them, as already said, in decreasing number going on with age. In addition, one main issue involved in the use of stem cells is the difficulty of inducing and maintaining their differentiation and proliferation *in vitro*, which requires specific and controlled physical and biochemical signals.

1.1.2 The scaffold

The second fundamental element which is required for a tissue engineering application is the scaffold. The scaffold is a tridimensional structure which, thanks to its particular characteristics, is able to host the cells, allowing them to grow and proliferate in an environment similar to the physiological one, carrying out what is done *in vivo* by the ECM. This structure needs to satisfy a series of requirements to be used. First of all, the material must not be cytotoxic to prevent a harmful reaction in contact with the cells. Then, the surface of the material must be hydrophilic in order to allow cellular adhesion and protein adsorption. Also, the volumetric properties of the scaffold must be tuned, finding an optimal range of porosity with a suitable size of the pores, so that cells can migrate inside all of the volume, but also allowing a good diffusion and movement of metabolites and gases. Since the idea is to implant the cell-laden scaffold inside the human body, this structure needs to be biodegradable and bioresorbable without inducing an immunogenic response and allowing the designer to tune the properties of the degradation, such as the time required to be fully degraded. Once the scaffold is inserted, it totally supports the growth of the cells, which, after a certain period of time, will form their own ECM, able to support stresses and movements. In this way, when the scaffold degrades and loses its mechanical properties, it allows

the newformed tissue to withstand the forces gradually. Finally, also the tridimensional shape of the scaffold is important and must be chosen according to the function it will have ⁴.

The techniques that are used to produce scaffolds are several, as well as for the materials. In this thesis, we will focus on the 3D printing techniques, a relatively new additive manufacturing technology with a very high ability to form complex structures rapidly and inexpensively. Specifically, we will use the fused deposition modelling (FDM) technique, which is based on the thermal fusion of a wire and its extrusion to form the tridimensional object. Moreover, 3D printing includes a technique with the possibility of directly involving cells during the print of the scaffold, called bioprinting. This technique is the state-of-the-art gold standard for the production of cell-laden scaffolds. Unfortunately, for this study it was not possible to develop a scaffold using this technique.

In the last few years, 3D printing has been a revolutionary technology, bringing innovation and a whole new way to approach engineering tasks, not only in the biomedical field. One of the aims of this thesis is to exploit the advantages brought by this new technology to produce a versatile bioreactor for *in vitro* tests suitable for the culture of innovative tubular scaffolds.

1.1.3 The bioreactor

The third and last element for a tissue engineering application is the bioreactor. A bioreactor is a dynamic system able perform different kinds of stimuli to the engineered tissue, while monitoring the important parameters to evaluate the viability and health of cells and improving their functionality, resembling the *in vivo* environment in a controlled and automatized manner. In addition to this, since the system is dynamic, it is possible to exploit the movement of the tissue or a part of the bioreactor to increase the perturbations of the culture medium, obtaining an improved diffusion of metabolites and a higher waste disposal. Bioreactors and dynamic systems have been widely used during the last years as they have been proven to be an efficient alternative to classical static culture using flasks or Petri dishes. In fact, the use of a tridimensional environment and all the benefits already cited lead to a faster maturation of the tissue and a higher functionality ⁵.

This thesis will be focused on the development of a dynamic system able to host tubular constructs, which can be versatile for different uses, for example as a culture chamber for the following engineered tissues: trachea, big vessels / aorta, ureter, esophagus, intestine. In this way, the developed system can be helpful for both tissue engineering and regenerative medicine approaches, but also to study *in vitro* biological phenomena in a more realistic as ever environment, especially

with respect to unrealistic flat, static culture. The bioreactor will involve the double chamber configuration, which will confer to the user the possibility to treat separately the cells on the outside and on the inside of the tubular scaffold. Briefly, the double chamber model consists of the separation of the environments inside and outside of the tubular construct, allowing co-culture of different cell types, which has been observed to produce better results in a multitude of applications and studies ⁶. Along with this, also the design of a 3D printed tracheal scaffold suitable for the bioreactor will be presented. Finally, the results, consisting of tests performed on the developed system, will be showed and discussed, introducing what needs to be improved and developed in the future.

1.2 The tubular tissues

As just introduced, this thesis will be focused on the design and development of a versatile bioreactor, by which it will be possible to culture different kinds of tubular tissues. Some of these are: the trachea, big vessels such as the aorta, the esophagus, ureter and brief tracts of small intestine. In this paragraph, the anatomy and physiology of these tissues and organs will be briefly introduced, along with the most common pathologies that affect them. This kind of approach is useful as it is vital for the tissue engineer to know the microanatomical cues of a tissue in order to recapitulate its characteristics in a scaffold and to understand the mechanical and physical behavior of the tissue in the human body, along with basic explanation of how an organ or tissue might be compromised from the pathological point of view.

1.2.1 Anatomy and pathophysiology of the trachea

The trachea is the main airway of the human body. It is a fibrocartilaginous structure with the function of connecting the larynx to the bronchi of the lungs. It is composed of a number of horseshoe-shaped rings, flat on the rear, connected vertically by annular ligaments. On the inside of the tubular structure its epithelium is made by column-shaped cells which have hair-like extensions, called cilia – from this its name *ciliated epithelium* -, and the lumen is covered by a mucosa. The trachea reaches the length of 10 to 12 cm, varying with the height of the individual, while its inner and outer diameters are usually between respectively 15 to 20 mm and 20 to 26 mm, hence causing an average thickness of about 6 to 8 mm, which varies during the breathing cycle and phenomena like cough. The tracheal rings are formed by hyaline cartilage and can vary in number between 16 and 20. Each ring is about 4 mm high and is C-shaped. Running on the back wall (membranous wall) of the trachea lays the flat trachealis muscle, while connecting the first to the last incomplete rings. The position of the trachea is comprised between sixth cervical vertebra (C6) and the fourth thoracic vertebra (T4). These are respectively the positions of the cricoid cartilage and the carina, that are the locations in which the trachea is linked to the larynx and the bronchi. In addition to this, the trachea lays on the median line of the body and is placed anteriorly to the esophagus. Its vascularization mainly depends on the branches of the thyroid lower arteries and bronchial arteries. An important characteristic from the tissue engineering point of view is the mechanical behavior of the trachea, in fact it is able to extend and change its shape, getting longer or shorter and withstanding rotations, allowing movement of the head and neck. The trachea has an anisotropic behavior due to the properties of the cartilage and smooth muscles which compose it, indeed the deformability is higher in the longitudinal direction while it is stiffer laterally. Another function of

the cartilaginous rings is to keep the lumen patent, withstanding the negative pressures caused by the breath; the tracheal muscle causes changes in the diameter of the structure through contractions; the connective tissue allows longitudinal strains.

The main pathologies that affect the tracheal tract can be of different nature, the most common are the inflammation or infection of the trachea, the tracheal stenosis and the tracheomalacia. Tracheal stenosis, like the other stenosis which affect other tubular tissues, consists of the stiffening of the tracheal walls and the loss of patency of the tracheal lumen; tracheomalacia instead leads to a loss of mechanical properties of cartilaginous sections of the trachea, caused by a softening of the latter; infection and inflammation of the trachea – known as tracheitis – usually is of viral or bacterial nature, since these pathogens can easily be inspired through the mouth and nose. While the pathologies related to inflammation are very common and in the majority of cases lead to mild symptoms such as cough and sore throat, tracheal stenosis and tracheomalacia are potentially lethal for the patient in case these are not treated with urge. In fact, an excessive narrowing of the airway or a collapse of the tracheal structure can potentially block all the oxygen exchange in the lungs and lead to death caused by an insufficient supply of oxygen to the brain. The causes that can lead to tracheal stenosis and tracheomalacia are often related to congenital pathologies and malformation, usually solved surgically in the first months of life, but they can also be related to injuries or illness such as tumors, in addition to prolonged use of endotracheal intubations, hence causing the insurgence of the pathology as a complication from other diseases ⁷.

1.2.2 Anatomy and pathophysiology of aorta and vessels

The aorta is the main artery in the human body, which originates from the left ventricle, then splitting into two smaller arteries, the iliac arteries. The function of the aorta, like every artery, is to bring oxygenated blood to all the districts in the body. Despite the aorta being subdivided in different sections according to its characteristics and the vessels having different structures according to their functions, now we will focus mainly on the structure of arteries and veins in general, paying attention to the relevant cues for the tissue engineering point of view.

Arterial vessels, including the aorta, play the role of conduits for the transport of oxygenated blood from the heart to the tissues. These vessels are formed by three concentric layers, different in both structure and function. The outermost layer is called tunica externa, or *adventitia*, and is composed mainly of relatively stiff and elastic tissue, thanks to the presence of collagen and elastin fibers. In the largest of the arteries, such as the aorta, small supplement vessels are present, called *vasa vasorum*, to nourish the largest ones. Below the outer layers lays the tunica media, similar to the

tunica adventitia, but with the difference of having the presence of smooth muscle in it, along with connective and elastic tissue. The last and innermost layer which composes an artery is the tunica intima, the only layer directly in contact with the blood. The main component of this layer are endothelial cells, laying on a basal lamina formed mainly by collagen. The functions of these three layers can be understood from their anatomical composition: the elastic tunica externa is the one that confers resistance to bending and stretching; the muscular tunica media thanks to the contraction of the smooth muscle fibers can propel the blood against gravitational and pressure gradients; the tunica intima can allow the exchange of substance from and to the blood, especially in the smallest vessels, the capillaries, in which most of the exchange of oxygen and other substances happen, being mainly formed from a fenestrated layer of endothelial cells. The pathologies which are commonly related to arteries and vessels in general are stenosis and aneurysm. These two respectively consist in a reduction of the transversal area of the patent lumen and an increase in vessel volume due to a collapse and loss of mechanical resistance of the vessel wall. These two conditions can often be related and present simultaneously in a patient, in fact, both are mainly caused by atherosclerosis. Atherosclerosis is a disease where the patient presents infiltration and accumulation of material forming atherosclerotic plaques. For their presence, patency of the lumen can be lost. In this situation, two clinical events can happen: the first one is represented by the aneurysm, since the decrease of surface area of the patent lumen causes an increase of intraluminal pressure, which in turn pushes too strongly on the vessel wall, causing its collapse. If the lumen loses its patency totally, the consequence is ischemia of the tissues after the vessel, as they lose the oxygen supply.

Venous vessels, instead, have the duty to bring the deoxygenated blood back from the tissue to the heart, where it will be pumped by another system of arteries and veins to the lungs to be oxygenated again. The main veins are the inferior and superior vena cava, which respectively collect the blood from the lower and upper parts of the body. Some notable differences between arteries and veins: veins are less muscular, in fact they do not need to urgently propel the blood; veins are closer to the skin, as arteries in fact run deep into the tissues; there are one-way valves in most veins, similar to Duckbill valves, to prevent backflow. From the microanatomical point of view, veins are similar to the arteries, hence are composed by three layers with different structures and functions. The outermost layer is the tunica externa, or *adventitia*, made mainly of connective tissue. The second layer is the tunica media, composed of smooth muscle, but, as already said, this is much less thick with respect to arteries. The interior layer, called tunica intima, is lined with endothelial cells. As far as pathologies which commonly affect veins are concerned, venous insufficiency and deep vein thrombosis are the two most widespread. As for venous insufficiency, this is a pathological

condition in which the patient's veins are not able to return all the blood to the heart, causing edema and swelling of the nearby tissues in the first place; the causes related to venous insufficiency can be related to low arterial pressure, hence causing a lower force driving the blood in the vessels, or to a malfunction of the valves that prevent the backflow. Deep vein thrombosis, instead, presents when a clot is formed in a deep vein and, just like edema, also thrombosis is more common in the veins of the lower limbs; the causes of deep vein thrombosis are immobility, cancers, obesity and unhealthy lifestyle, traumas or congenital disorders ⁸.

1.2.3 Anatomy and pathophysiology of the esophagus

The esophagus, also informally known as food pipe, is in of the first tract of the digestive system and it is composed of a fibromuscular tube which connects the pharynx to the upper part of the stomach, allowing so the passage of food for further digestion. The esophagus is long about 25 cm in adults and passes behind the trachea and the heart and through the diaphragm. Its location in the human body is between the sixth cervical vertebra (C6) and the eleventh thoracic vertebra (T11). The passage of food inside the esophagus is driven by peristaltic contractions of its walls. The organ which allows food to enter the esophagus and air to enter in the trachea is the epiglottis, a small muscle flap which can tilt one way or another, opening the right channel. Two sphincters, that are muscular rings, close the esophagus in its connections with the pharynx and the stomach; the second of these prevents acidic stomach content to reflux into the esophagus. In addition to this, the esophagus is richly supplied by arteries and drained by veins and lymphatic system. The anatomy of the esophagus is composed by layers, each one with different structure and functions. The outer layer is made of connective tissue, which covers a sandwich of fibrous – muscle – fibrous layers. Inside these ones there is another layer of connective tissue, called *submucosa*, and more internally there is the *mucosa*. The mucosa is a tough, keratin-free, stratified squamous epithelium made of 2 to 4 layers of squamous cells. Thanks to its rapid cellular turnover, the role of this layer is to protect the tissue from the abrasive effects of food deglutition. Moreover, in the mucosa and submucosa there are different glands which secrete mucus, allowing higher protection and isolation. As for the muscle part of the esophagus, it is mainly made of smooth muscle in the lower part and striated muscle in the upper part (closer to the pharynx), whereas these two muscles are mixed in the middle section. Similarly to other conduits in the body, also in the esophagus the muscles are divided according to their orientation with respect to the structure of the tissue, indeed they can be lined longitudinally or circumferentially. These two different layers of muscle are separated by a highly innervated network of fibers, called the *myenteric plexus*. Finally, the outermost fibrous connective tissue is the *adventitia*.

The main diseases which affect the esophagus are the following: inflammation, Barrett's esophagus, cancer, varices, motility disorders and malformations. Esophagus inflammation, or *esophagitis*, can be caused by reflux of gastric acid from the stomach, infection, ingestion of harmful substances, certain drugs and allergies related to food. Esophagitis can cause a painful swallowing and is usually treated aiming to erase the moving cause. In case of prolonged esophagitis, a condition called Barrett's esophagus can happen. In this condition, the stratified squamous epithelia which characterizes the esophagus can undergo metaplasia, that is a cross-differentiation of a group of cells *in vivo* into another phenotype, in this case simple columnar epithelia. The main consequence of this is cancer, specifically adenocarcinoma of the cuboidal cells. Another type of cancer, which instead affects the squamous cell linings of the esophagus, is the squamous cell carcinoma. Radiotherapy, chemotherapy and surgical operation are the most common therapies for esophagus cancer. Another solution is to insert a stent into the tissue, allowing the patient to ingest food more easily, although neglecting the pathology itself. On the other hand, esophageal varices are swollen branches of the esophagus veins, which in the worst cases can obstruct the patency of the lumen. The main cause of this condition is hypertension of the portal hepatic system, which drives the veins in the esophagus to anastomose wrongly. The biggest issue with this disease is when a varix breaks, causing the patient to vomit blood painfully. Therapy of this condition is the most common approach to solve this issue. Finally, motility disorders are disorders which alters the physiological peristaltic motility of the esophagus walls, possibly causing the food to clot into the lumen or to induce the esophagus to enlarge its size, increasing the pressure on the other surrounding tissues. Stiffening of the esophageal walls is also directly related with this condition. However, malformations must be considered into the pathophysiology of the esophagus, especially from a tissue engineer, as replacement of the esophagus are the only solution to defects larger than a certain threshold, hence it is necessary to develop new ways to obtain substitutes for the tissue ⁹.

1.2.4 Anatomy and pathophysiology of the ureter

Ureters are small tubes made of smooth muscle which propel the urine from the pelvis of the kidneys to the back of the urinary bladder. A number of structures pass by, above or around the ureters on their path. The length of the ureters in the human body is about 20 to 30 cm and its diameter is 3 to 4 mm. Urothelial cells form a type of transitional epithelium which lines in the ureter and their characteristic is to be able to respond to stretches, in fact this epithelium appears as a layer of column-shaped cells when relaxed and as a layer of flat cells when relaxed. Below the epithelium lays the lamina propria, which is a complex network of connective tissue and elastic fibers with a rich vascularization, innervation and lymphatic system. Surrounding the ureter there

are two layers of smooth muscle, one running internally and longitudinally while another running externally and circularly or spirally. A third muscular layer is present in the part of the ureter closer to the bladder, allowing more peristaltic force. An adventitia lays on the outermost part, involving blood and lymphatic vessels.

The pathologies which can affect the ureters are for example urinary tract infections and kidney stones formation. Inflammation of the ureter can lead to stenosis of the lumen of the conduit. Malformation or congenital abnormalities can happen in this tissue and can exhibit in two ureters on the same side or misplaced ureters. More common in children is the condition in which a reflux of urine from the bladder back up in the ureter happens ¹⁰.

1.2.5 Anatomy and pathophysiology of the small intestine

The small intestine is an organ of the digestive system, which is part of the gastrointestinal tract. In the small intestine, the largest part of the absorption of nutrients and minerals happen. Its position is between the stomach and the large intestine, while it is connected to the pancreas and liver, from where it receives bile and pancreatic juice, through the pancreatic duct, to help in the digestion of food. The small intestine is mainly formed by three regions: the duodenum, the jejunum and the ileum. The duodenum is the shortest tract (20 to 25 cm), it is C-shaped and it is where the food is prepared to be absorbed through small protruding extension called *villi*. The duodenum receives gastric substance from the stomach, along with digestive juices from the pancreas and liver. In this section of the small intestine, secreted bicarbonate neutralizes the acidic content of the stomach. The jejunum (2.5 m long) is lined by enterocytes, cells which are specialized in absorbing small particles of nutrients which have been previously digested in the duodenum. The suspensory muscle of the duodenum marks the line between jejunum and the ileum. Finally, the ileum (3 m long) is in charge for absorption of vitamin B₁₂, bile salts and all the products that were not digested or absorbed by the previous tracts. The length of the small intestine can vary greatly, starting from 3 m up to 10 m, according to the technique used to measure it. The length of the intestine also depends on the height of the person. In adults, its diameter is around 3 cm. The total surface area of the small intestinal mucosa, thanks to the present villi, can reach 30 square meters. The layers which compose the small intestine can vary according to the tract we are referring to, even though they are all similar, but in general the possible layers present are the following: serosa, muscularis externa, submucosa, mucosa (muscularis mucosae, lamina propria, intestinal epithelium). Finally, the small intestine is an important resource for the immune system thanks to the presence of its flora.

The pathological conditions which affect the small intestine can be divided in five main categories. The first ones are the obstructive disorders, characterized by loss of the patency of the lumen of the intestine and obstruction of the passage of substance. The second category is composed of infectious diseases, caused by the presence of bacteria, viruses or other disease-causing agents. The third category is represented by developmental, congenital or genetic disorders. Finally, the last two classes can be listed as neoplasms (cancers) and diseases of other nature, of which the most famous are endometriosis, Crohn's disease and duodenal ulcers ¹¹.

1.3 Clinical significance of the work

An injury or a disease can lead to the damage and possibly loss of a tissue or organ, causing serious health issues. In fact, transplantation of tissues and organs, despite being between the most common solutions, is affected by the extremely high lack of donors. In these cases, the quality of life of a patient is damaged, increasing the medical and social costs. The most fortunate patients, which received an allograft for example, are still required to assume immunosuppressants for all the duration of their lives. Alternatives to transplants can be the use of mechanical devices and prostheses, which lack in the capability to restore the function of the tissue or organ. Moreover, prostheses and artificial implants have a limited lifespan, requiring substitution after several years.

As already said, tissue engineering is an emergent field enjoying an increasing interest in the clinical and research world, which offers alternatives to conventional therapies.

As for the relevance of this study, we can point out the importance of a well-functioning trachea in the human body. Indeed, the trachea acts as the only conduit for ventilation, hence being vitally important. Despite still functioning, also injuries and damage to the trachea can result in a dramatic decrease of life quality, as activities like breathing, speaking and swallowing might be severely hindered. Surgical intervention is only possible for low entity defects, for example performing direct anastomosis for damaged segments shorter than a maximum of 6 cm, since the mechanical tension in the anastomosis site would be too high. Not properly managed surgical interventions can bring further complications, which could become fatal for the patient ¹². Disorders like this still have no satisfactory solution. Despite allogeneic tracheas have been widely used as a replacement for damaged ones, the administration of lifelong immunosuppressants usually leads to another family of health problems related to the high risk of infection. Obviously, the same issue affects also tracheal xenografts. Tissue engineering is trying to cover its role and solve these issues, providing sustainable alternatives, both for the patient and the clinical world – because of its use of highly available materials.

The required conformation of a tracheal reconstruction is based on a longitudinally flexible, but laterally rigid tube coated with a layer of ciliated epithelium and able to host integration of chondrocytes. The aim of tissue engineering is to make this artificial tissue able to self-repair, remodel, revascularize and regenerate, without the risk of rejection¹³. A multitude of studies have faced the topic, many of them getting closer to the clinical applications of these new approaches. Nevertheless, there are still many issues and further development is required, but the premises are high.

What has been said for the trachea, which is the tissue for which the bioreactor presented in this thesis was initially thought, is also valid for the other tissues that have been previously listed, that are first of all blood vessels, specifically arteries, along with ureter, small tracts of intestine and esophagus. Indeed, all of these tissues can easily be damaged by an injury or can present malformations, pathologies such as tumors and so on. The wide range of tissues and dimensions they assume and the wider range of injuries and defects they can undergo open the possibility to perform aimed tissue engineering studies, which would require a significantly long period of time to be performed with a relatively restricted outcome. One of the steps for these studies would be the design and development of bioreactors able to host the different artificial tissues.

The relevance of this study lays in this process, which would be faster and easier, allowing researchers to focus more on the biological counterpart of the study, if standardized bioreactors, suitable and versatile for a series of applications could be in commerce. However, it must be said that there are limitations and the one-for-all idea of compatible bioreactors for all tubular tissue is still primitive and needs much more work on it. For instance, it is hard to think to clinically implant a tract of intestine with a maximum length of 15 cm, which is more or less the highest length reachable by the bioreactor presented in this work. But still, it would be suitable for a mouse intestine, allowing studies *in vitro* with a high biological relevance. The versatile bioreactor here presented is more suitable for arteries and trachea studies.

1.4 3D printed bioreactors and bioreactors for tubular constructs

This project will be focused on the development of a bioreactor specifically designed to host tubular constructs. The applications for which the bioreactor will be useful are mainly two: the first one is represented by the already described classical tissue engineering application, in which the scaffold grown in the dynamic system will be studied and developed with the final aim of implanting it in a patient with a defecting tissue or organ; the second application is more focused on research and study of unknown conditions that must be recapitulated *in vitro* exploiting the characteristics of the

bioreactor itself, which allows to create a highly controlled environment, both from the physicochemical and biological points of view. The usefulness of this kind of study is dual. Indeed, recapitulating *in vitro* a certain biological phenom can allow researchers to study both a therapy for the related disease or to deepen the knowledge about the phenom itself. One example of this concerns atherosclerotic plaques in arteries or aorta. Developing an atherosclerotic vessel in a bioreactor can help in understanding the development of the disease, but also allow for treatment of it, trying to destroy the plaque using a catheter.

Despite these premises and despite the bioreactor being a powerful mean, from the biological point of view it has always been very challenging to recreate faithful and functional environment and tridimensional structures *in vitro*. In fact, the parameters that have to be handled, interpreted and monitored are countless and starting this approach fully based on single cells is very ambitious. It must be considered, for example talking about cell culture and cell phenotype, that all these parameters are often influenced by each other, making studying them even harder and more complex. For this reason, each application and design of a bioreactor must be finely tuned around the tissue that is wanted to be developed, in this way allowing the researcher to focus on and monitor only some of the parameters and qualities that the tissue is showing. Indeed, decoupling the cause and the effects has always been an important aim in the biology research field in order to gain significance in the results obtained. For example, in this case, the concentration of a certain chemical compound and a specific cellular phenotype can be related. Hence, in this paragraph some of the solutions that have been found and used in the last few years will be listed and discussed. In particular, we will pay more attention to the ones designed to host tubular constructs and that were developed using 3D printing techniques, both for the culture chamber itself and all the mechanical components involved in the system.

1.4.1 3D printed bioreactors

Thanks to the technological advances in the fields of material science and manufacturing it has been always easier for researchers to produce objects of increasing complexity in terms of shape, surface texture and restrained dimension. 3D printing has been and still is a revolutionary procedure, which allowed to obtain a never seen before level of control on the printed objects, offering the capability of manufacturing intricate architecture. Before its invention, machine tools were the only mean to operate and design the shape of a product. As for certain materials, such as metals, this is still the best choice, however, in order to be able to perform certain processing a considerable expertise is required, for example using common and widely used materials such as glasses and stiff polymers -

polycarbonate (PC) and polymethylmethacrylate (PMMA) are the most relevant examples. 3D printing advent gave to a higher number of consumers the possibility to create models and produce them in a wide range of materials in a relatively cheap, fast and repeatable way. In addition, it must be specified that some materials already used in the biomedical field are compatible with the 3D printing techniques, such as polyesters like polylactic acid (PLA), polyglycolic acid (PGA) and polycaprolactone (PCL). These materials, in addition to present high printability, are also biodegradable, favoring their use in tissue engineering and regenerative medicine applications. Nonetheless, as far as bioreactors are concerned, the biggest advantage introduced by 3D printing is the possibility to have 3D computer-aided drafted (CAD) models of the objects we produce, or better, the possibility to physically produce a 3D CAD model. In fact, the workflow behind the 3D printing technique starts from the development of the CAD model, then a process called *slicing* writes the G code, which contains the instructions that the 3D printer has to follow to produce the object. The steps for the production of a 3D printed object will be analyzed more in detail in the Materials and methods chapter. Using this procedure, it is easier than before for the researcher to obtain small and highly defined objects, useful for the assembly of a bioreactor or a scaffold, like in the work shown in this thesis, obviously respecting the constraints imposed by the chosen material properties and the 3D printer work temperature and minimal or maximal dimension limitations.

In literature, many groups designed and developed bioreactors made by several smaller functional units produced by 3D printing, outperforming traditional methods in the results. Indeed, a number of 3D printed bioreactors have shown improved performance in tissue engineering and other applications, such as drug screening, thanks to their 3D cell culture microenvironment with precise spatial control. It is necessary to precise that, in this thesis, every 3D printed apparatus, including culture chambers, filters and scaffold holders are considered as or part of the 3D printed bioreactors. Following, an analysis, with brief discussions, of some of the most relevant 3D printed bioreactor features in literature.

a. Advantages of 3D printed bioreactors

One of the most recent and important improvement in biomedical research field has been the passage from the bidimensional - or flat - analysis to a more faithful and biologically relevant tridimensional study. It is clear that cells, organs and tissues in the human body grow and sense an environment developed in every direction and dimension, hence, it has always been a big limitation to the validity of *in vitro* study to perform bidimensional assays. Despite being a faster solution, still useful for screening tests and first approach analysis, using traditional bidimensional surfaces to perform a biological assay provides results which cannot be fully reliable, as the studied conditions

do not represent faithfully the *in vivo* environment and tissue morphology. Nevertheless, producing this advanced kind of device using traditional methods is challenging. 3D printing allows bioreactors to have higher performance in terms of experimental throughput, liquids controllability and stability ¹⁴. 3D printing both grants freedom to produce complex architectures, enhances cellular functionality and bioreactor suitability for highly specific applications ¹⁵.

b. 3D printed bioreactors fabrication methods

The applications of 3D printing in research devices production are mainly two. The first one is bioprinting, in which cells are embedded in a biocompatible printable matrix, hence allowing cell survival and growth inside of the desired shape. For obvious reasons, this method is widely used for the production of scaffolds. The second application, that is the one on which we are focusing and that will be used in this thesis, regards the use of 3D printing to produce substrates for cell culture *in vitro*. Moreover, the techniques that allow to produce these substrates are the following: selective laser melting (SLM), direct metal laser sintering (DMLS), fused deposition modeling (FDM), fused filament fabrication (FFF), inkjet, PolyJet, material jetting, stereolithography (SLA), digital light processing (DLP), micro-SLA and multiphoton lithography. The most relevant of these techniques in the field of bioreactors will be analyzed more deeply in the Materials and methods chapter. The one we are going to focus on and that will be mainly used for this thesis work is FDM. Some drawbacks of these listed techniques are related to biocompatibility issues, difficulty in removing support materials, low printing resolution, unsuitable surface texture and poor dimensional accuracy. However, FDM has been chosen because of its affordability, high availability, reliability and versatility – this and other technical choices will be further discussed in the Materials and methods chapter. Some of the parameters that have to be considered while choosing the best 3D printing method for a specific application are manufacturing capability of the printer, type of material, desired shape of the object, functionality – such as mechanical properties - and visual appearance.

c. Biological applications of 3D printed bioreactors – some examples

- One of the applications that have exploited the advantages introduced by the 3D printing has been carried out by Cristopher Chen *et al.* ¹⁶, in a study that used the versatility of the objects that can be printed and used as a **substrate for cell culture** to analyze what are the effects of certain architectures, geometric arrangements and mechanical properties on cell viability and apoptosis rate. Indeed, once tridimensionality is conquered for *in vitro* modeling of scaffolds and constructs, it is vital to finely tune several properties and characteristics that need to be added, and not excluded, from the lone dimensionality factor.

For example, porosity, roughness and curvature play a fundamental role in how the microenvironment conditions cellular adhesion, growth, alignment, proliferation and differentiation.

- **Microfluidics** is a growing technology in which the capability of producing cellular scale constructs allow to perform precise and highly controlled experiments. Typically, chambers and tubes for inter-connections are etched on a wafer and then a system of micropumps and microvalves accurately controls the flows of medium with cells, inducing them to adhere and grow where the device wants them to. Hang Lin *et al.*¹⁷ managed to include this technology in a multichambered 3D printed bioreactor performing experiments about the phenomena related to the pathogenesis of osteoarthritis. In this case the group used the tissue specific environment to study the interactions between chondral and osseous tissues during osteochondral differentiation. In this way 3D printing, working synergically with microfluidics, showed to be a valid approach to study with high reliability and biological relevance an *in vitro* model of a pathology unknown at the cellular scale.
- **Organ-on-a-chip devices** (OOC) can be produced by 3D printing to assemble organ models in 3D specific architecture on a microfluidic chip. Ying Wang *et al.*¹⁸ developed a continuous perfusion model of the blood brain barrier (BBB) environment exploiting the precise geometrical features attained by 3D printing coupled with controlled flow dynamics of microfluidics. Moreover, another advantage of microfluidics is the compatibility with most of the imaging techniques, allowing, in addition to high physic control, also the possibility to have an optical feedback. A 3D printed cell insert was used to accommodate cell monolayers on the side of a porous membrane, allowing their coculture. In this way, it was possible to study the coupling between two different cell types without involving physical contact, but only the chemical signals that they exchanged. Indeed, coculture is another new technique which has shown highly significant results in a huge number of applications. The development of tridimensional *in vitro* apparats has allowed researchers to recreate more faithfully the real disposition of cells in the human body, including more than one cell type and being able to study the interactions among them.

The use of 3D printing in this thesis will be limited to the production of small objects required for the assembly of the culture chamber. The possibility to study and design a CAD model before the true assembly of the bioreactor gave us the freedom to experiment different approaches and ideas without any cost, except for the time required to create the model. The steps and choices taken will be listed in the Materials and methods chapter, as well as descriptions of the paths that have been abandoned during the work.

1.4.2 Bioreactors for tubular constructs

After introducing the role of 3D printing in studies which used bioreactors, in this paragraph the characteristic and some examples of bioreactors will be presented. These were used for some of the tubular tissues that were previously discussed. Specifically, we will focus on the trachea and blood vessels, being, among the tubular ones, the most suitable tissues for the bioreactor that we designed.

a. Bioreactors for tracheal tissue engineering

In order to develop a system able to mimic and favor the growth of a tracheal graft to be implanted in a patient, the use of mainly two cell types is required: chondrocytes and ciliated epithelial cells. In fact, the aim is to form a tubular structure with a cartilaginous inner backbone to reach mechanical stability, coated with ciliated epithelium both on the outer and luminal surface. These two cell types are essential to provide proper tissue functionality and also reduce the risk of graft stenosis, airway blockage and infection due to impaired mucus transportation¹⁹. A trachea tissue engineering bioreactor must have three functions: i) it must have two separate chambers (so called, double chamber model) in order to culture separately the two main cell types; ii) it must rotate or produce a physical movement to provide homogenous cell distribution in the matrix, enhance oxygenation and waste removal; iii) consequently, it must furnish to the cells a hydrodynamic stimulus for proper cell differentiation and maturation. The first bioreactor for tracheal tissue engineering which followed these guidelines was developed in 2008 by Macchiarini *et al.*²⁰. For this study, chondrogenic-induced mesenchymal stem cells and epithelial cells were used. Further studies^{21,22} showed a more evenly distributed and more highly proliferated chondrocyte population when a perfusion system was used for cell seeding, along with increased matrix secretion, cellular alignment on the direction of flow and more native-similar morphology of the tissue, confirming the importance of the role played by the shear stresses in cell function regulation. Despite these successes, Haykal *et al.*²³ showed that the tracheal graft was not able to support cell survival *in vivo*, probably due to the lack of vascular support, as they failed to detect labelled epithelial and cartilage cells 3 days after the transplant and no formation of epithelium was seen in the first two weeks. Indeed, the development of a system able to produce an artificial construct with angiogenic properties is the main goal of research in this field at the moment.

b. Aorta and blood vessels bioreactor

Similarly to other tissues, tissue engineered vascular grafts need to recapitulate both the mechanical properties of the native tissue and its biological function. For this purpose, stem cells are the most

widely used source of cells for the production of vascular grafts. However, in this paragraph we are focusing on the bioreactoristic counterpart of such studies. Indeed, once the scaffold is fabricated and potentially seeded with cells, it does not present the mechanical properties suitable for *in vivo* implantation, hence it needs a period of culture in a bioreactor. Such systems were first used for this application in 1999 by Niklason *et al.*²⁴. In this study, the main characteristic of the bioreactor was to present a pulsatile pump in order to introduce flow through the inner wall of the seeded scaffold. According to this first study, and confirmed by many others through the years, the use of a biomimicry-deduced pulsatile flow inside the scaffold induced the cells to behave more similarly to the native tissue. Specifically, this flow was necessary for the stem cells to migrate inside the scaffold. In the following years, other external stimuli were applied by the developed bioreactors to the grafts: the most important consist of shear stress and matrix stretching. As a consequence of these, various parameters were enhanced, such as stem cell senescence (decreased), matrix deposition, contractility of muscular cells, differentiation from progenitor cells. Through these studies, also various signaling pathways were elucidated which regulate vascular barrier function, survival, proliferation and maturation of stem cells into smooth muscle cells. Obviously, as specified in previous paragraphs of this thesis, along with mechanical stimuli, also biochemical ones must be used, such as dissolution of growth factors in the culture medium.

Chapter 2

Materials and methods

In this chapter, an analysis of the device will be presented, focusing of its various parts and how they assemble together, along with the reasons behind the choices made. First of all, the evolution of the bioreactor design will be given, explaining which have been the steps that have led to the final device. Finally, also the techniques and materials used for the objects production will be discussed.

2.1 Evolution of the bioreactor design

In this paragraph, as already said, the various steps which led to the design of the final bioreactor will be analyzed, discussing the several small changes required to improve the system. The device itself was first thought to be a bioreactor for tracheal tissue engineering, but then the aim was moved to obtain a higher versatility to be compatible with other tubular tissues. Hence, since the first idea, the double chamber model was adopted, in various forms.

The bioreactor for tubular tissues is composed of different parts. The skeleton of the structure, that is the polysulfone (PSU) container which hosts all the other parts, will be referred to as *culture chamber* for simplicity, even if usually in this field with culture chamber we intend all the parts that work synergically to allow the hosting, culture and monitoring of the tissue. The culture chamber will contain several smaller parts produced by 3D printing that have various functions, such as: allowing the exchange of metabolites and media inside and outside of the system while keeping the inner chamber sterile; conditioning the inner part of the tubular construct and the outer part separately, as this will be needed due to the different cell types involved; monitoring both visually, thanks to the transparency properties of the chosen materials, and through sensors the health and evolution of the tissue.

2.1.1 The first model

In figure 2.1 it is possible to see the three main views of the first conceived bioreactor: top view (top left), side view (top right), front view (bottom left), isometric view (bottom right). The represented dimensions are not fully determined, as this project was changed after its ideation and was never practically developed. As can be seen, this bioreactor is composed only of the culture

chamber in this representation, even though it was thought to add an external perfusion system. The structure of the chamber is cylindrical, with smoothed borders. This approach was used in order to avoid the accumulation of substance in the edges of the chamber and not to hinder in the removal of catabolites.

The idea was to develop this device in Pyrex glass or other transparent material, such as polycarbonate, for example by blowing air in a 3D printed mold. However, polycarbonate is a hard to model material, but the design of this chamber is relatively simple, hence it might have been possible to produce it. Pyrex glass has the characteristic of being sterilizable multiple times, so the most suitable application for this device would be in the research field, as it is mandatory for clinical applications to use disposable materials, in order to avoid contaminations between one patient and another. The side surfaces of the cylinder are free, as it was intended to use this part for optical analysis of the phenoms inside the chamber, whereas the top and bottom surfaces of the chambers both present three holes: a larger one in the middle and two smaller, identical and specular holes on the sides. Inside of the largest hole, a thin, hollow and circular extrusion is present, on both sides.

The idea was to introduce the scaffold in the chamber and place it as a tube between these two extrusions, hence creating the inner chamber, and then securing it through the use of two O-rings. In this way, it would have been possible to perfuse the scaffold internally from the largest holes and externally through the other smaller holes. This is the so called “double chamber model”. In addition to this, a ball bearings system had to be added on the two central holes in order to allow the rotation of the scaffold, required for the reasons already explained in the Introduction chapter. For obvious reasons, this chamber is intended to host one single scaffold at a time. As for the medium, in each chamber would be used the one relative to the cell type present (ciliated epithelium and chondrocytes in the case of the trachea) and the medium level could fill the chamber only for half of its height or for its total volume, according to the application. Indeed, for tracheal applications, it would be better to allow the scaffold to be in contact both with the medium and the air, to recreate more faithfully the physiological environment. Whereas for vascular applications, a total filling of the chamber would be better for the same reason. As far this feature is concerned, this bioreactor shows a good versatility.

Another cue that can help in tailoring the design of the chamber for various applications is the physical conditioning due to the rotation which is regulable according to the parameters required. As for the oxygenation of the tissue, since Pyrex glass and polycarbonate are not permeable to O₂, it is necessary to use a perfusion system made in silicon, being it permeable to O₂ molecules. The

necessary length of this perfusion circuit must be calculated and the tubes can be rolled up a turret which would make its transport easier. Sensorization of the system is important for a bioreactor, hence in this case it was planned to use indirect sensors – so placed before and after the chamber, in the perfusion system – for pH and CO₂ gas concentration. The perfusion system is closed, but it would be possible to have access to it through syringe pumps using 0.22 microns filters. Finally, it would be possible to automatically seed the cells in the scaffold directly in the device. To do so, it would be necessary to perform a confined seeding using centrifugal pumps. The use of roller pumps would cause the death of cells through mechanical lysis.

The main issue of this project consisted of how to access the chamber, as it would have required an opening on one of the sides and an interlocking between the vitreous and fragile material of the chamber would have been hard to develop and to maneuver. Another problem regards the central hole, which should be used both for rotation and for perfusion, requiring the shift of the rotation axis far from the chamber through a system of gears. Finally, the confined perfusion could be hard to realize because of the limited dimensions of the system – the thickness of the outer chamber would be only of 6 mm.

However, the first model of the bioreactor proposed valid ideas for further developments.

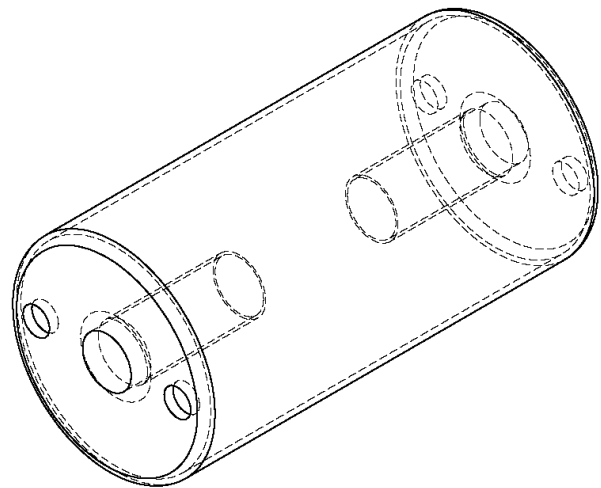
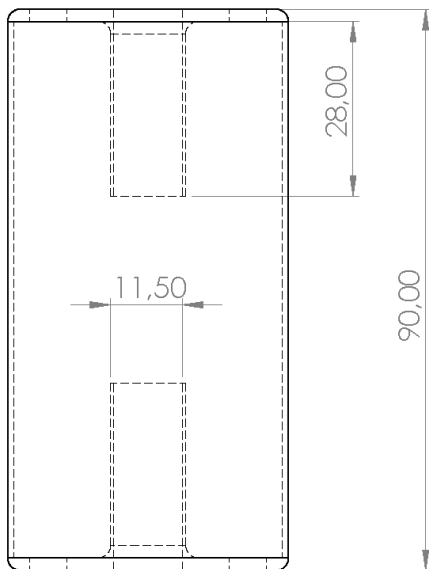
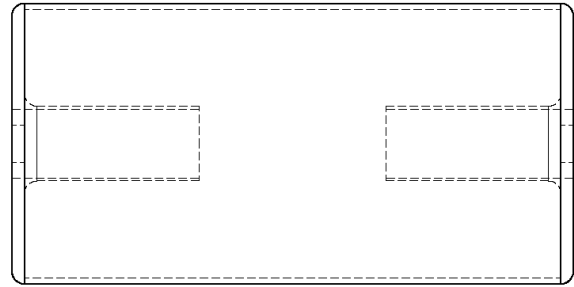
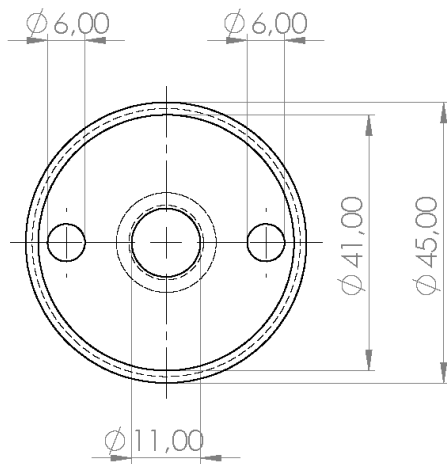


Figure 2.1 Views of the first model: top view (top left), side view (top right), front view (bottom left), isometric view (bottom right). Measures in mm.

2.1.2 The second model

On the ideological principle of the first model, it has been decided to simplify it and rebuild the bioreactor with a different approach, giving higher importance to the versatility of the system. The main reason behind this choice was that it resulted too complicated and time consuming to use the first model and to find a way to make it work with perfusion and rotation through the same hole. Since perfusion is the most important feature in bioreactors which distinguish a dynamic system from static culture, it has been decided to set aside the rotation of the scaffold, focusing on the perfusion and its versatility. Moreover, it is possible to add the rotation to the system in the aftermath.

In this moment it was first thought to develop intelligent grips, which were tunable and versatile for tissues such as trachea, but also big or small vessels, ureters, short tracts of intestine and esophagus. The requirements of this device, hence, were to have mobile grips which were tunable for their length and width of working. In addition to this, it was thought to preserve the outer design of the culture chamber. The reason of this choice was their fast availability in Professor Mantero's laboratory and their already obtained good results in terms of sterility and easy handling. More information about this chamber and its characteristics will be given in The final model paragraph, since this was the final design of the external chamber containing the inner 3D printed components. The basic idea behind the new approach was that it was required to be simple to open the lid of the chamber and to move only one or two components to allow grip of tubular scaffolds of various length and diameter. Moreover, the chamber had to use, for now, simple perfusion with an inlet and an outlet. The aim of the range of grip was between 3 and 20 mm for the diameter and between 1.6 and 12 cm for the length, allowing suitability for tracheas and vessels of various sizes. From the design point of view, the new bioreactor is totally different from the one described in the previous paragraph.

The design of the grips was based on the idea of placing them below the lid (Figure 2.2). In this way it would be allowed to place the lid upside down, to position the scaffold and then to close the lid, preserving sterility and avoiding introducing other holes in the structure. The hold of the scaffold and its variability is based on the fact that one of the grips is fixed, while the other is mobile on a guide, giving the possibility to use scaffolds of different lengths. The fixed grip is directly screwed on the lid, such as the guide of the mobile one. In order to improve stability of the mobile grip, it

was thought to use a couple of magnets: one directly on the lid and one between the guide and the mobile part of the grip (magnets shown in black in Figure 2.2).

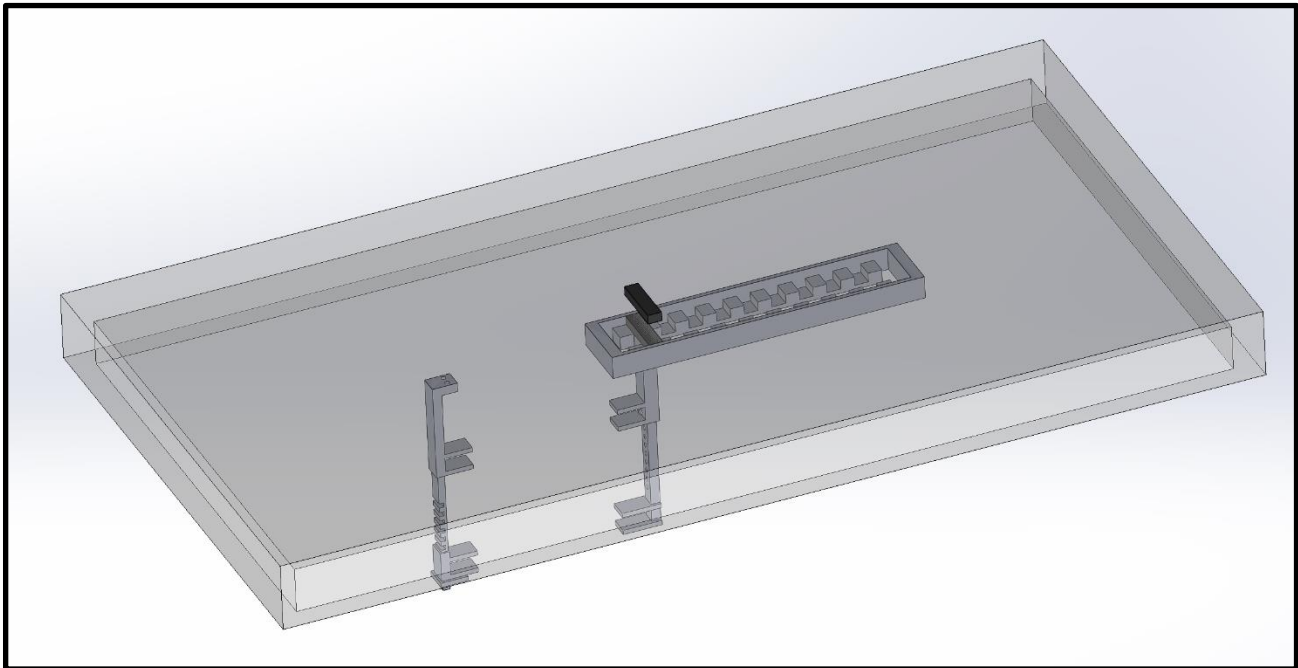


Figure 2.2 *The lid of the second model bioreactor, with the grips fixed on it. Fixed grip (left), mobile grip (right). Magnets shown in black.*

As shown in Figure 2.3, each grip was formed by three parts: one part (green) is the one which is fixed to the lid or which can move inside the guide, one part (grey) has the degree of freedom to move vertically and another part (red) is a plate or a screw which has the role to stop the vertical movement in the desired position. While the movement of the mobile grip inside the guide allows for the hold of scaffolds of different lengths, the vertical movement of the grey parts allow tunability as far as different diameters are concerned. The choice of using a plate or a screw to block the vertical movement of the grip would have been made after the production of the objects, according to which one would have behaved more properly.

There are several problems to this design. The fixing of the grips to the lid makes it impossible to culture more than one scaffold simultaneously. Indeed, opening the lid and mounting one scaffold when there is already one inside would probably induce the loss of sterility. However, both the dimension of the chamber and their use do not contemplate the utilization of more than one scaffold. In addition to this, the system used to hold scaffold of different diameter causes the two holes of the tubular constructs to be obstructed by the grips themselves. In this way, perfusion is highly hindered. This was the main reason to develop a new system and discard this one. However, this design allows for a versatile static culture of tubular scaffold which do not require perfusion of

two different chambers. In fact, the perfusion of the whole chamber is still possible, despite not being optimal to reach the lumen. It must be noted that this system keeps a good sterility of the chamber, since additional holes to the ones for the perfusion are present. One possible solution to this problem involves the tradeoff between keeping the sterility and the patency of the lumen. Indeed, in case the grips were fixed on the sides of the chamber, and not on the lid, it would be possible to utilize the double chamber perfusion system, despite losing the advantages related to the grips being fixed to the lid.

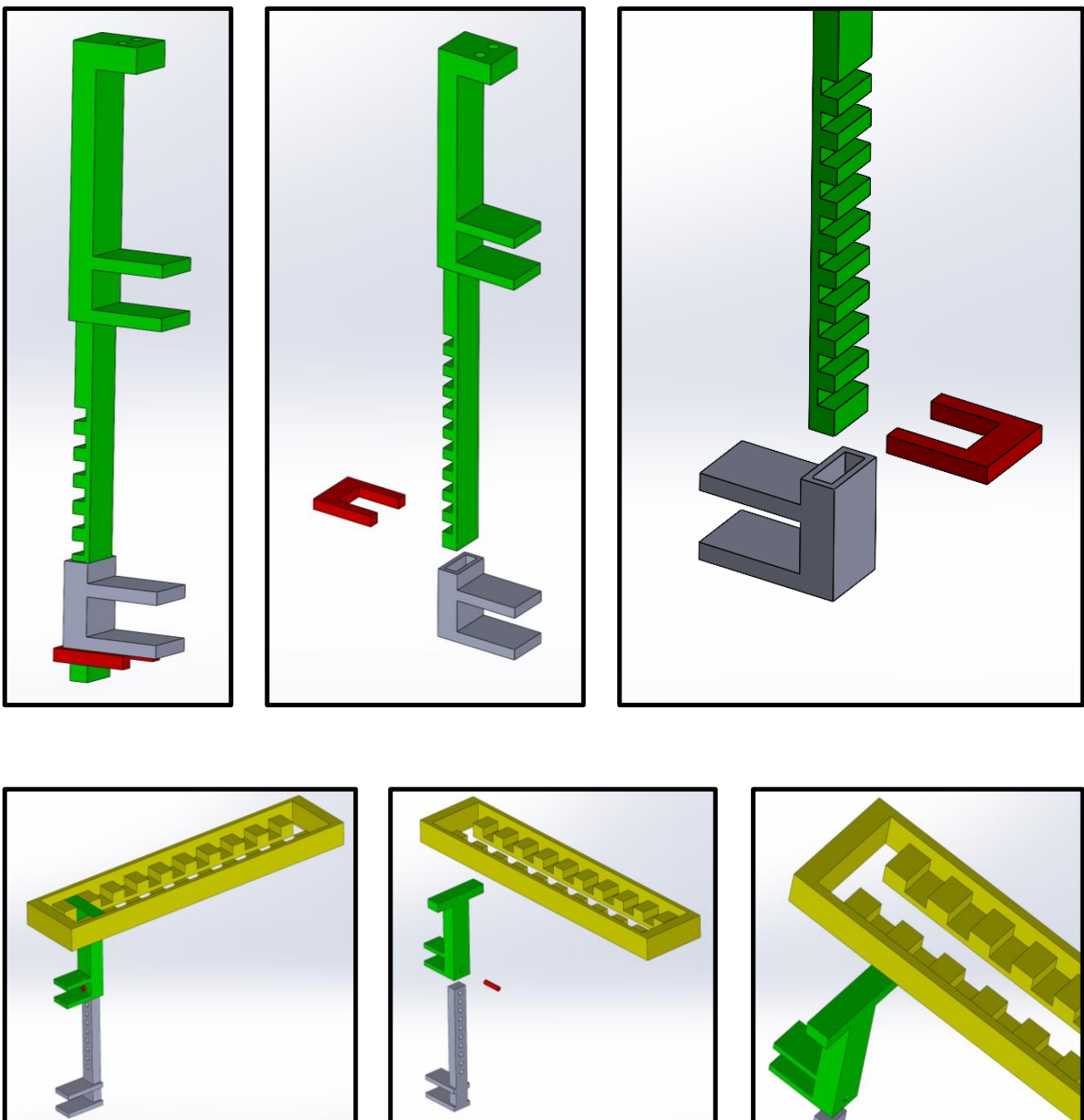


Figure 2.3 Global views (left), exploded views (middle) and details (right) of the fixed grip (top row) and the mobile grip (bottom row).

2.1.3 The third model

Because of the issues explained in the previous paragraph, it was necessary to find a new design for the bioreactor and its versatile grips. For the new approach, the same chamber was used, even though this time the exact dimensions of the available chambers were measured and implemented, as the production of the components was closer. Indeed, a digital precision caliper was used to measure accurately each part of the chamber. This was required to produce its CAD model and to guarantee the fit with the 3D printed components.

A change that was done to the chamber is to make the lid concave, exploiting the transparency of the material. In fact, with this optical artifact it is possible to see the inside of the chamber with an appreciable magnification. The lid closes the chamber creating a tortuous path of Pasteur, leaving a distance of 0.2 mm between their edges thanks to four small extrusions in the four corners of the structure (Figure 2,4, highlighted in the red circle).

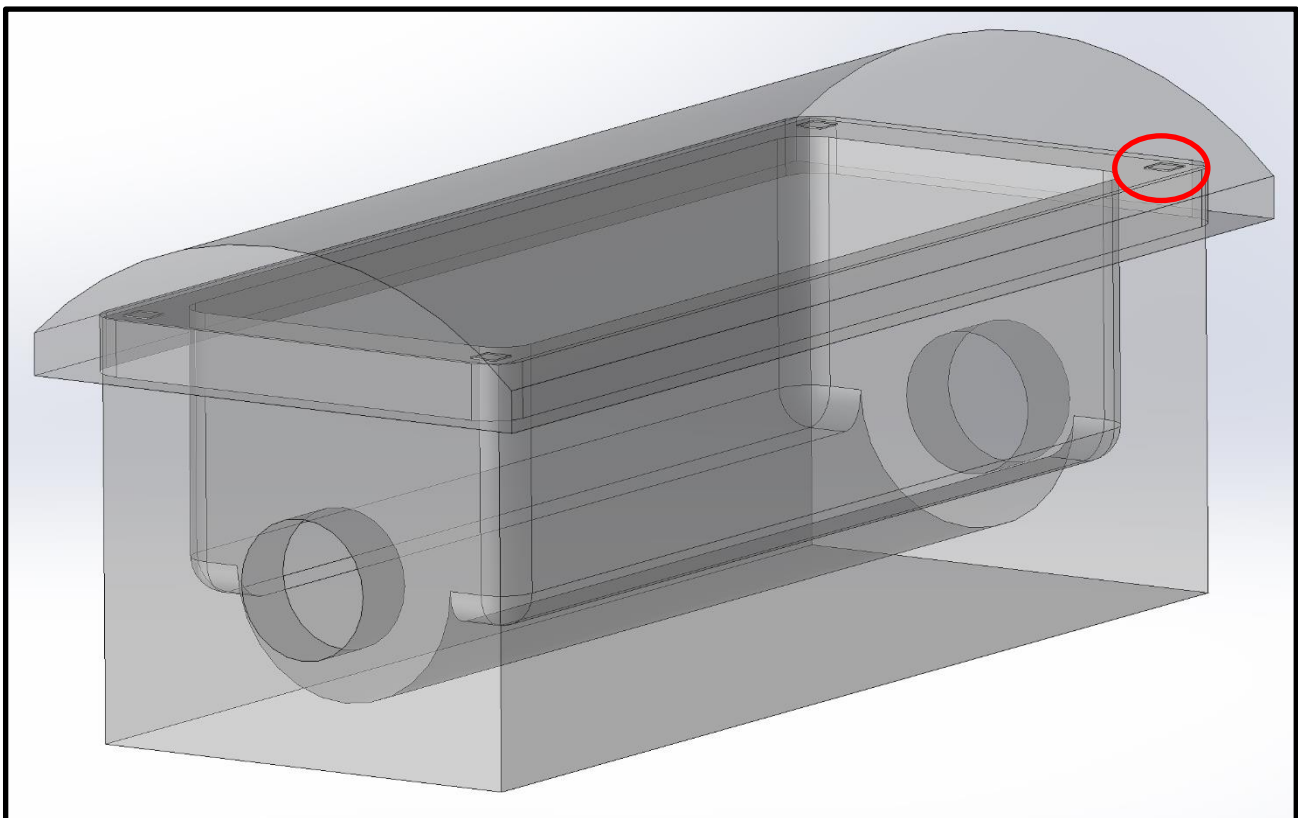


Figure 2.4 *The chamber and the lid create a tortuous path of Pasteur thanks to the extrusion on the corners of the structure (circled in red).*

To explain briefly what a tortuous path of Pasteur is, it is necessary to introduce the spontaneous generation theory, which Louis Pasteur proved to be wrong in 1864. Indeed, the spontaneous generation theory stated that life could spontaneously arise from non-living matter and that such

processes were commonplace and regular. This theory was opposed to the biogenesis theory, which stated that life could only come from other life. Louis Pasteur was a supporter of the biogenesis theory and, through an experiment, showed that the spontaneous generation theory was wrong. In this experiment, he developed a swan-neck shaped flask, putting nutrient liquid in it and then sterilizing it by boiling. The long and tortuous inlet of the flask allowed oxygen and gas exchange, but did not allow microorganisms to enter, also thanks to its opening being upside down. After a certain time that Pasteur removed the neck from the controls of the experiment, he observed presence of microorganisms only in these, confuting the spontaneous generation theory ²⁵. In this way, Pasteur also invented an effective way to keep sterile a flask, or whatever system such as a bioreactor, while allowing diffusion of gases in and outside of it. Our culture chamber and its lid form a similar apparatus.

The chamber presents two holes on the shorter sides. One of these entrances will be the inlet for the perfusion system (from now on called *perfusion inlet*), while the other will be necessary firstly for the assembly of the grips and the hold of the scaffold (*assembly inlet*) (Figure 2.5). However, as it will be explained later, the assembly inlet also has the function of being an entrance for test devices, such as catheters. Since their designs will be kept in the final model of the bioreactor, only presenting negligible changes, further information about their structure and functions will be explained in the following paragraphs.

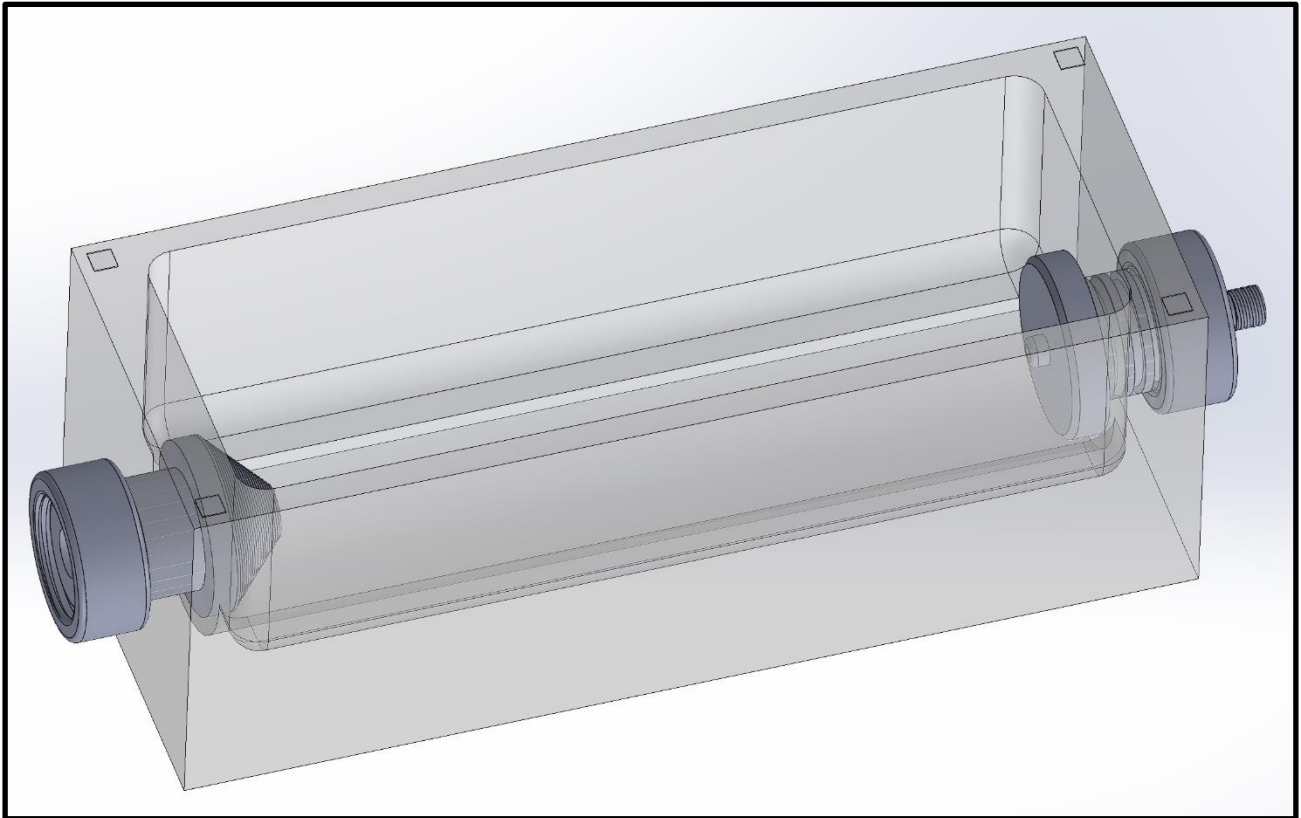


Figure 2.5 *The chamber with the assembled inlets. Perfusion inlet (right), assembly inlet (left).*

However, the assembly inlet includes one of the two grips for the scaffold, hence we will now focus shortly on its structure and then on how the components assemble in this model. The inlet is composed of two parts: one of these crosses the hole in the chamber from the inside (Figure 2.6, left) and the other is simply a sort of bolt which closes the structure granting sterility maintenance (Figure 2.6, right).

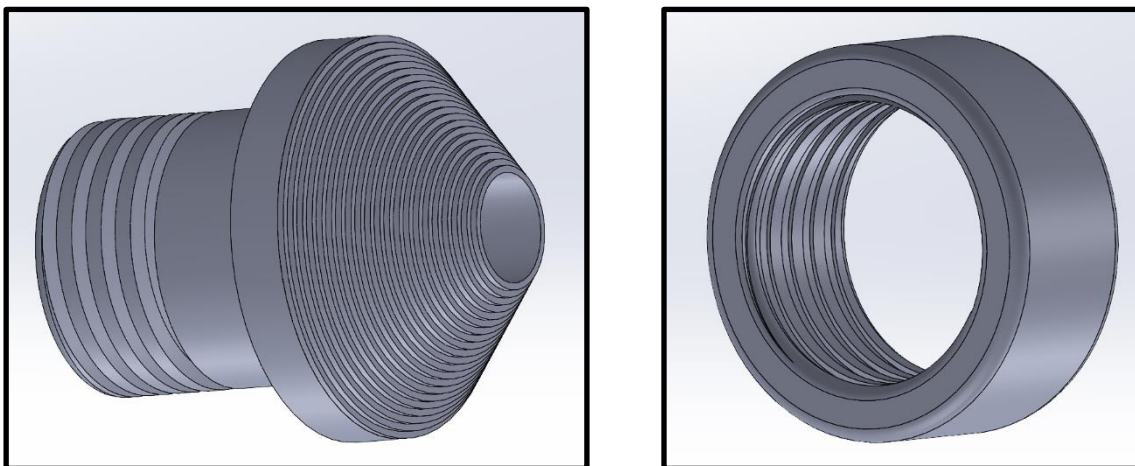


Figure 2.6 *Details of the components of the assembly inlet.*

The part represented on the left includes the grip of the scaffold, which is the conic structures with the discrete steps. This cone is designed to allow the hold of one of the extremities of the tubular

scaffold, which will adhere to the most suitable step of the cone according to its diameter. The inclination of the cone side is 45° . As can be seen in the previous figures, the assembly inlet presents a hole in the middle of the cone which crosses the component in all its length. This hole is needed to allow an axis to enter the structure. This axis is long enough to reach the perfusion inlet (Figure 2.7).

Moreover, the axis also presents another cavity for all its length, allowing to perfuse the inner part of the structure through the small holes on the side surfaces of the axis. On this axis a thread is present which allows another grip, similar to the one bound to the assembly inlet, to be screwed onto the axis while it is being inserted, before reaching the perfusion inlet. This second grip presents a thread complementary to the one on the axis. In this way, during the mounting of the bioreactor, it is possible to also insert the tubular scaffold and to fix it onto the two grips. Moreover, the thread system allows this second grip to be placed in the most suitable position to host scaffolds of different lengths. To sum up, the versatility of this system for tubular scaffolds of different diameters and lengths is given respectively by the steps on the cones of the grips and by the movement of the grip screwed on the axis. In figure 2.7, top panel, there is the system while it is being assembled; in the middle panel, there is a detail of the thread present on the axis and inside the hole of the mobile grip; in the bottom panel there is another detail of the hole present in the axis which allows communication with the perfusion system. In figure 2.8, instead, there is a picture of the assembled system.

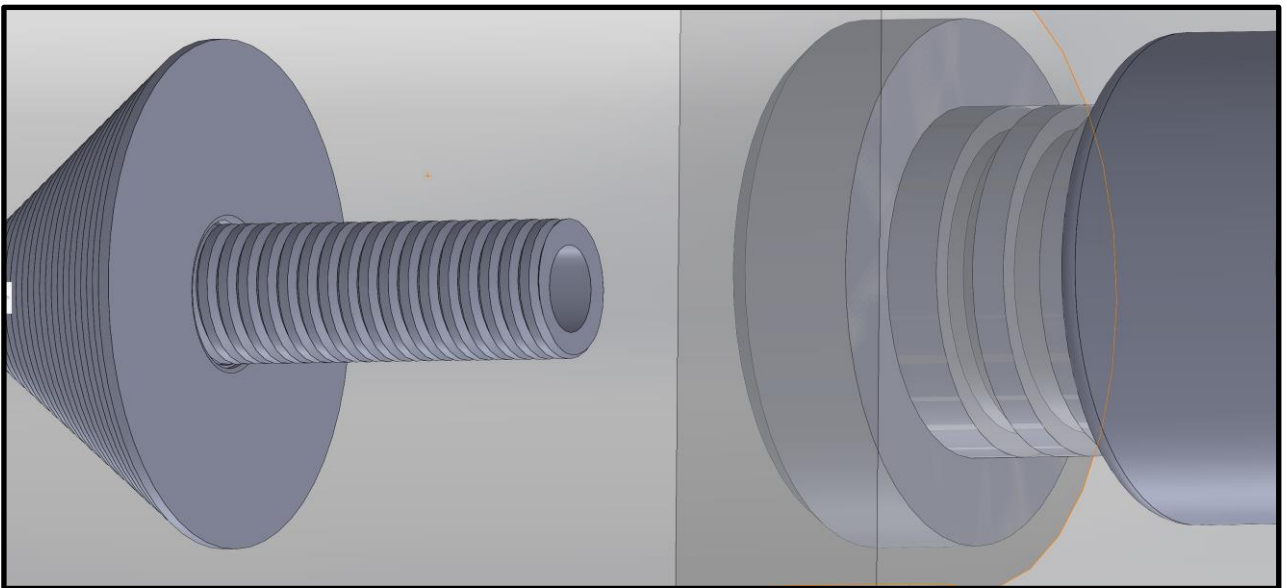
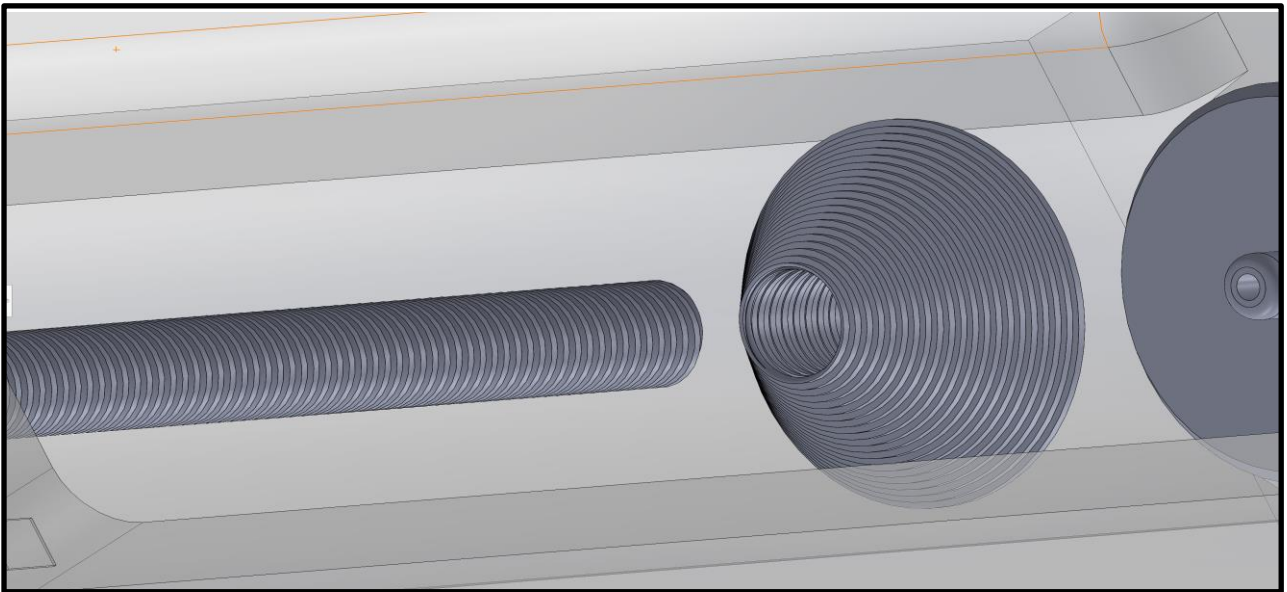
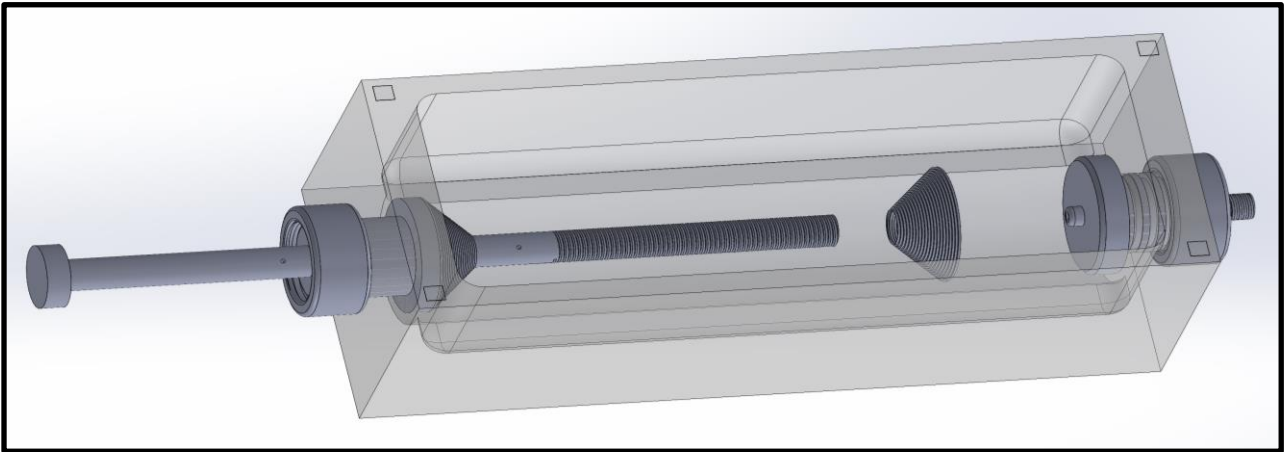


Figure 2.7 Top panel. *Assembling of the system.* Middle panel. *Detail of the threads on the axis and the mobile grip.* Bottom panel. *Detail of the hole in the axis reaching the perfusion inlet.*

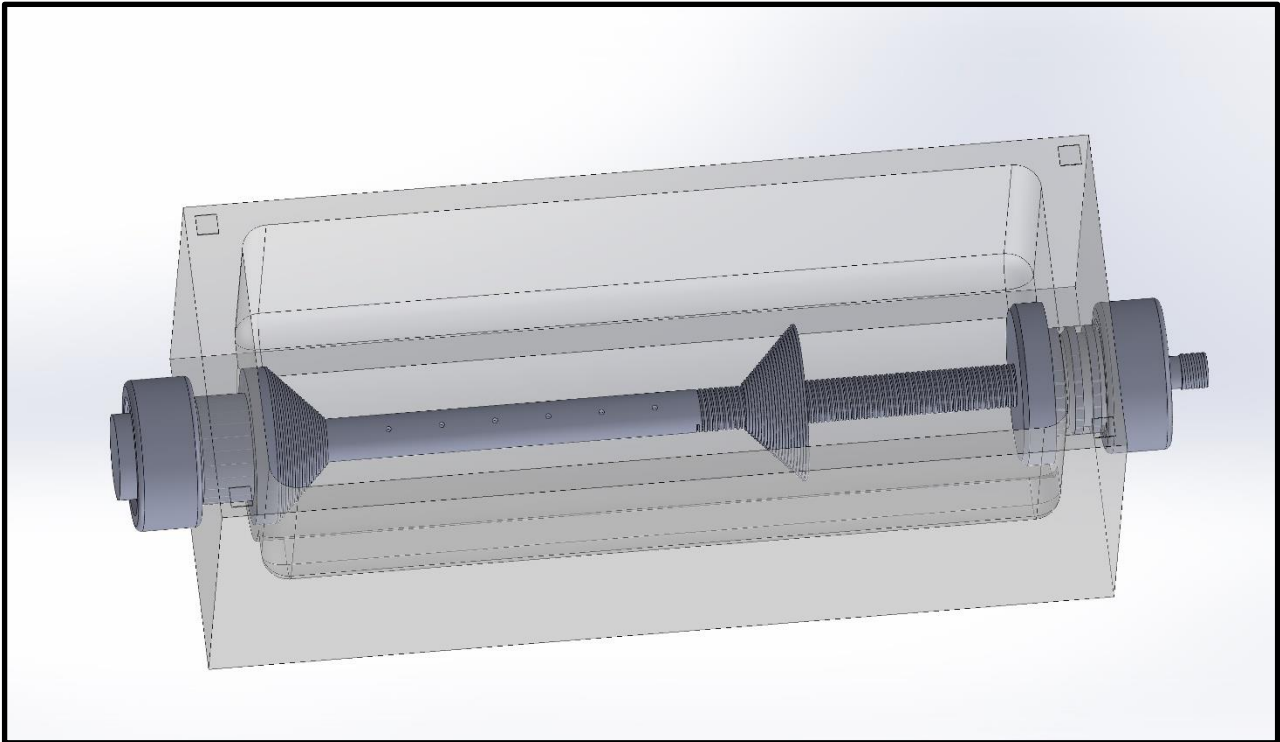


Figure 2.8 *The assembled bioreactor, without the lid.*

As already said, on the axis, between the two grips, there is a series of holes which will allow the perfusion of the scaffold from the inside through the perfusion inlet. The reasons behind this approach have been explained in the Introduction chapter when it was talked about the double chamber model for trachea tissue engineering and bioreactors.

However, this system present some issues. The first one regards the capability of the grips to hold the scaffold. Indeed, because of the thinness of the steps on the cones' sides, the scaffold has a too narrow space to solidly settle. In addition to this, soft tissues, like blood vessels, are often collapsible, requiring a relatively strong hold and often to be pretensioned. During the cell culture, several types of grafts also tend to undergo shrinking, making this process even more unlikely to work. A possible solution to this problem is to change the design of the grips, reducing drastically the number of steps to just three different sizes, allowing more space for each step, with the possibility to secure the tubular scaffold to the most suitable step through the use of an O-ring. In this way, despite the hold of the scaffold being improved, a reduction of the versatility of the system is caused. However, because of the modularity of the bioreactor and the relatively ease by which a component is 3D printed, it will be possible to print a series of different grips and use the most suitable for each application, allowing us to cover a higher range of scaffold diameters.

Another issue affects the threads present on the axis and the mobile grip. These small cavities, in an environment like a bioreactor, would be perfect spots for catabolites, wastes and possibly pathogens

accumulation and stagnation. Hence, instead of the thread and bolt model, it was thought to create a series of grooves on the outer surface of the axis, at a distance equal to the length of the grip component, allowing it to be placed and secured with two O-rings. To conclude, it is right to mention that these and other changes to the system will be further discussed and pictured in the following paragraphs, being these the final design chosen for the bioreactor.

At this moment of the development of the system, the material for the production of these 3D printed objects was selected and it was polylactic acid (PLA). The reasons behind this choice will be discussed in one of the following paragraphs. The same goes for the choice of the material of the outer chamber. However, for the first approaches to this study, an already available chamber was used as model. This model is the one which has already been presented, characterized by the concave lid. The material of this chamber was plexiglass. Nevertheless, this was only an expository chamber, as the material, despite being cytocompatible, is not suitable for the real use of the bioreactor.

2.2 Final design of the bioreactor

In this paragraph, the single components of the bioreactor will be presented and analyzed. In addition, pictures of the final 3D printed products will be shown. The final model is based mainly on the ideas discussed when talking about the third model. However, some parameters had to be improved, since when trying to 3D print the objects many issues have been met, driving us to modify the structure to make its print possible. More details will be furnished for each component singularly.

2.2.1 The culture chamber

We will now discuss, first of all, the properties of the main culture chamber. Until now, the chamber has been the transparent container already shown in the previous paragraphs. This was the chamber used from the second model on, with only neglectable changes in its dimensions. In Figure 2.10, the chamber with the final dimensions is showed. This chamber, in addition to presenting new dimensions, has a different shape for its lid, which will be discussed in the following paragraph. As shown, the structure has a rectangular base, presenting symmetrical disposition on the longitudinal plane, with two circular openings on the shorter walls. These holes are needed to allow the perfusion of the system, the mounting of the components or the scaffold and the insertion of testing and analysis devices such as catheters. The chamber presents smoothed angles and walls since the presence of right angles would imply the accumulation of catabolites and possibly pathogens that

would harm the tissue. The top of the container is open, as it will be closed by the lid. This kind of approach has been chosen as it is planned that the user should open the lid inside a sterile environment to operate inside the bioreactor. Some possible operations consist of assembling of the components, insertion of the tubular construct or change of the outer culture medium. In fact, the inner medium is introduced through the perfusion system. On the top surface of the chamber four extrusions are present, each tall 0.2 mm. As previously discussed, the function of these thin structure is to create a tortuous path of Pasteur, which means that, when the bioreactor is closed, there will be enough space for the oxygen to diffuse inside the container and so into the medium, but the access of pathogens will be highly reduced and mainly avoided, also because the opening will be facing downwards. Finally, the material chosen for this chamber is polysulfone.

In Figure 9, a photo of the chamber.



Figure 2.9 *Photo of the culture chamber.*

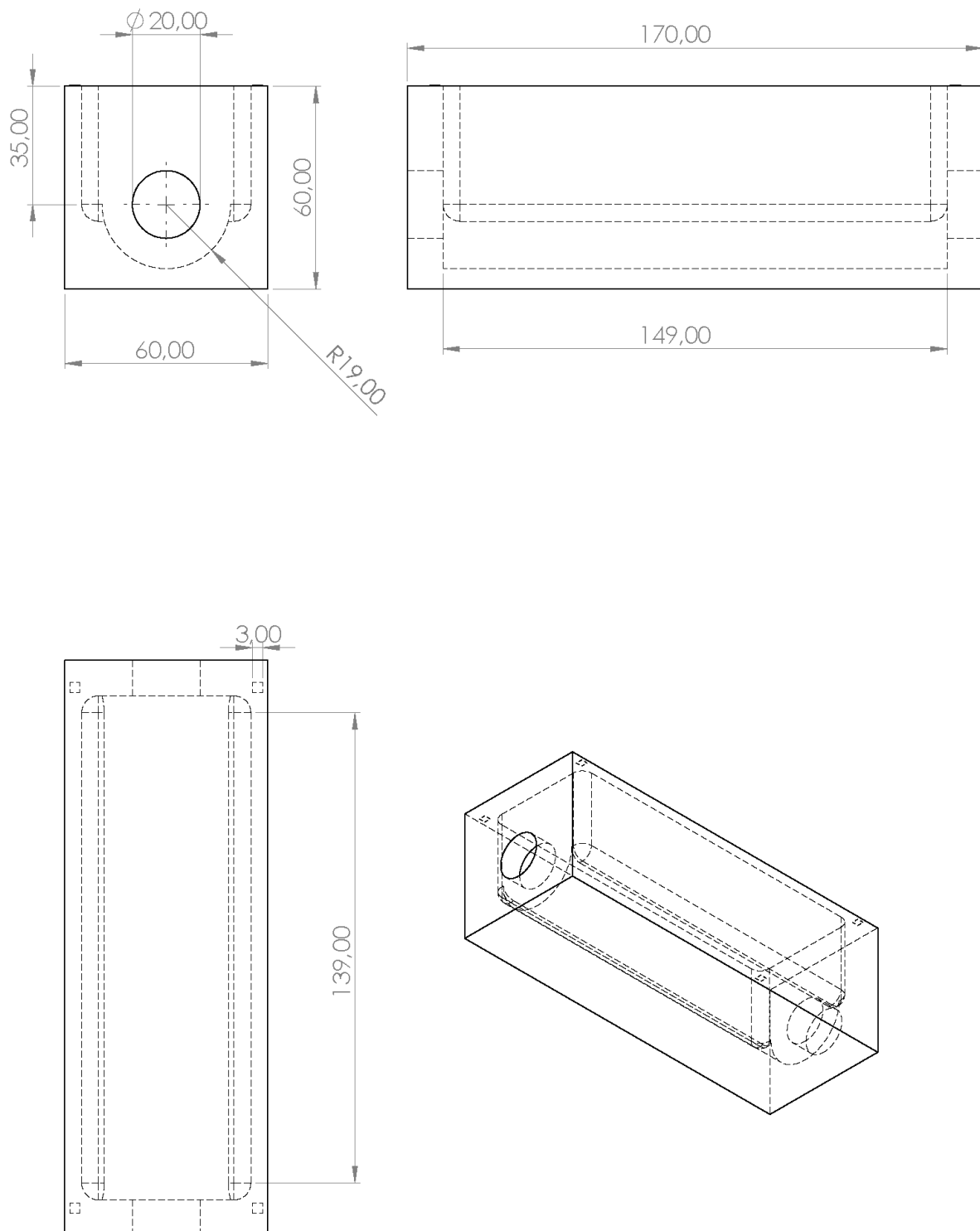


Figure 2.10 Views of the final culture chamber: front view (top left), side view (top right), top view (bottom left), isometric view (bottom right). Measures in mm.

2.2.2 The lid

The lid has the function of closing the structure on the uppermost side. It fits with the outer edges of the culture chamber and, as already said, thanks to the four extrusion of the chamber, the lid creates a tortuous path of Pasteur. It has been previously said that the lid has a concave shape in order to create a magnification effect when looking inside the chamber, exploiting the transparency of the material. However, the transparent material (plexiglass) was not suitable for real use of the object and was produced only for aesthetical effects. The material was indeed changed with polysulfone, a non-transparent, yellowish material, which does not allow the magnification effect. For this reason, the lid is now flat (Figure 2.11).



Figure 2.11 *The lid of the final model. Note that it is now flat.*

2.2.3 Inlets and outlets

Some of the most important components for the good functioning of the bioreactor are the inlets, since these have the duty to keep the inner part of the system sterile while allowing exchange of substance with the outside. As already said, the inlets are two: the perfusion inlet, connected to the perfusion system, allowing perfusion of the innermost part of the future scaffold; the assembly inlet, with the functions of allowing assembling of other components, but also handling the start and stop of the perfusion, along with insertion of test devices such as catheters. In this paragraph, these two sub-systems and their sub-components will be analyzed and described.

2.2.3.1 Perfusion inlet

The perfusion inlet is assembled on one of the two holes on the culture chamber. It is formed by several smaller components. The most important is what has been called the perfusion screw (Figure 2.12, bottom left). This component is formed by a wider base, which goes inside the chamber and a screwed extrusion which goes on the outside through the hole. Through a nut-and-bolt-like system another component, simply called ring (Figure 2.12, top left), closes the screwed part from the outside of the chamber. As it is possible to see, the perfusion screw presents a hole through all of its length, which is not obstructed by the closing ring. Halfway through the screwed extrusion it is possible to see a cavity, designed to host an O-ring to improve sterility maintenance and contact with the chamber hole. A similar cavity is present on the part of the ring that will be in contact with the outer wall of the chamber for the same reason. The thread on the inner wall of the closing ring is not complete on all of its length for practical reasons, indeed, adding a small, non-threaded part here helped in the 3D printing of the object. Finally, two smaller pieces (Figure 2.12, top and bottom right) close the holes on the inside and outside of the perfusion screw, allowing communication with an outer perfusion system and other inner components, that will be explained later. It has been preferred to produce these two smaller components separately since it would have been harder to print them included in the perfusion screw due to the diameter changes on the longitudinal axis and it would have been necessary to print a support and detach it subsequently. Every time a similar approach has been chosen in the development of other components it will be due to this reason. In Figure 2.13 it is possible to see the assembled perfusion inlet.

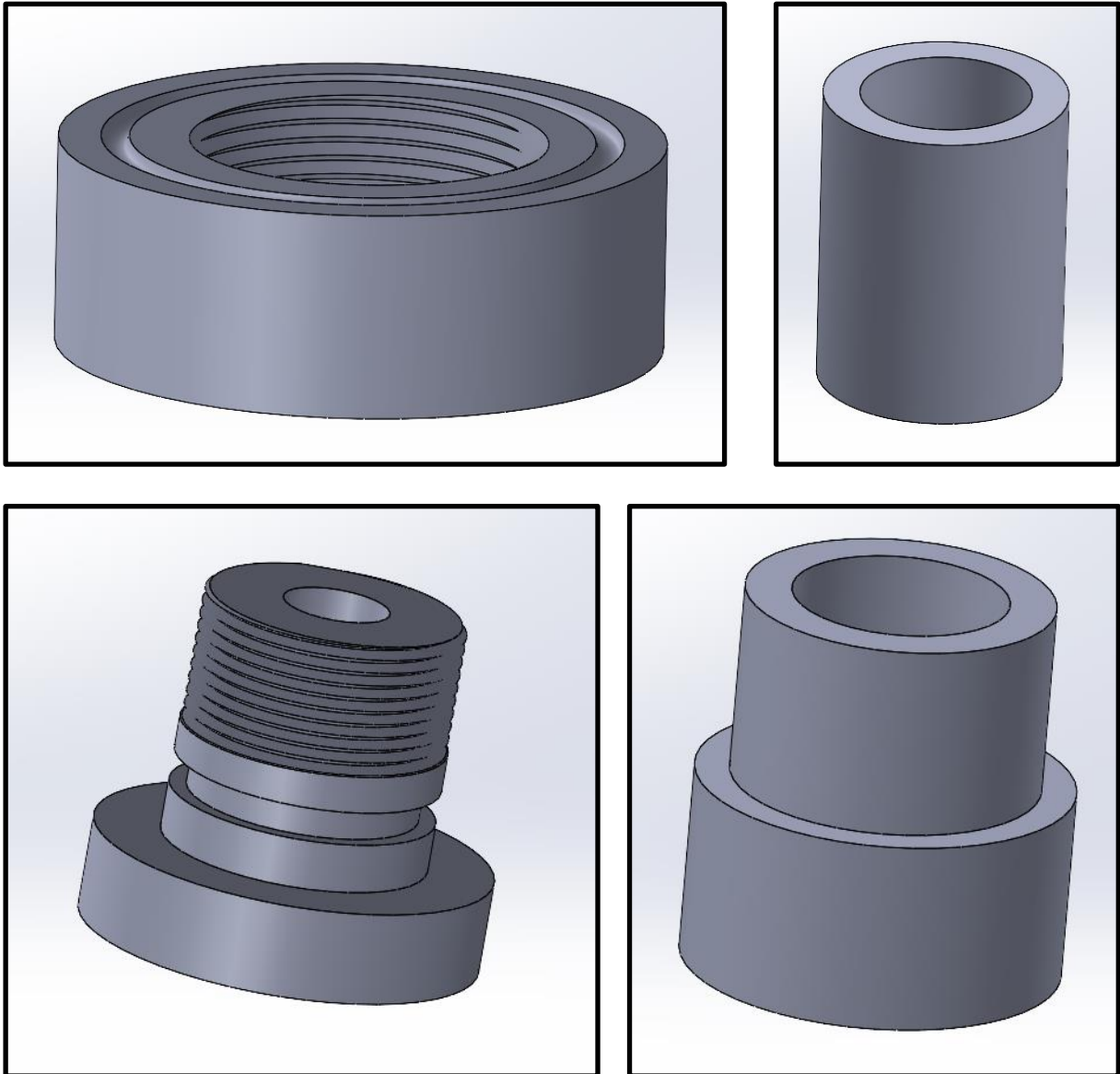


Figure 2.12 *The components which form the perfusion inlet. Top left. Ring. Bottom left. Perfusion screw. Top right and bottom right. Supplementary components to connect the various components.*

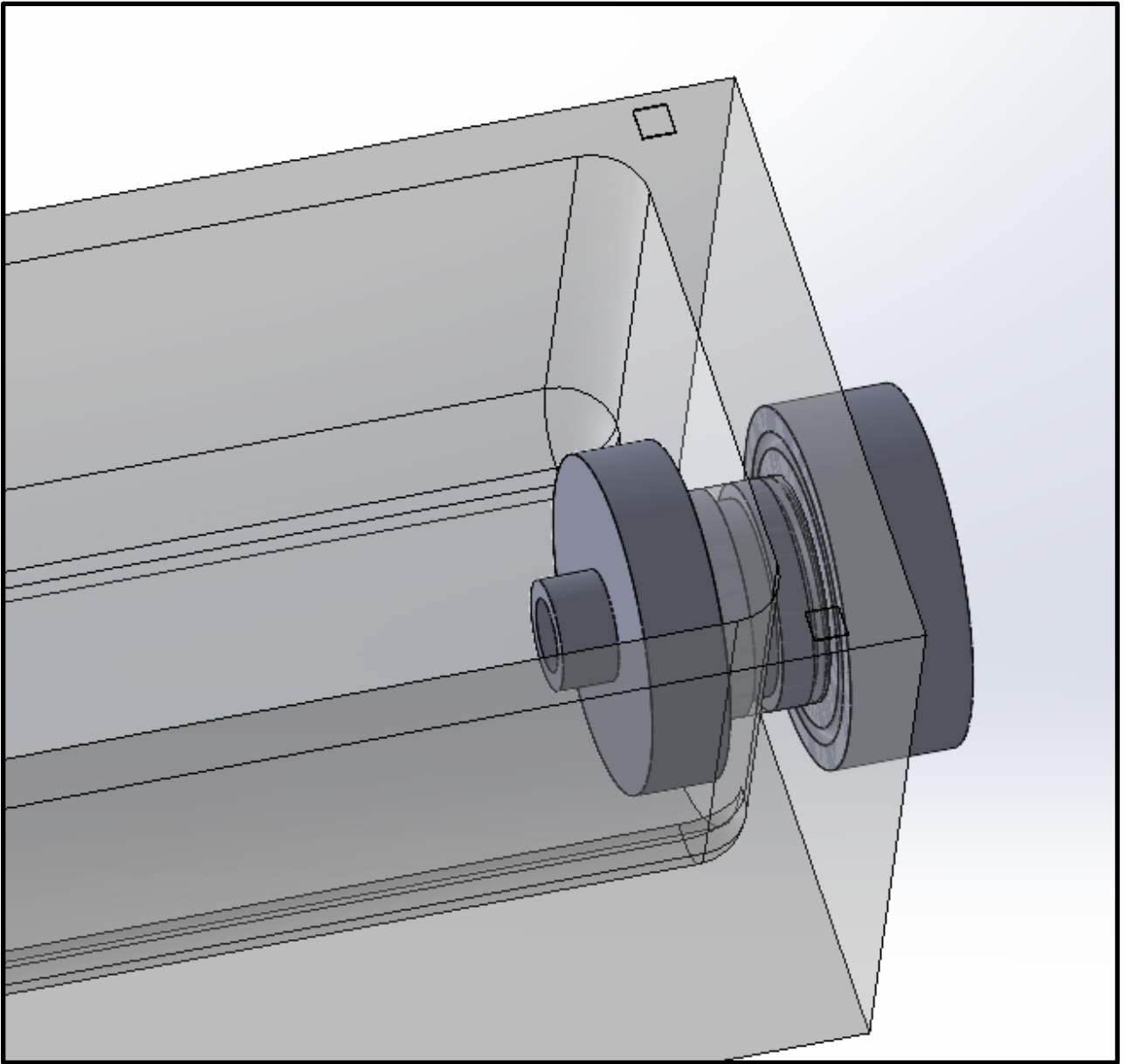


Figure 2.13 *The perfusion inlet fully assembled with the chamber.*

2.2.3.2 Assembly inlet

The other important inlet is the assembly inlet, mounted on the other hole. The assembly screw here is very similar to the perfusion screw, with minimal changes in its dimensions to allow coupling with other components. The structure is the same, hence having a wider base which goes on the inside of the chamber and a threaded extrusion which goes on the outside. A closing ring, identical to the perfusion inlet one, closes the system on the outside. The cavities for O-rings are present also in this sub-system. For these reasons, a figure of these two components will not be inserted.

The major difference between the perfusion screw and the assembly screw is the size of the longitudinal hole. Indeed, in the assembly screw the hole has a diameter of 12 mm, whereas for the perfusion screw this diameter is 8 mm. The reason for this difference is the function of the two screws. The perfusion screw only has to allow the passage of medium to perfuse the scaffold internally. The assembly screw has to allow the entrance of both other components that will allow the grip of the scaffold and also devices such as catheter to study the artificial tissue. Finally, a picture of the assembled assembly inlet is shown in Figure 2.15.

It is possible to see in Figure 2.14, instead, two views of both the perfusion screw and the assembly screw. In these pictures, however, it is present the Teflon tape, which was necessary to apply for further studies, which will be explained in the following chapters.

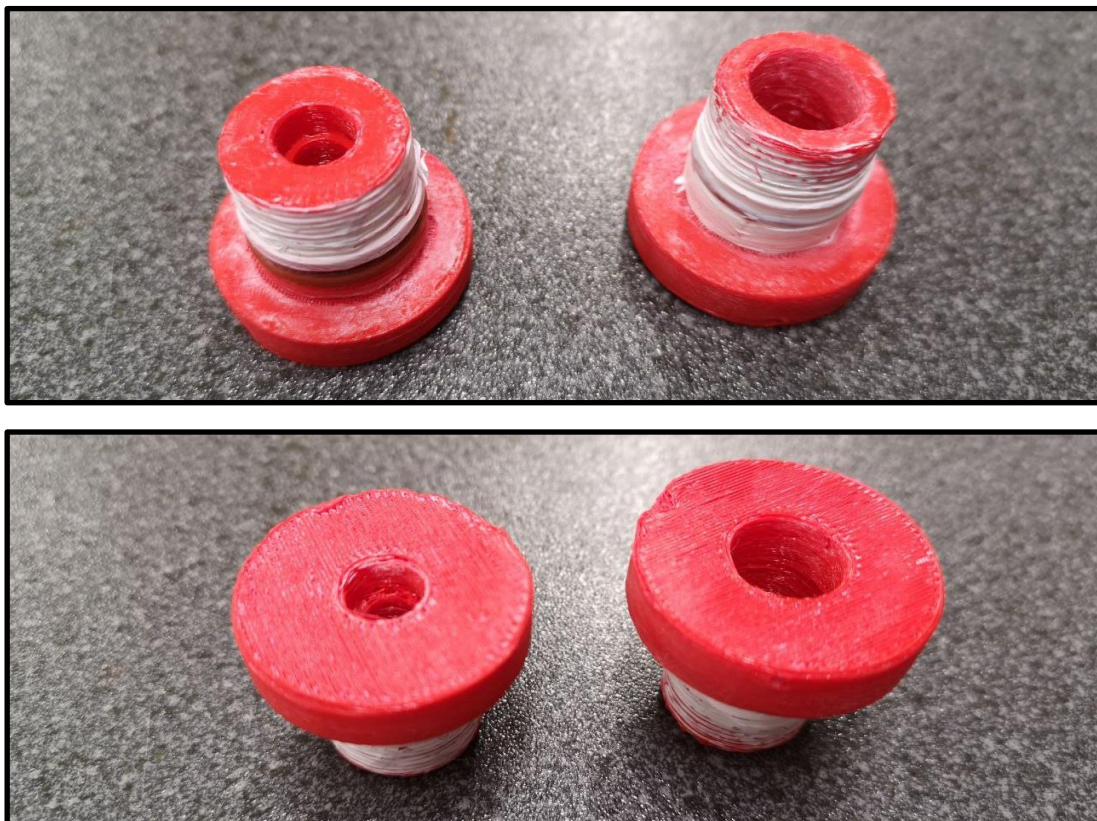


Figure 2.14 *Top and bottom views of the perfusion inlet (left) and assembly inlet (right).*

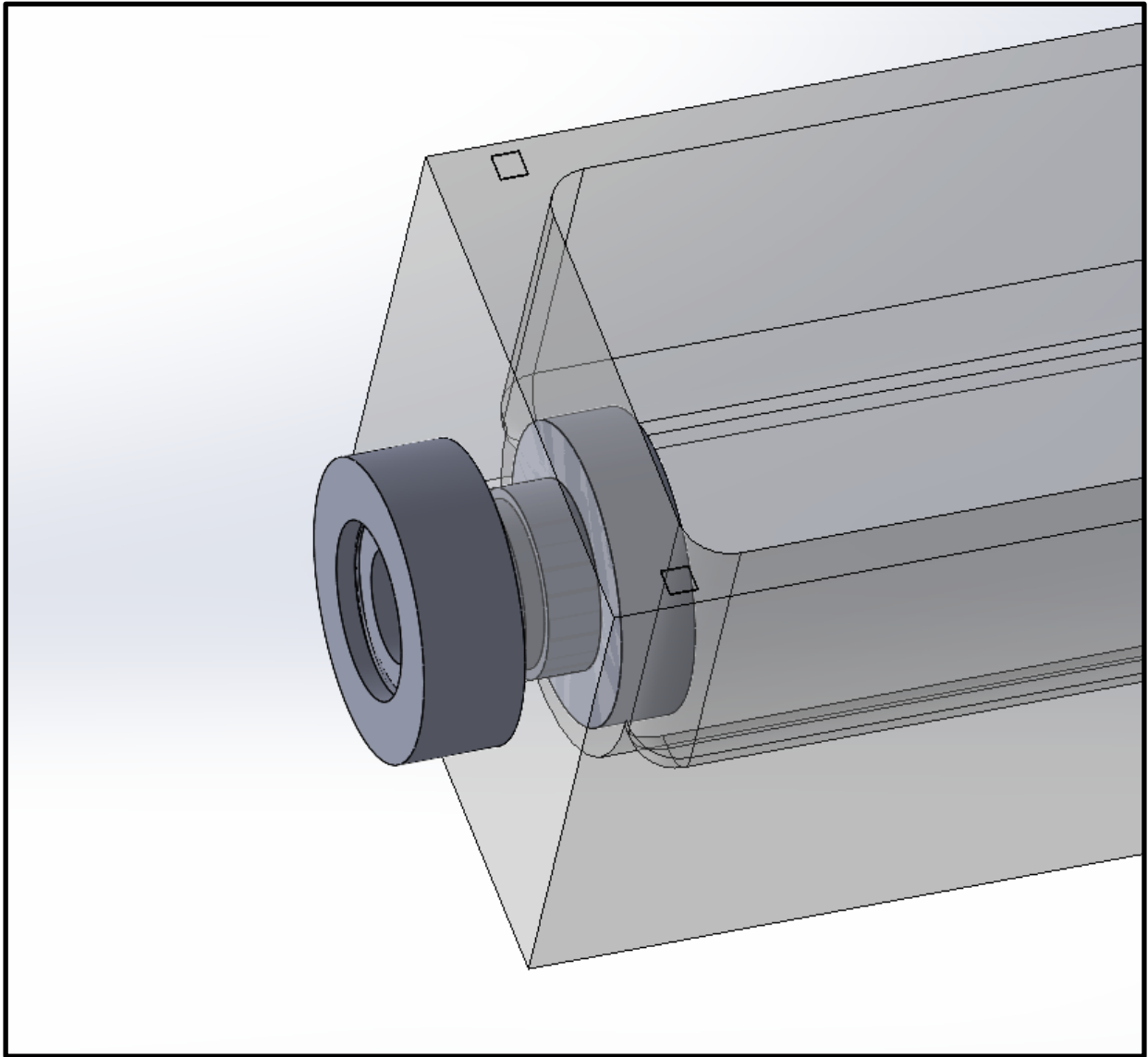


Figure 2.15 *The assembly inlet fully assembled with the chamber.*

2.2.4 Inner perfusion axis

The inner axis (Figure 2.17) is the most complex component of the system. The role of this axis is both to allow the assembly of the grips which will hold the scaffold and also to allow the perfusion of the inner part of the scaffold. Indeed, the structure of this axis is basically a cave tube which presents holes on its sides. The axis communicates with the perfusion inlet interlocking with the smaller component mounted inside the perfusion screw towards the inside of the chamber. From here, the medium is pumped inside the axis, around which the scaffold is placed. Then, the medium can go out through the holes of the axis to wet the scaffold. On the other side, the axis is assembled with other components which enter from the assembly inlet. However, other components had to be added for practical reasons to ease the 3D printing process. Outside of the assembly inlet a three-way stopcock is present, allowing to block the perfusion flow at pleasure (Figure 2.16).

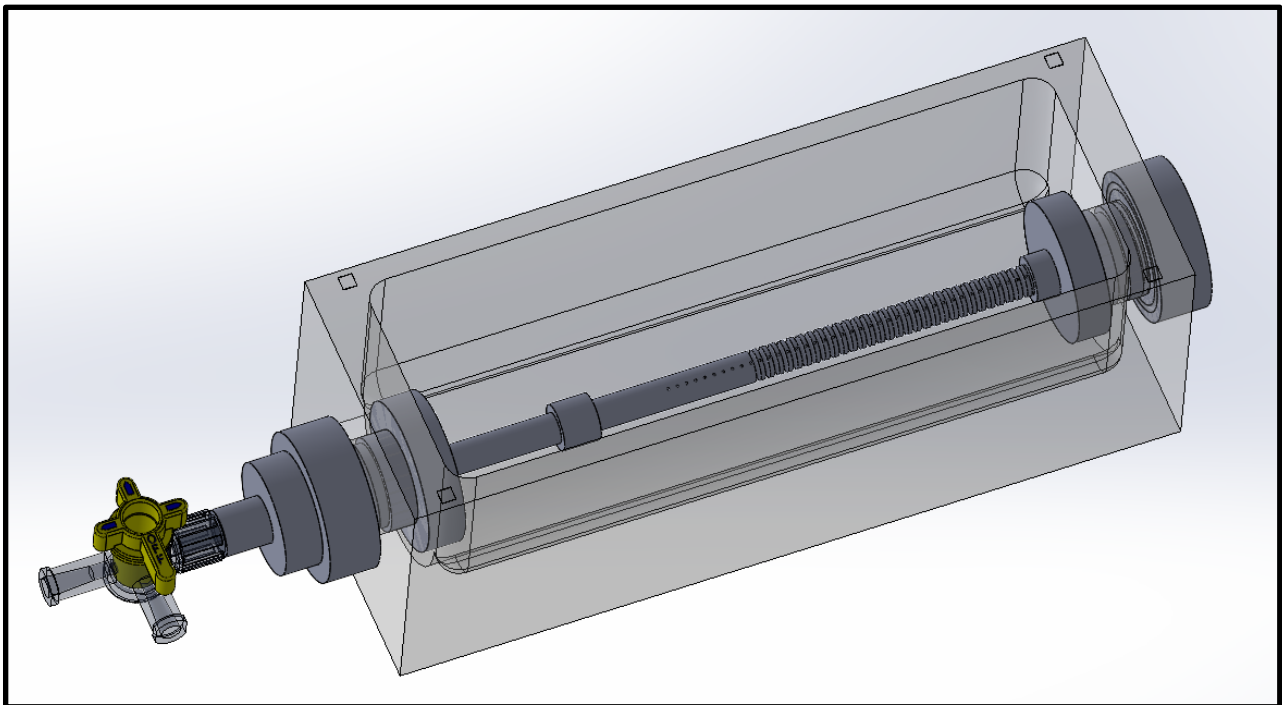


Figure 2.16 *Assembly of the bioreactor with the components listed until now: perfusion inlet, assembly inlet, inner perfusion axis, three-way stopcock. Note the addition of smaller components to improve feasibility of 3D printing.*

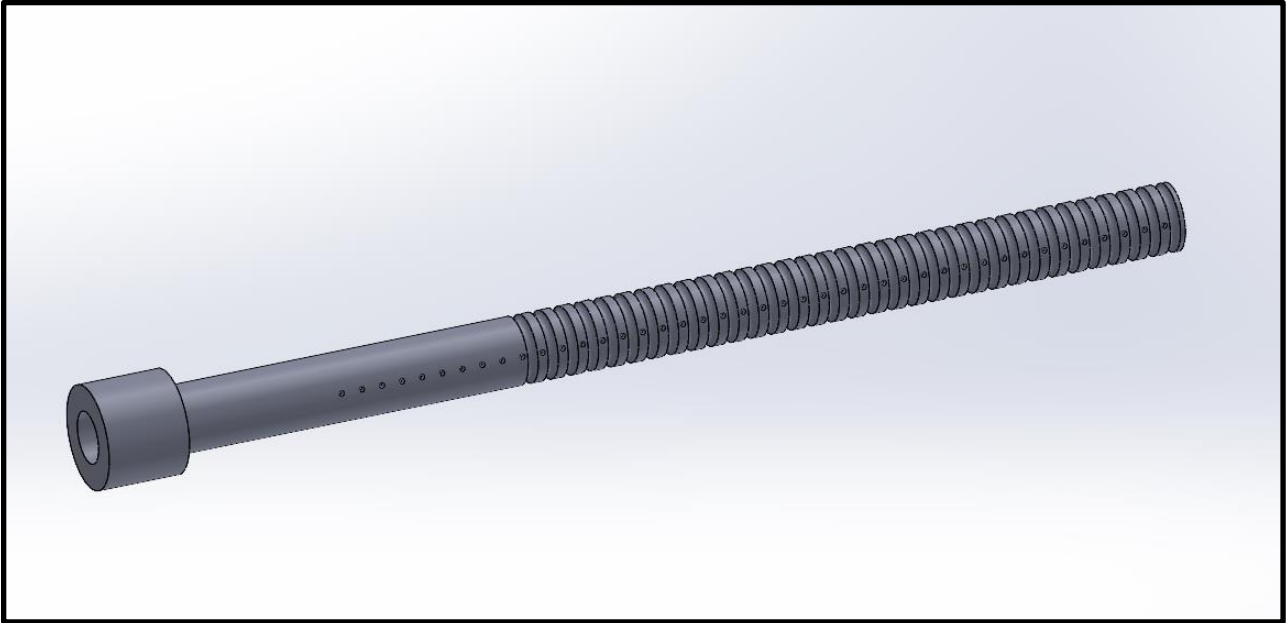


Figure 2.17 *The inner axis. Note the holes and the grooves on its sides.*

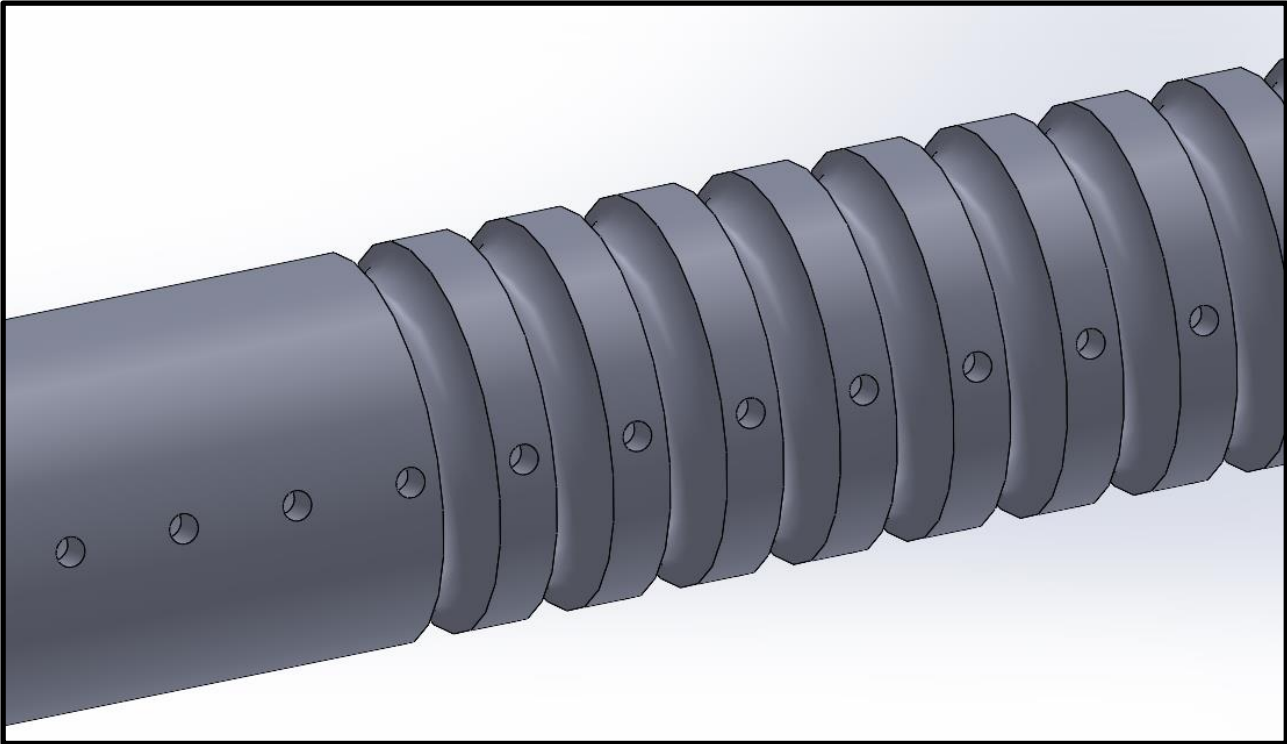


Figure 2.18 *Detail of the holes and grooves on the inner axis.*

2.2.5 Scaffold grips

The grips, which have only been shown in its original design in The third model paragraph, are the most innovative part of this project, not due to their shape, but due to their interaction with the other components. The aim of these grips is to allow the versatile use of the bioreactor for tubular constructs of different and custom diameter and lengths. The placings of these two grips are on the perfusion axis. One of the grips, which has been called fixed grip, is in contact with the assembly screw and is fixed there, blocked between the assembly screw itself and the perfusion axis. The other grip is still mounted on the perfusion axis, but this is not fixed. Indeed, this grip has been called the mobile grip. The mobile grip is free to move between the perfusion screw and the fixed grip. Thanks to this system, scaffolds of different lengths are free to be host inside the bioreactor. However, this is not the only versatility of these grips system. Indeed, looking at their structure, it is clear to see two different diameters. These diameters can be customized, obtaining a wide range of possible diameters for the scaffold. The advantage of using PLA for the print is that it is highly available, so a specific diameter in one of the possible three can be designed and developed rapidly and easily. The lengths for scaffold which can be host in this system range from about 20 to 80 mm, whereas the diameters range from 6 to 35 mm. Having two possible diameters on a single couple of grips is a big advantage, but however is less relevant with respect to the first project, where these possibilities were more than 10 to 15. It has been preferred to reduce the number of steps in the structure of the grips to improve the hold of the scaffold. Indeed, a too thin step width would have caused a loose and weak hold of the scaffold, considering its mechanical properties and the fact that often grafts need to be pretensioned. So, it has been preferred to obtain a more satisfying hold of the scaffold with respect to the possibility of hosting a wider range of diameters. However, since PLA present a low durability, it would have been necessary to produce the components again after some time of use. In this case, the necessity of producing a new component to host a different diameter scaffold is less heavy and more understandable. The structure of a single grip is shown in Figure 2.19 and a photo is given in Figure 2.20.

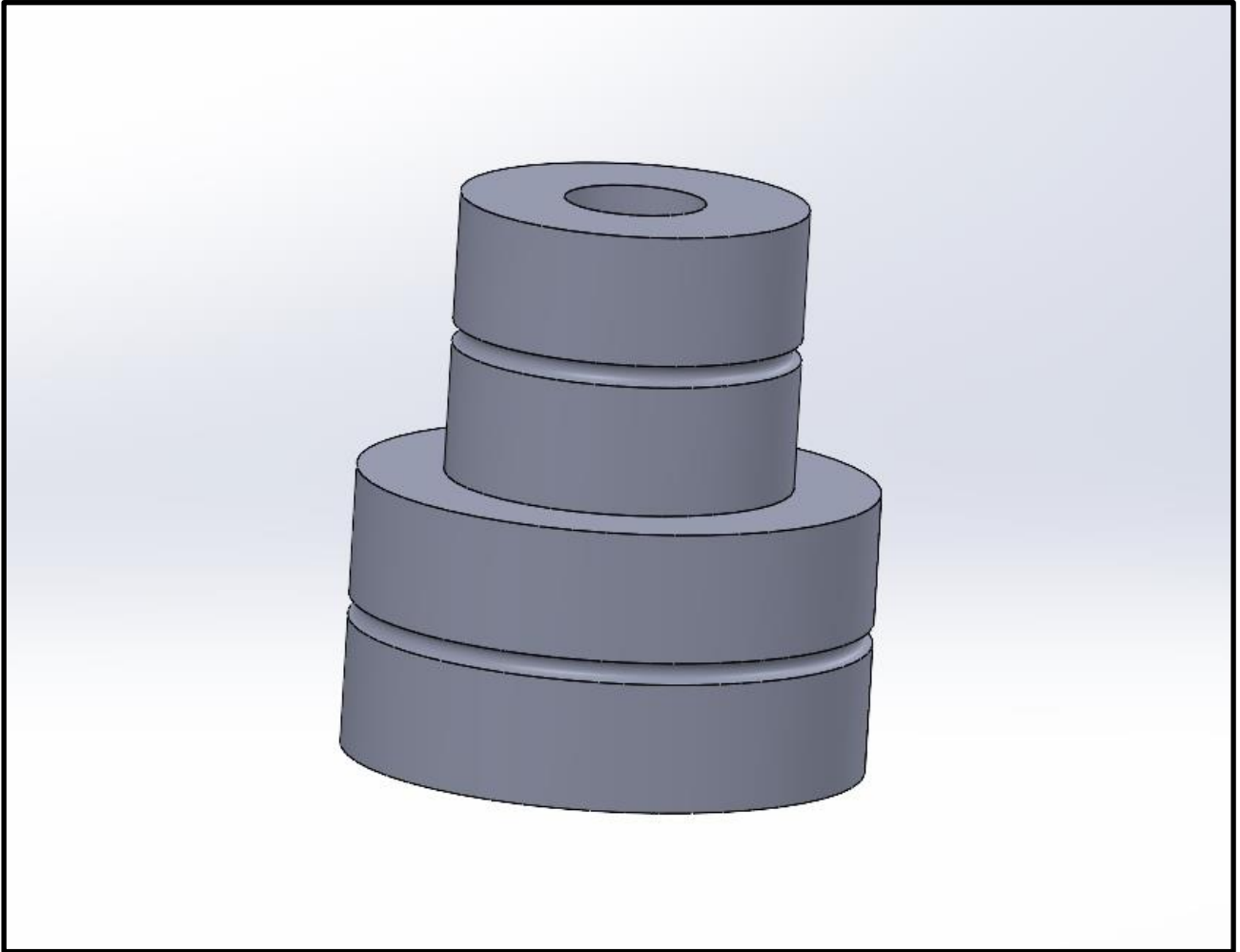


Figure 2.19 *Single scaffold grip. The fixed and the mobile grip have the same shape and dimensions, hence only one is shown here.*



Figure 2.20 *The two 3D printed scaffold grips.*

2.2.6 Assembled chamber

In this paragraph, brief considerations on the assembled chamber will be listed. First of all, it is possible to see the assembled bioreactor in Figure 2.22. In order to allow better understanding of the design of this complex 3D printed system, a section view is shown in Figure 2.23. It is possible to appreciate how the components have been thought and produced in order to avoid printing of supports and to allow patency of the inner lumen and sterility maintenance.

In these two CAD models it is possible to note that not all the components have been explained now. Indeed, some of the present components have only a supportive function, allowing the assembly of the whole system. In Figure 2,21 you can see all the additional 3D printed components that it was necessary to produce to assemble the whole bioreactor.



Figure 2.21 *Additional 3D printed components required for the full assembly of the system.*

After explaining the design that the bioreactor was thought to have, in the following paragraphs the process behind the production of the components will be explained, along with clarifications about the feasibility of the project and how issues have been met and solved.

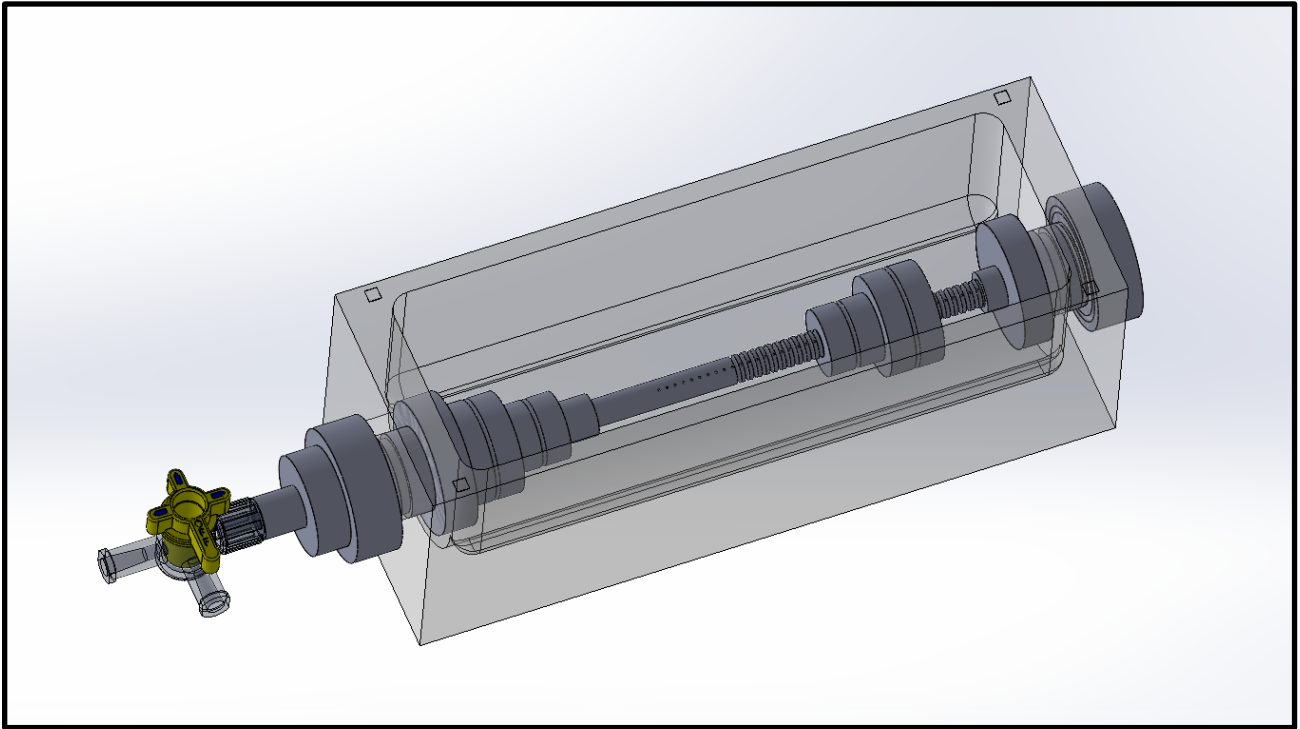


Figure 2.22 *Assembled chamber with three-way stopcock (without lid).*

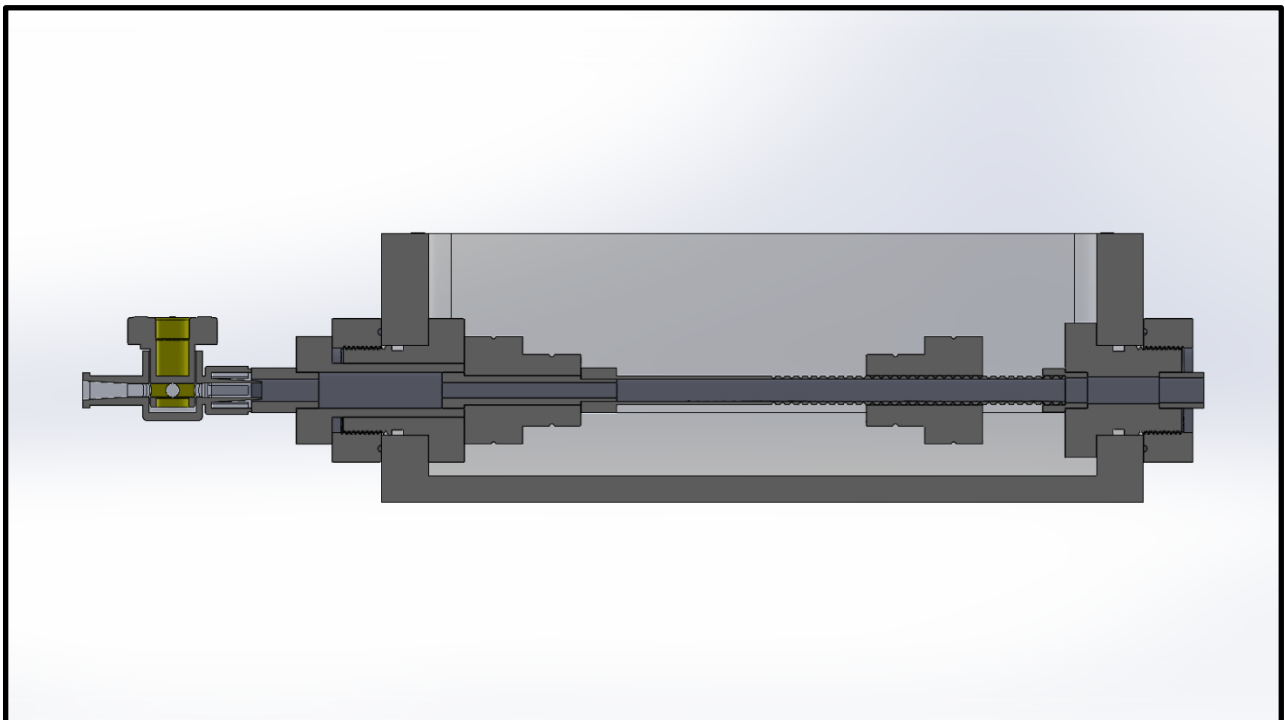


Figure 2.23 *Assembled chamber with three-way stopcock (without lid). Section view.*

2.3 Steps for the production of a 3D printed object

In this paragraph, the process behind the production of a 3D printed object will be presented, taking as example one of the simplest yet very important object produced for this thesis, that is the scaffold grip (Figure 2.20).

The production of a 3D printed object is based on the fact that we can print any object, with some constraint, that can be three-dimensionally and virtually designed using a computer. In fact, once we obtain the 3D model of the object, we can produce a code that will be read by the 3D printer, which will follow the path leading to the production of such object. First of all, we must use a CAD (Computer-Aided Drafting) modeling program: the most used are Dassault Systèmes SolidWorks²⁶, Autodesk AutoCAD²⁷, Rhinoceros²⁸ and many more. For all the work showed in this thesis, SolidWorks was used. Using this or one of these programs allows the researcher to exploit simple or complex commands based on geometrical shapes to create a model starting from a simple one (a cube, a sphere etc.) or from the object's bidimensional draft and then extruding it. What is obtained by working on a CAD program for the object we are taking as example is shown in Figure 2.24.

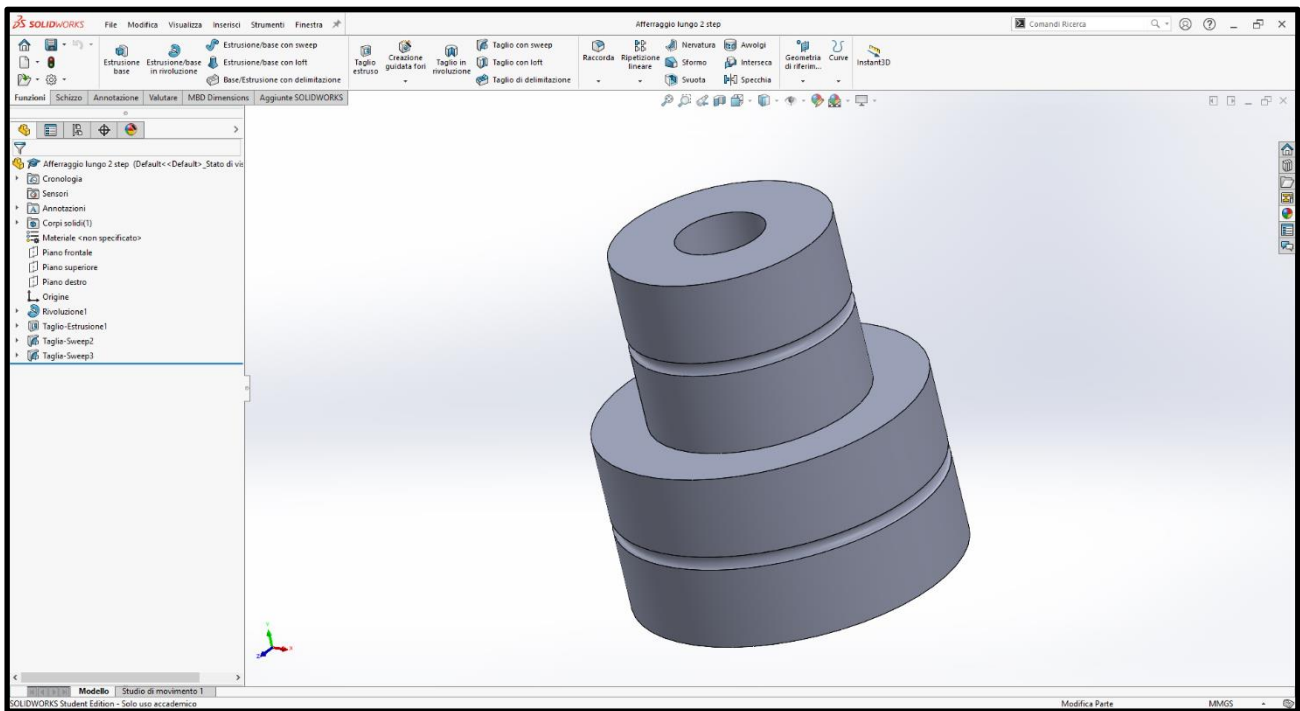


Figure 2.24 CAD model of the scaffold grip shown in SolidWorks.

Once obtained this file/model, the 3D printer is not yet able to read it and produce it, since two other steps are required: triangulation or tassellation and slicing.

Triangulation, as the word says, is the process by which the surface of the CAD file/model is discretized in triangles, obtaining an STL file (Standard Triangulation Language). STL is one of the main formats used in 3D printing. An STL file is just a series of numbers which consist of the coordinates in the space X, Y and Z of each vertex of each triangle and a vector describing the orientation of the normal to the surface. Of course, higher numbers of triangles allow higher resolution of the object. Differently from modelation and slicing, saving a CAD file as STL is normally a built-in process for the main operative systems, hence it does not require the use of specific programs. In Figure 2.25 there is the STL file of the example object, shown in the Windows 10 built-in 3D viewer program.

After the triangulation process, slicing is required. As for modeling, slicing needs computer programs: the most used are Slic3r²⁹, Ultimaker Cura³⁰ and Autodesk Netfabb³¹. In this thesis, Ultimaker Cura was used for slicing. Slicing is the process which allows to pass from a 3D STL model to its sliced version, allowing the writing of the G-code, that is basically the list of commands that the 3D printer is able to read and operate. In the slicing process, the object is cut and translated in a series of flat horizontal layers, which then will be piled one on top of the other by fused material deposition. In some applications and using certain devices it is possible to see these layers with naked eye. The slicing programs usually allow to modify the thickness of the layers,

allowing higher control on the printing quality and time. These programs also automatically produce supports that must be removed at the end of the printing process, as they only need to keep the structure still while it is being printed. These are the supports that have already been talked about in the previous paragraphs. Indeed, for this study, supports have been avoided, as they are usually difficult to remove without damaging the printed object, while separation of components in smaller ones has been preferred.

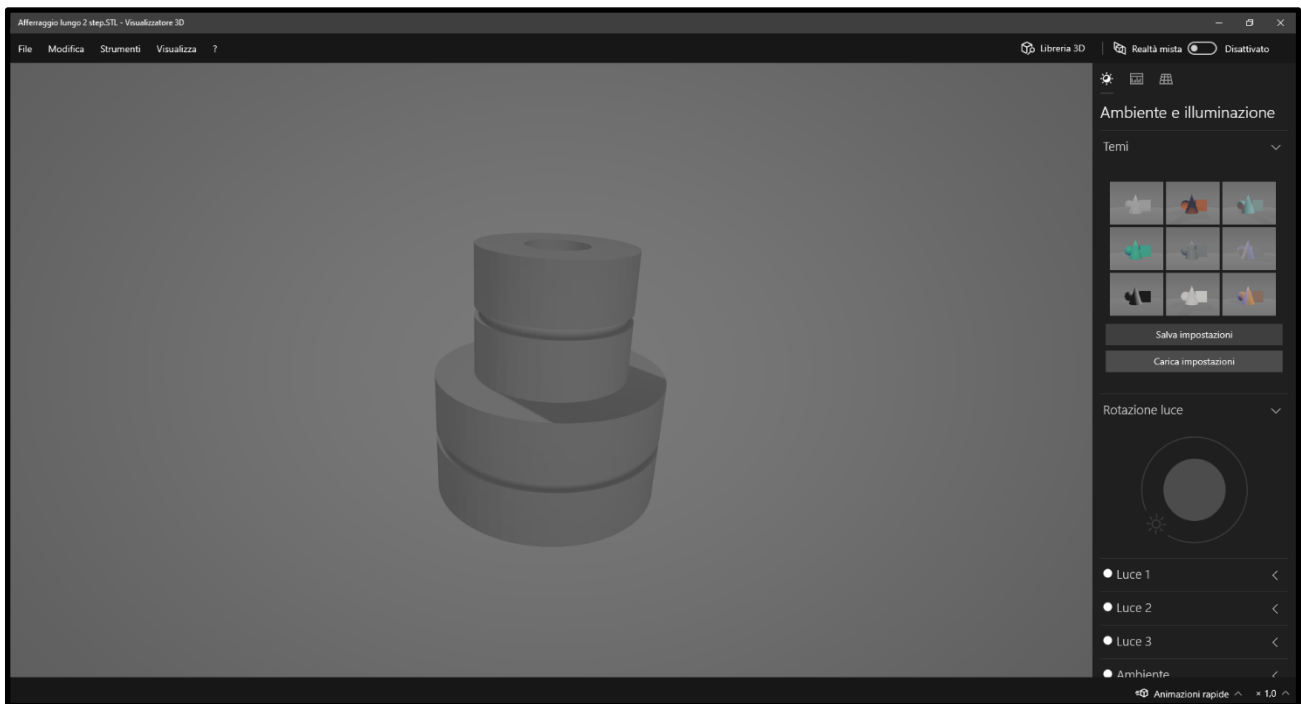


Figure 2.25 STL file of the mobile grip shown in the Windows 10 built-in 3D viewer program.

So, the input to the slicer program is the STL file, and the output is the G-code. The G-code is the list of the movements that the head of the printer must follow on the X, Y and Z axis, for each layer. Sometimes, also printing parameters, such as temperature, time and cooling fans working can be included in the G-code, according to the devices used. In the next figures, the sliced example object shown in Cura (Figure 2.6) and the diagram showing the workflow for the production of a 3D printed object (Figure 2.27).

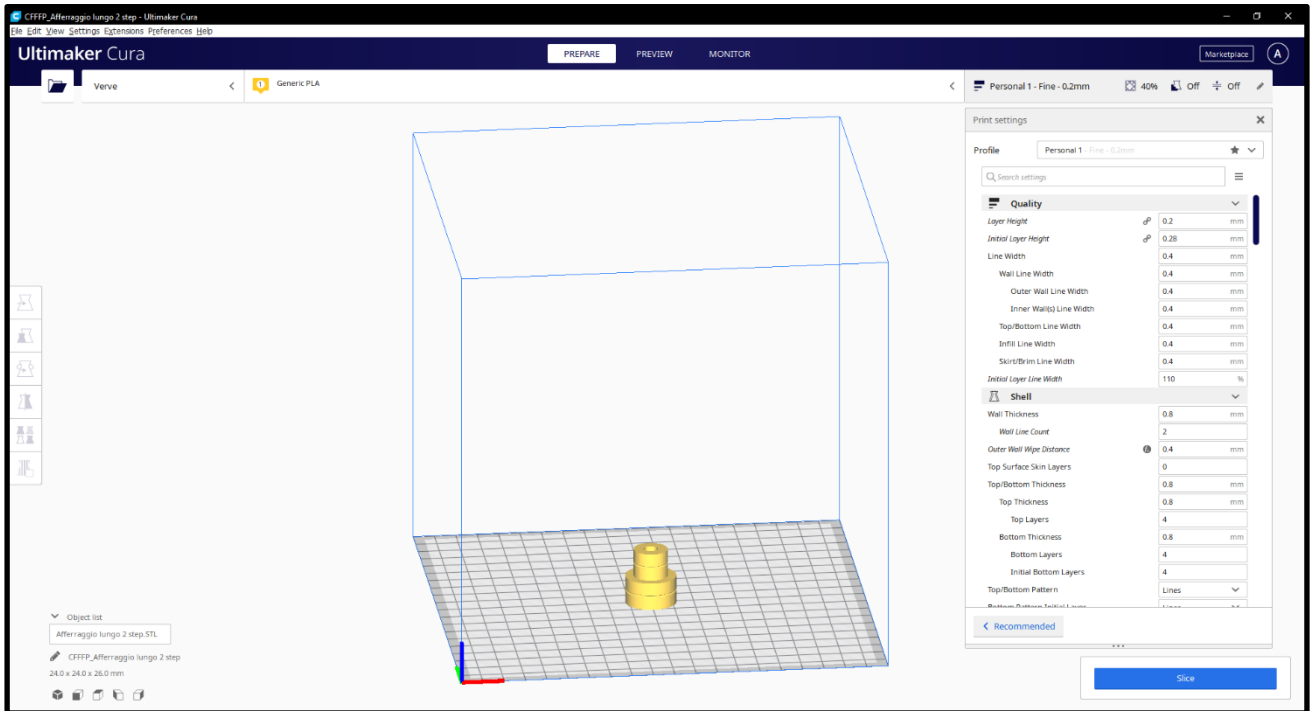


Figure 2.26 Interface of Ultimaker Cura, the slicing software used in this thesis. The sliced object is the scaffold grip.

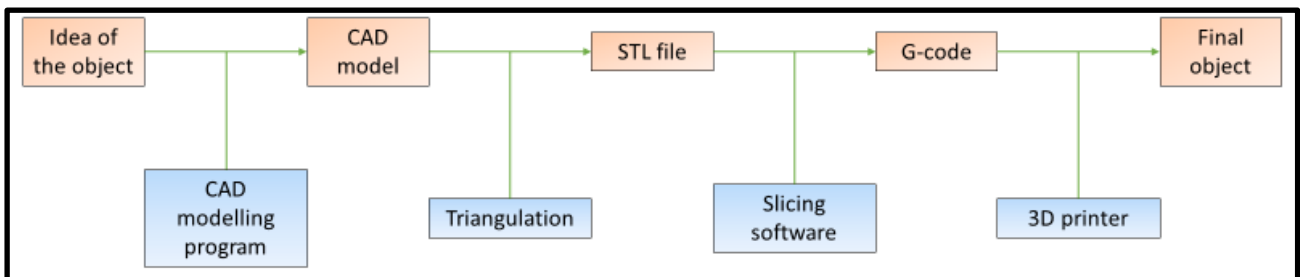


Figure 2.27 Diagram of the workflow for the production of a 3D printed object.

2.4 Production of the bioreactor 3D printed components

In this paragraph, an explanation of how the parts and components that are part of the bioreactor designed in this thesis will be presented. First of all, all of these components were printed by the Kentstrapper Verve 3D printer (Figure 2.28) in the Laboratory of Biological Structures Mechanics (LaBS), at Politecnico di Milano. Indeed, in order to obtain the desired shape and mechanical properties, while avoiding relatively high costs and long printing time, the chosen printing technique has been FDM (Fused Deposition Modeling) and the chosen material PLA, both for its availability and properties. These choices will be more deeply motivated in the following paragraphs.

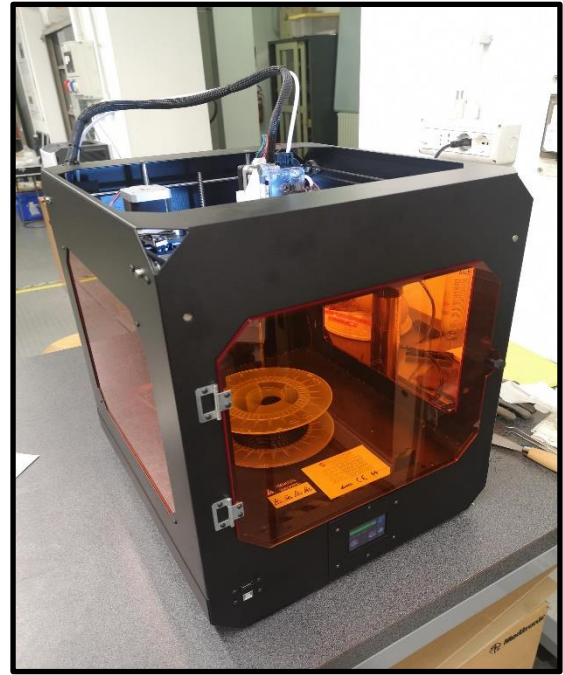
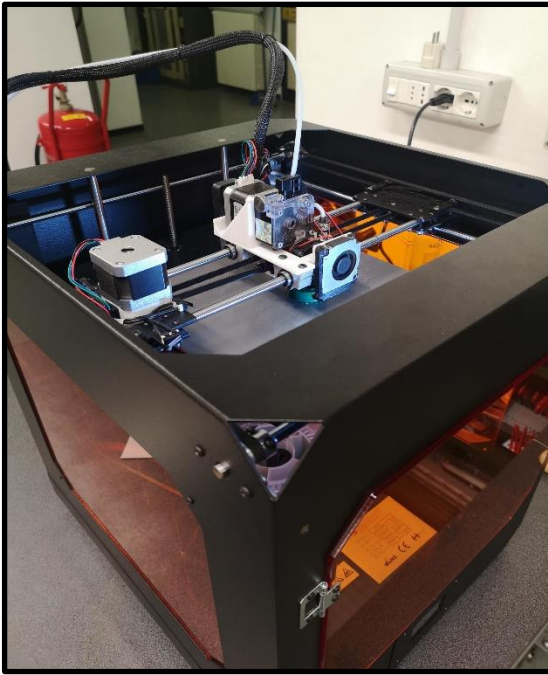


Figure 2.28 *The Kentstrapper Verve 3D printer used for all the 3D prints in this thesis.*

2.4.1 The choice of the printing technique

Additive manufacturing is the larger family of manufacturing techniques in which 3D printing belongs. The basic idea behind additive manufacturing is opposite to the one of subtractive manufacturing, indeed in the latter the approach is to start from a coarse piece of material and to itch and model it in order to obtain the final form. The final consequences of this are to cause a waste of material, to possibly damage the structure of the material and to have a low number of suitable materials for this treatment. In fact, subtractive manufacturing is not used anymore in most of the biomedical applications, but it is more suitable for other fields and approaches. Instead, additive manufacturing is based on the deposition of material, moved by different physical forces, on a supporting structure to obtain the final object. As already said, 3D printing is one of the branches of additive manufacturing. According to the process of material deposition, it can be classified into four main categories: inkjet 3D printing, laser 3D printing, stereolithography and extrusion 3D printing, also called fused deposition modeling.

- Inkjet 3D printing consists of the release of small droplets of heated material, defining with high precision the fall point of these and giving them the right size through the use of mechanical impulses of piezoelectric or thermal nature. The advantage of this technique is the capability to produce high resolution objects, despite its times that are rightfully very long. Moreover, the requirements for the chosen materials include a low viscosity, in order

to prevent clots, and a high crosslinking speed after the printing, in order to keep the shape properly. Finally, this technique has a relatively low cost in general.

- Laser 3D printing technique is based on the phenom of LIFT (Laser-Induced Forward Transfer). In this technique a laser pulse is focused on a layer of absorbing material such as gold or titanium, which is covering the printing material. When the laser is absorbed, the material heats up and eventually evaporates, creating a high-pressure bubble which pushes the local part of biomaterial away towards the printing collector. Also, this technique has high resolution and low speed, but does not present issues with the viscosity of the material as it is free from nozzles of any kind. However, a fast crosslinking is still required, and its cost might be prohibitive, as devices like lasers are highly expensive. This technique is used for microscopic constructs, still too far from the length scale of clinical applications.
- Stereolithography-based 3D printing or Light-Assisted 3D printing are quite different from what shown until now, indeed their working principle is not based on the deposition of material, but on the photopolymerization of specific parts of a bath of material. The used light is typically a laser of UV (ultraviolet) or IR (infrared) nature. Different kinds of light-assisted 3D printing exist, such as Selective Laser Sintering and Digital Light Processing. High resolution and high efficiency are two benefits of this technique; however, the choice of the materials is limited to the range of photosensitive polymers. Finally, just like laser 3D printing, also light-assisted 3D printing has a high cost because of the light source.
- The last 3D printing technique family, which is the one that has been selected for the production of the components of the bioreactor presented in this thesis, is extrusion-based 3D printing. As the word suggest, this technique is based on the extrusion of heated material out of a nozzle and deposition of this material on a heated bed, where it will cool and form the final object. The physical forces that can push the material out of the nozzle define the subfamilies of this technique, mainly classified in mechanical forces, developed by a rotating screw or a piston, and pneumatic forces. Each has its advantages and disadvantages. The use of a piston confers a higher control of the extrusion of the material through the nozzle, as it allows to tune the pressure more accurately, whereas the screw configuration requires a much more careful design to control the spatial distribution of high viscosity materials. The Kentstrapper Verve 3D printer used in this thesis presents an E3D Lite6 Extruder based on a rotating screw. As already explained in the previous paragraph, the head of the printer moves on X and Y axis, depositing material layer by layer (moving on the Z axis) according to the instructions furnished by the G code. The advantages of this technique are relative to the possibility to produce clinically relevant sized objects in a low amount of

time (a few hours for some centimeters of object, varying according to shape, infill and printing velocity). Moreover, the hardware used is cheap and so the cost is low, making it accessible also for unexpert workers. Through this technique it is possible to obtain anatomically correct porous constructs, while this is hard or impossible for other techniques (exception made for stereolithography). The tradeoff between size of the final object and resolution is present, indeed the resolution of this technique is nearly one order of magnitude higher than technology based on lasers and inkjet printing. Some limitations are given by the melting temperature and viscosity of materials, which might be hard to make into cylindrical filaments, but however the number of available materials is satisfactory.

Because of the availability of this last technique and its simplicity, in addition to the size of the objects that were needed, fused deposition modeling has been chosen as 3D printing technique.

A brief summary is reported below in Table 1.

PRINTING TECHNIQUES	ADVANTAGES	DRAWBACKS
<i>Inkjet 3D printing</i>	<ul style="list-style-type: none"> - Multiple nozzles working simultaneously - Gelation happens at moderate speed during complex structures production - Possibility to print bioactive material 	<ul style="list-style-type: none"> - Materials must have low viscosity to prevent obstruction of the nozzle - Limitations in the size of the produced objects for the small dimension of the used droplets - Vertical structures hard to produce
<i>Laser-assisted 3D printing</i>	<ul style="list-style-type: none"> - No nozzle is used, avoiding obstructions - High precision print - Possibility to include a wide variety of bioactive materials - Wide range of material viscosities 	<ul style="list-style-type: none"> - Hard to produce complex structures - Heat produced by the laser must be considered - A metallic coat is required
<i>Stereolithography-based 3D printing</i>	<ul style="list-style-type: none"> - Inks have no restrictions in their viscosity - Slow production times and independent on the structure to be produced - Good vertical printability - Nozzle-less technique, avoiding obstruction issues 	<ul style="list-style-type: none"> - Limited to photosensitive materials - Residual photocurable dust presents reduced granulometry, causing microfractures and voids - Use of UV-light might be dangerous for bioactive components and for the user
<i>Fused deposition modelling</i>	<ul style="list-style-type: none"> - It is possible to print material and cells together (bioprinting) - Working at environment temperature - Cells can be directly incorporated and homogeneously distributed (bioprinting) - High post-print shape fidelity - Possible inclusion of bioactive factors - Good vertical printability - Able to print high viscosity materials and high cellular density structures (bioprinting) 	<ul style="list-style-type: none"> - Printing time relatively slow - Gelation of material must be finely tuned and timed - The size of the nozzle is critical in certain applications - High stresses on the material could harm cells (bioprinting)

Table 1. Summary table of the different 3D printing techniques properties.

2.4.2 The choice of the material

In Table 2 a brief analysis of the most important requirements for the printing material is shown. As for printability, the requirement was that the material needed a melting temperature lower than 300 °C, which is the highest temperature printable by the available 3D printer. Resilience regards the capability of the material to withstand mechanical stresses, being basically a coarse parameter to evaluate mechanical properties. Elasticity means the capability to change shape without losing the initial one. The durability represents the time it takes to degrade a certain object or material. Finally, the cost is self-explicative.

The choice of PLA was made since firstly it satisfied all the requirements, as its melting temperature is about 200 °C (lower than the limit of 300 °C) and its cost is the lowest. This last feature allowed to run a trial and error approach avoiding a high money expense, which is necessary and suggested for who is learning for the first time the use of the 3D printing technology. In addition to this, the mechanical properties of PLA are good for the purposes that the final pieces will have, as none of them will support stresses, but they will only have a structural function to the scaffold of other components of the bioreactor. Finally, despite the low durability might appear as a drawback of this material, it is indeed a suitable characteristic. Indeed, the aim and major quality of this bioreactor is its versatility, both for the type of tissue to be hosted and also its dimension (length and diameter). So, as it has already been explained earlier in this chapter, it has been thought to develop different components for each use it will have, with the same shape but different size, allowing the bioreactor to be suitable for a high variety of tissues.

Material	Printability	Resilience	Elasticity	Durability	Cost
<i>PLA</i>	High	Medium – high	Medium – high	Low	Low
<i>ABS</i>	High	Medium – low	Medium – low	Medium – high	Medium – high
<i>Polypropylene</i>	Low	Low	Low	High	Medium – high
<i>Nylon</i>	Medium – high	Medium – high	Medium – low	High	High
<i>Polycarbonate</i>	Medium	High	Medium	High	High

Table 2. *Important properties of the main printing materials. Color-code for positive and negative values. Note how the color-code for Cost is in reverse.*

2.4.3 Choice of the printing parameters in Ultimaker Cura

When printing using the extrusion 3D printer it is necessary, as already described in the previous paragraphs, to produce the G code. To do this, the software Ultimaker Cura was used. In this software it is required to choose several printing parameters to obtain the best printing quality specifically for each object or material. The parameters to choose are divided in the following groups: quality, shell, infill, material, speed, travel, cooling, support, build plate adhesion, dual extrusion, mesh fixes, special mode and experimental. The program provides different standard profiles, also designed for the use of a particular material. Indeed, also the choice of the material is one of the parameters that needs to be specified, so that the program can set the working and printing temperatures and the speed of the cooling fans. The first print test was performed using one of these standard profiles as a basis, modifying only two parameters, that are the printing speed and the infill percentage. Specifically, the printing speed was reduced, while the infill percentage was increased. The reasons behind these choices will be explained below.

With a trial and error technique, the final optimal parameters were chosen. Following, an exhaustive analysis of the choices made will be presented, divided by the already listed groups.

Quality

The *layer height* was set to 0.2 mm. This is the height of each printed layer in the Z direction. This has been found to be a good tradeoff between high resolution and slow printing speed for low values of this variable and low resolution and high printing speed for high values of this variable.

The *initial layer height* was set to 0.28 mm, so a significative higher value than the other layers in order to ease the adhesion to the plate. This choice was made due to issues related to the adhesion of the first layer to the printing bed, which consequently compromised the whole print.

The *line width* was set to 0.4 mm, since generally this should correspond to the width of the nozzle. Moreover, this was the value for all the lines in the print, consisting of inner and outer walls, infill lines, top/bottom lines and skirt lines.

The *initial layer line width* was set to 110% of the normal line, hence 0.44 mm. Underextrusion was observed in the initial phases of the print (Figure 2.29), so a higher flux of material in the nozzle was required to obtain a satisfying first layer width.

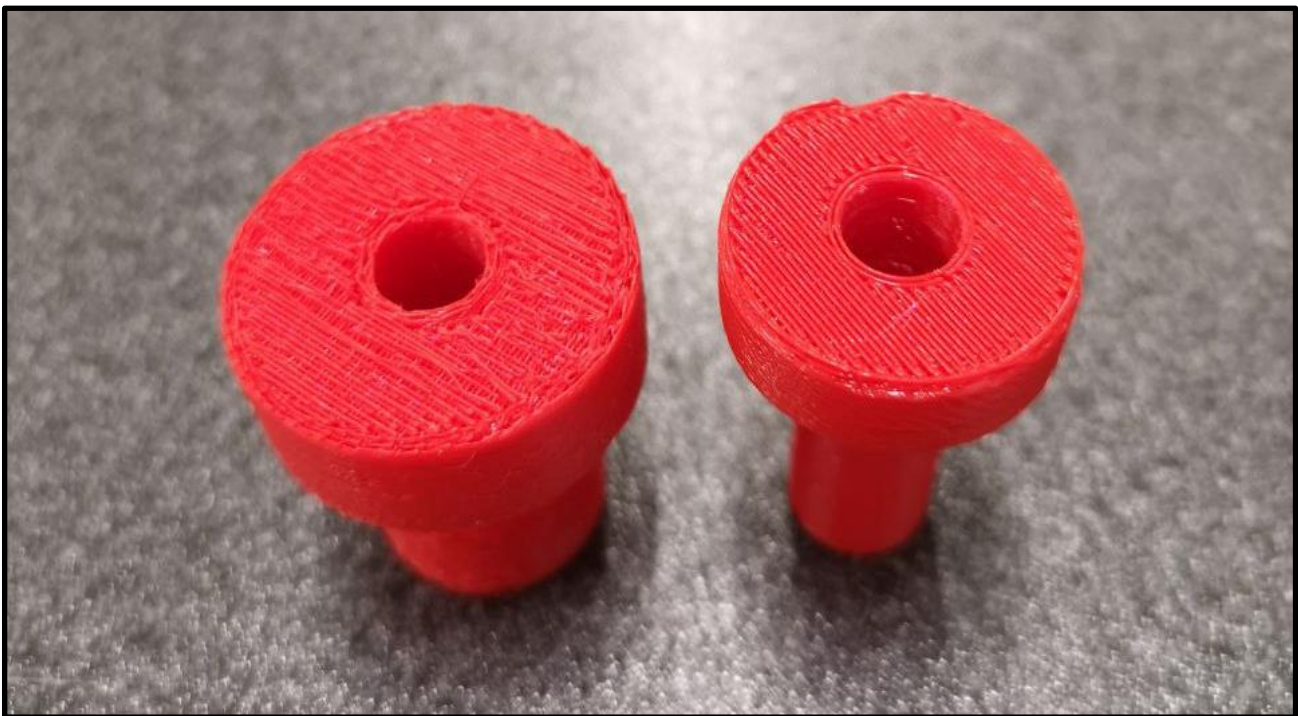


Figure 2.29 Underextrusion was observed in the first 3D printed components (left), but enhancing some parameters allowed to obtain satisfying first layers (right). As it is possible to see, underextrusion causes rough and unflat first layers, in which the extruded material often detaches.

Shell

The *wall thickness* was set to 0.8 mm, corresponding to twice the width of the line, including in the wall 2 lines.

The *outer wall wipe distance* is the small movement that the nozzle does without extruding material after finishing to print a wall. This was increased from 0.2 mm to 0.4 mm to avoid a phenom called hairing, consisting of the formation of a sort of fuzzy tangle in proximity of the most detailed parts, caused by uncontrolled extrusion.

The *top surface skin layer number* was set to 0, that is the number of additional top layers to be printed to increase the quality of the top surface print. This was done since it was required that the components had precise dimensions that would be thrown off by this parameter being different.

Also the *thickness of the top and bottom layers* was set to 0.8 mm and, because of the layer height being 0.2 mm, these are formed by 4 layers each. This approach is to form a shell around the object and increase its mechanical resistance.

Similarly, the *pattern inside the top and bottom layers* was chosen as 90° staggered lines, forming a sort of tridimensional grid inside the top and bottom layers.

No *inset for the outer wall* was set, since the nozzle and the wall width were the same.

Optimization of the wall printing order was disabled, as it was observed to increase the printing time.

Outer walls were printed before the inner walls. Indeed, what is printed first, solidifies first and feels less the pushing force of the rest of the layer being printed. In this way, the outer walls could keep better dimensional accuracy on the X and Y axis, allowing more precise joints with the other components. However, for inner threads present in the two ring components, inner walls were printed before outer walls to reduce the overhang distance of the thread itself with respect to the lower layers. As can be seen in Figure 2.30, printing outer walls and producing large overhangs caused the fail of the print.



Figure 2.30 *For the ring components, presenting an internal thread, it was necessary to print the inner walls before the outer ones to avoid large overhangs.*

No *alternating extra wall* was set in order to reduce the printing time, sacrificing slightly the mechanical resistance of the print.

No components had in the 3D model overlaps between the walls, so it was not necessary to choose the *Compensate wall overlap* parameter.

In case the model causes the walls not to fit between them, the program was set to *fill all the voids* which will form.

The program was set to avoid *printing tiny gaps* in order to avoid blobs inside the model.

For the same reason, *thin walls* were avoided, both in the 3D model and in the printing process.

Horizontal expansion was set to 0 mm, as issues which should be solved by changing this parameter were already fixed using other parameters, such as the adhesion of the first layer to the printing bed.

The *Z seam alignment* was set to random, both for estetical reasons and also to avoid discrepancy of mechanical properties between the walls around the circular components.

No *skin in Z gaps* was printed, since the components did not present the structures affected by this parameter.

Extra skin wall count was set to 0, for the same reasons already explained when talking about the *Top surface skin layer* parameter.

Ironing was enabled, to improve the quality of all the top surfaces (Figure 2.31). The *pattern chosen for ironing* was zig zag. *Ironing line spacing* was set to 0.1 mm. *Ironing flow* was set to 10%. The *ironing inset* was set to 0.38 mm. *Ironing speed* was set to 5 mm/s.

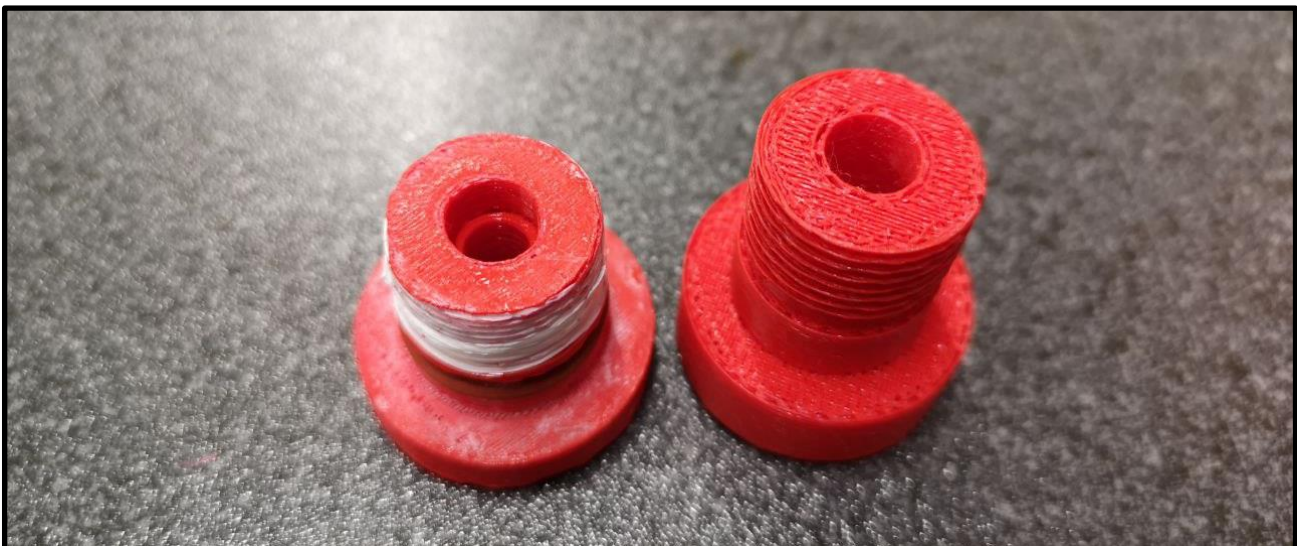


Figure 2.31 Enabling ironing allows to obtain smoother and more defined top surfaces (left) with respect to unironed parts (right), in which it is possible to see the extruded PLA lines and the presence of small holes.

The *skin overlap percentage* was a critical parameter for the prints in this study. One of the main issues encountered during the printing process was underextrusion and this caused detachment of the infill from the skin, especially in the initial layer. Increasing this parameter allowed to balance the underextrusion effect, leading the printer to increase the overlap between the infill and the walls, increasing the mechanical resistance of their bond. This percentage was set to 25%, corresponding to 0.1 mm, being the width of a line 0.4 mm.

Infill

One of the most important parameters to choose is the *infill density*, which is the percentage of full volume inside the object. On this parameter the tradeoff between mechanical properties and printing time depends. In fact, a highly filled object will have high mechanical properties, but will take much more time to be printed, and vice versa. According to this parameter, the *distance between the infill lines* will be calculated, depending also on the dimension of the object. Moreover, despite most of the components of the bioreactor present a circumferential symmetry, the chosen *infill pattern* was “lines”. Indeed, it has been observed that a grid-like structure, similar to the shell one, supports the structure better and provides higher resistance to mechanical stresses. The *infill density* was set to 40%, causing a *infill line distance* of 1 mm. *Infill lines were not connected*, to avoid blobs in the smallest parts, and *no offsets* were chosen.

The *start of the infill* was randomized for the same reasons that the Z seam was set to random when talking about the shell parameters.

No *extra infill lines* were set and the *overlap between infill and walls* was set to 10%, corresponding to 0.04 mm.

Infill wipe distance, similar to the Outer wall wipe distance, was set to 0.1 mm.

The *infill layer thickness* is 0.2 mm, as the other lines.

No *gradual steps in the infill* printing process was selected.

The *infill could have been printed before the walls*, allowing higher resistance of the structure. However, similarly to the reason why the outer walls were printed before the inner ones, printing the wall before the infill allows more dimensional accuracy, as the walls solidify first. This was required for the several joints that components had to form.

Minimum infill area was set to 0 mm², avoiding void spots.

No *support for the infill* was printed, being it unnecessary.

Similarly, the *skin removal width* was set to 0.8 mm, which is exactly the width of the skin, allowing that all the skin had to be printed.

Skin expand distance was set to 1.6 mm, allowing higher bond between infill and walls. This parameter had to be increased to reduce the effects of underextrusion.

Material

All the parameters regarding the printing and working temperatures depend on the chosen material, hence these values are already set when PLA was selected. However, underextrusion had to be mitigated, and increasing the *printing temperature* is one of the way to do it. So, the *printing temperature* was increased from 200 °C to 205 °C. Additionally, also the *flow of material* in the nozzle was increased from 100% (normal value) to 110%. Moreover, for the initial layer this parameter was set to 112%. Optimal initial layers could be obtained only changing these parameters.

Speed

This, similarly to the infill density, is one of the most important parameter to choose. In this case the tradeoff is between the accuracy of the print and its printing time. In fact, high speeds allow fast prints, but might compromise the quality of the structure. This might be caused mainly by unproper deposition of the filament, caused by the high speed. This values was brought from 40 mm/s down to 15 mm/s, more than doubling the printing times, but allowing good prints. Most of the parameters in this family depend mathematically on the *print speed*, but they needed to be changed. Indeed, the infill could be printed at higher speeds (25 mm/s), for its simple shape, but the walls and the initial layers (number of initial layers was set to 2) had to keep the printing speed at 7.5 mm/s to maintain their shape. The *travel speed* was set to 80 mm/s, exception made for the initial layer, which had this parameter set to 40 mm/s. The *skirt speed* was also set to 7.5 mm/s. The *Z hop speed* was set to 10 mm/s, that is the speed at which the printing bed goes down, to allow print of the next layer.

The *control of the filament flow* to equalize thinner lines with higher speeds was not enabled. Also the *acceleration control* and the *jerk control* was not enabled. Indeed, these parameters were observed to cause bad prints.

Travel

Retraction of the nozzle was enabled, allowing it to be retracted after each layer to avoid contact with the model. The retraction distance was set to 1 mm and its speed to 40 mm/s.

The *combing mode* was set to “Within infill”. This mode allows the nozzle to move only inside printed areas while moving. This causes longer printing times, but avoid issues like hairing and bridging.

Cooling

The *cooling* was not changed, as these parameters are automatically set accordingly to the printing temperatures, speeds and material.

Support

No *support* was generated for all the components to avoid the difficult process of detaching it from the already brittle structures. Instead of printing a support, the pieces were divided and printed separately.

Build plate adhesion

The *printing speed of the skirt*, that is the trial circular line which the extruder prints before printing the object, was increased, doubling its minimum length. In this way, it is more probable to obtain a well heated and extruded filament by the time of the start of the object.

The *Z offset*, maybe the most important parameter for the good print of initial layers, should have been set to -0.1 mm, according to the manufacturer guide. This parameter is the offset which the printer head reads when auto-calibrating, in order to find precisely the correct height. As it is possible to see in Figure 2.29 (left), prints with Z offset set to -0.1 mm were clearly underextruded, caused by the nozzle being too far from the printing bed. After this parameter was set to -0.18 mm, the problem was solved, as it is shown in Figure 2.29 (right).

Dual extrusion

Dual extrusion was not used for this study, as all the components were made exclusively of PLA.

Mesh fixes

Being the 3D CAD model without any issues which hinders the print, the parameters in this sections were all set to disabled.

Special modes

None of these parameters needed to be changes, as the prints were traditionally made, one component by one and from the bottom to the top.

Experimental

The parameters in this group are still being tested by the developers, so it was decided not to use any of them.

In Figure 2.32 it is possible to see the main interface of Ultimaker Cura, showing on the right the list of parameters to choose and in the middle the resume of what has been changed from the standard profile and the chosen material.

However, the Table 3 below summarizes the most important parameters.

Parameter	Value	Comments
<i>Layer height</i>	0.2 mm	Optimal layer heights correspond to half of the nozzle diameter.
<i>Line width</i>	0.4 mm	Optimal line widths correspond to the nozzle diameter.
<i>Infill density</i>	40%	This value of infill density was observed to be suitable for proper mechanical properties of the objects.
<i>Printing temperature</i>	205 °C	Despite standard printing temperature of PLA is around 200 °C, this parameter had to be raised to counteract underextrusion.
<i>Bed temperature</i>	65 °C	Despite standard bed temperature for PLA is 60 °C, this parameter had to be raised up to improve first layer adhesion.
<i>Wall and top/bottom print speed</i>	7.5 mm/s	This parameter was kept low to improve the final skin quality.

<i>Infill print speed</i>	25 mm/s	This parameter was raised to speed up the prints, not varying the print fidelity.
---------------------------	---------	---

Table 3. A summary table of the most relevant printing parameters.

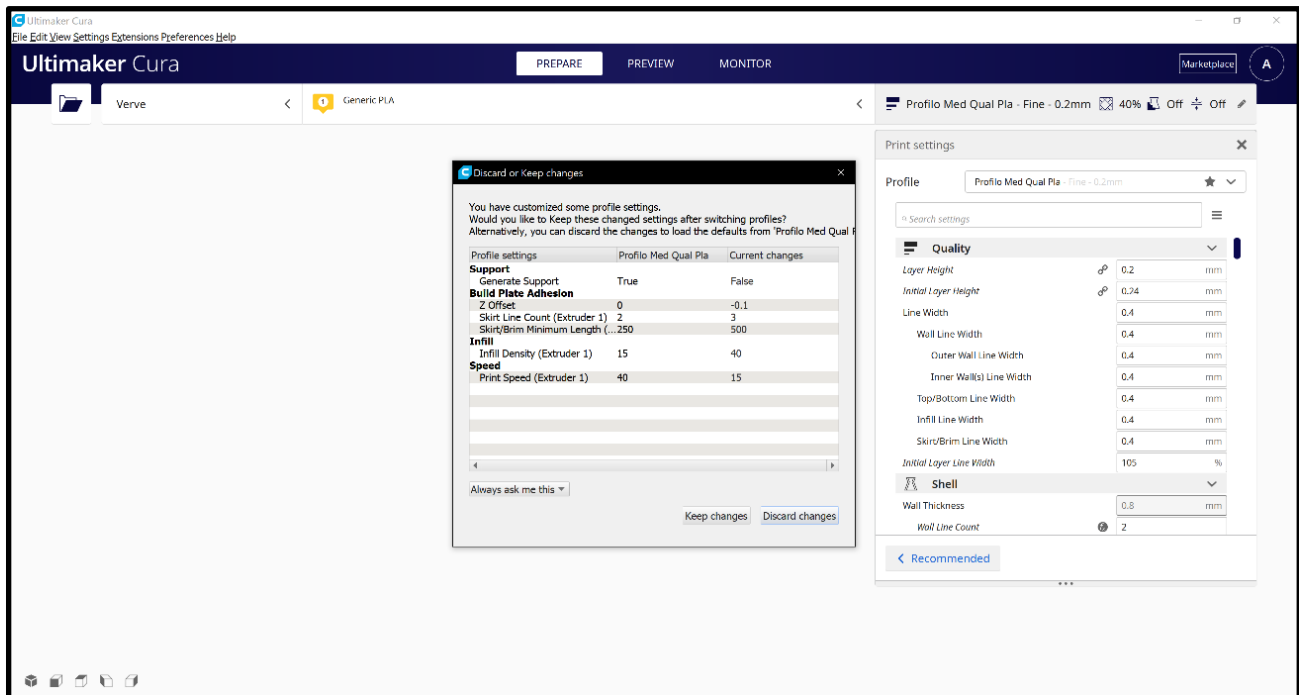


Figure 2.32 Main interface of Ultimaker Cura. Note the list of parameters to be set on the right and the material chosen on the top, in the middle.

2.5 Design of a tubular scaffold suitable for the bioreactor

Dimensions. As previously anticipated, in this paragraph a scaffold for tracheal regeneration will be presented. Such construct must meet some requirements. First of all, the dimensions must be included in the range allowed by the bioreactor. The lengths for scaffold which can be host in this system range from about 20 to 80 mm, whereas the diameters range from 6 to 35 mm. According to the tracheal structure, which has been briefly resumed in the Introduction chapter, the scaffold should present a structure made of rings, flat on the rear and linked between them one on top of the other. The allowable sizes in the bioreactor would suggest designing this scaffold as formed by three to five rings. Indeed, each ring is thick nearly 5 to 7 mm, whereas the annular ligament is 3 to 5 mm thick. In this way, a structure presenting 4 rings and 5 annular ligaments would be about 45 mm tall, being optimal for the bioreactor.

Bioprinting. Then, since this scaffold has to host cells in the future, it is required that it presents sufficiently large holes and cavities for the cells to settle and grow. Also the porosity of the material should be suitable for the diffusion of nutrients, avoiding cell death. Moreover, it has to be possible to host mainly two different cell types and to locate them in different portions of the structure. Specifically, it is required to include ciliated epithelial cells on the lumen of the scaffold and chondrocytes on the outside and inside the volume of the structure. For this purpose, it is thought that the best way to produce the scaffold would be through 3D bioprinting. This technology, similar to the traditional 3D printing and already cited previously in this thesis, allows for the production of objects which include cells inside its structure. However, as it is possible to imagine, the print procedure and constraints are much more difficult and stricter. First of all, the material must have the right properties for cell vital activity, not being harmful for them. In addition to this, it also must be printable at way lower temperatures with respect to traditional 3D prints, in fact such high temperatures would cause cellular death. In general, this temperature should not overcome the 50 to 60 °C limit and should be in this range for the shortest time possible. However, the maximal temperature reachable during this process is cell type and cell source dependent ³². Finally, since this procedure has not been included in this thesis, we will not linger additionally on it.

Material. As for the choice of the materials to be used to produce this scaffold, it is necessary to choose the one regarding the supporting structure. In general, tissue engineered constructs must present biodegradability properties and their degradation times must be long enough to allow cells to migrate outside of the scaffold into the host tissues. In addition to this, it is necessary that cytotoxic substances are not released by this degradation process. Also, the mechanical properties of the material should be compatible with the stresses that it will have to withstand. In particular, a tracheal scaffold will need to withstand bending and torsion properly. Also, soon after the print, the material has to keep its shape. Finally, cost and availability of the material must not be prohibitive and must favor cellular adhesion. According to these premises, polycaprolactone (PCL) was selected. Indeed, PCL is biodegradable in up to three years through hydrolysis of ester bonds, which is a process happening physiologically, producing no toxic wastes. It has been observed that it has a melting temperature of 60 °C and printing cells with this material allows a cell viability of about 70% ³³.

Structure. In Figure 2.33 you can see the structure of the designed scaffold. First of all, the scaffold is a cave column formed by four rings, linked between them through the flat backbone on the rear and which presents a close surface on the innermost side. The height of a ring and the distance between them are both 5 mm, so the height of the whole structure is 45 mm. The thickness of the

whole structure is 4 mm on the thinner rear part and 6 mm on the circular parts. The diameter of the rings is 26 mm. However, dimensions of this project have not been deeply studied as this was never produced. In order to allow the bioprint of a cell-laden gel inside the structure, different series of holes are present, in various directions. It is possible to appreciate that the rings are substantially empty, presenting a nearly grid-like structure. The rings present holes both radially and circumferentially. These are the main parts where chondrocytes should stay and produce fibrocartilaginous material. The inner part of the scaffold is occupied by the gray part (in Figure 2.33). This is basically a wall which has to prevent the exchange of cells and growth factors during the culture. Also, this structure must provide support to the ciliated epithelium during its deposition and growth. Indeed, the holes in this portion are much smaller and are all present toward the lumen of the tracheal graft. Finally, the red part is the backbone which has to withstand most of the mechanical stresses. Holes here cross all the length of the structure but no transversal holes are present. Indeed, this structure, despite needing to host chondrocytes, required a higher mechanical resistance, especially during the first phases of development.

If this construct ever had to be produced, first of all a test of its shape maintenance would have been done. First of all, ABS would have been used. Indeed, despite being a highly available and cheap material, ABS presents suitable mechanical properties for a comparison with PCL. Hence, if the 3D printed structure would present defects and problems in maintaining its structure, surely also PCL would do so. After the print in ABS, some stress tests should be performed, in order to study the properties of the structure. Finally, it would be possible to include cells in the study. Nevertheless, such application is very far from what we have presented and discussed here, so we will not go deeper into this topic.

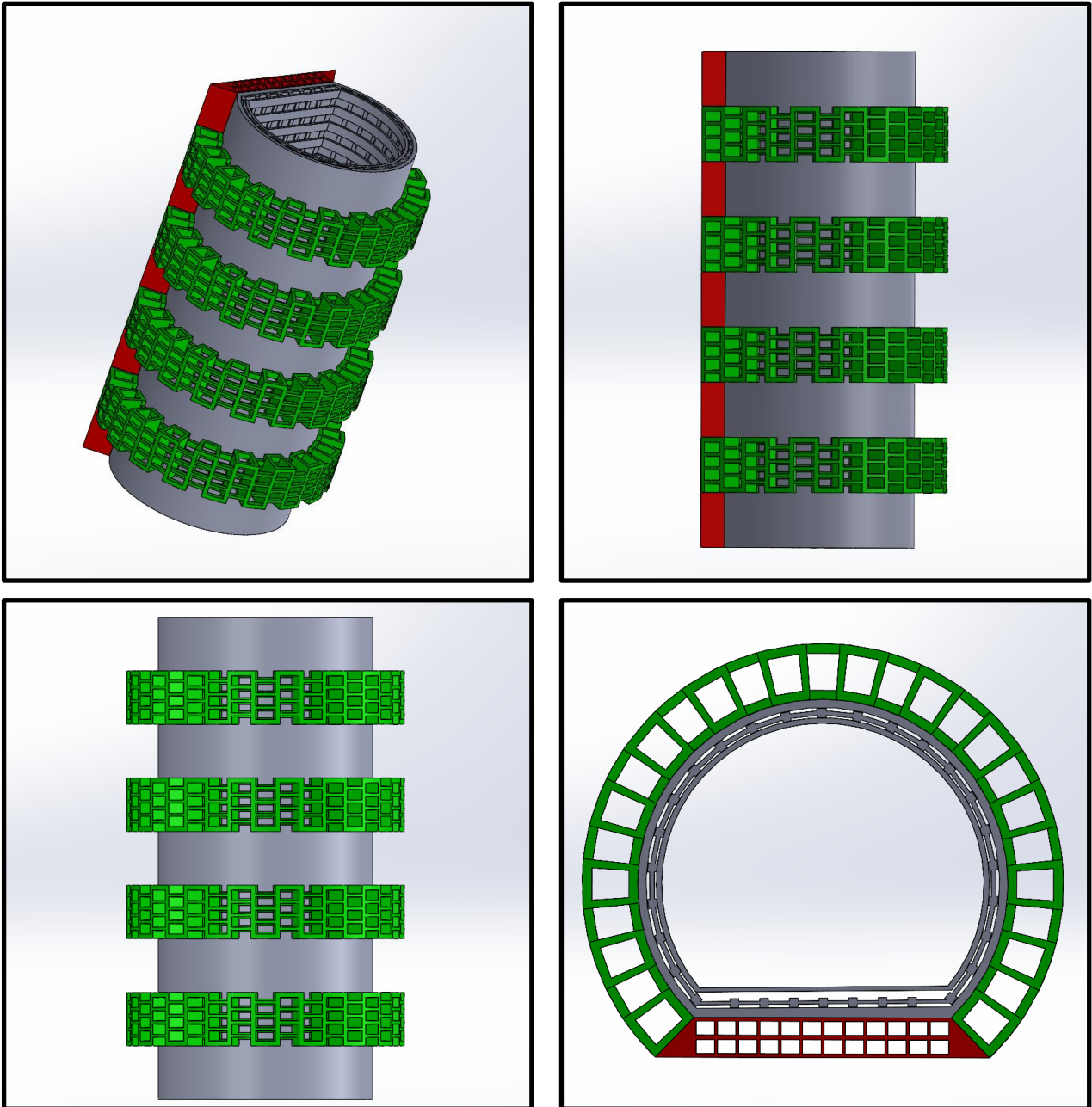


Figure 2.33 *Isometric (top left), side (top right), front (bottom left) and top (bottom right) views of the designed tracheal scaffold. Tracheal rings in green, inner surface in gray, flat rear portion in red.*

Chapter 3

Results

3.1 Study of the functionality of the developed components

In order to evaluate the proper functioning of the designed system and to assess the satisfaction of the prerequisites, additional studies had to be performed. These consist mainly of three parts: assessing the hydraulic seal of the bioreactor; guarantying a proper sterilization method for the components and the chamber; assessing the maintenance of sterility of the system. These three correlated studies will be discussed in the following paragraphs.

3.1.1 Assessment of the hydraulic seal of the bioreactor

The bioreactor, when in function, is thought to be filled with culture medium. In addition, this liquid should be kept at 37 °C in an incubator and presents a relatively low pH and aggressiveness towards materials. For this reason, it is necessary to guarantee that, when assembled, this liquid does not leak out of the structure. In order to study this feature, the culture chamber and the components forming the inlets were assembled. Then, the chamber was filled with water and the holes in the two inlets were closed using parafilm, that is a film made of wax, largely used in scientific laboratories to seal various kinds of containers.

However, parafilm showed up to be not suitable for this duty, as the jagged borders of the 3D printed components would create holes in the brittle film. In addition, water sealing capacity of parafilm was not high enough to withstand the pressure of all the water filling the chamber, corresponding about to 150 to 200 ml. Also the widths of the holes, respectively 8 and 12 mm in diameter, were too high to be closed with this method.

As a second solution to try to close the holes in the bioreactor, silicone was used. Transparent silicone was casted inside two 3D printed molds with the same holes as the ones used in the bioreactor. The silicone was allowed to dry for 24 hours, but however, the product did not come out of the suitable consistence and mechanical properties suitable for its duty.

Hence, it was thought to use a polydimethylsiloxane (PDMS) gel. Sylgard 184 Silicone Elastomer Kit was used, putting PDMS in 9:1 ratio with the crosslinking agent. After the solution was formed, it was cast in one well of a six-well cell culture plate and it was allowed to dry at environment

temperature overnight. The diameter of the well was 38 mm. This size was sufficient to create two couple of PDMS caps, respectively of 9 and 12 mm of diameter. One couple of caps was made of 9 mm in diameter, and not 8 mm, to try to enhance the water sealing capacity of it. First, the PDMS shapes were cut using a set of punchers (Figure 3.1, right) and then the punched material was cut in half for its length, to obtain two similar parts (Figure 3.1, left). These PDMS caps were used to close the holes in the 3D printed PLA components on the inside and on the outside with respect to the chamber. This technique showed failure of the water sealing after a few seconds.

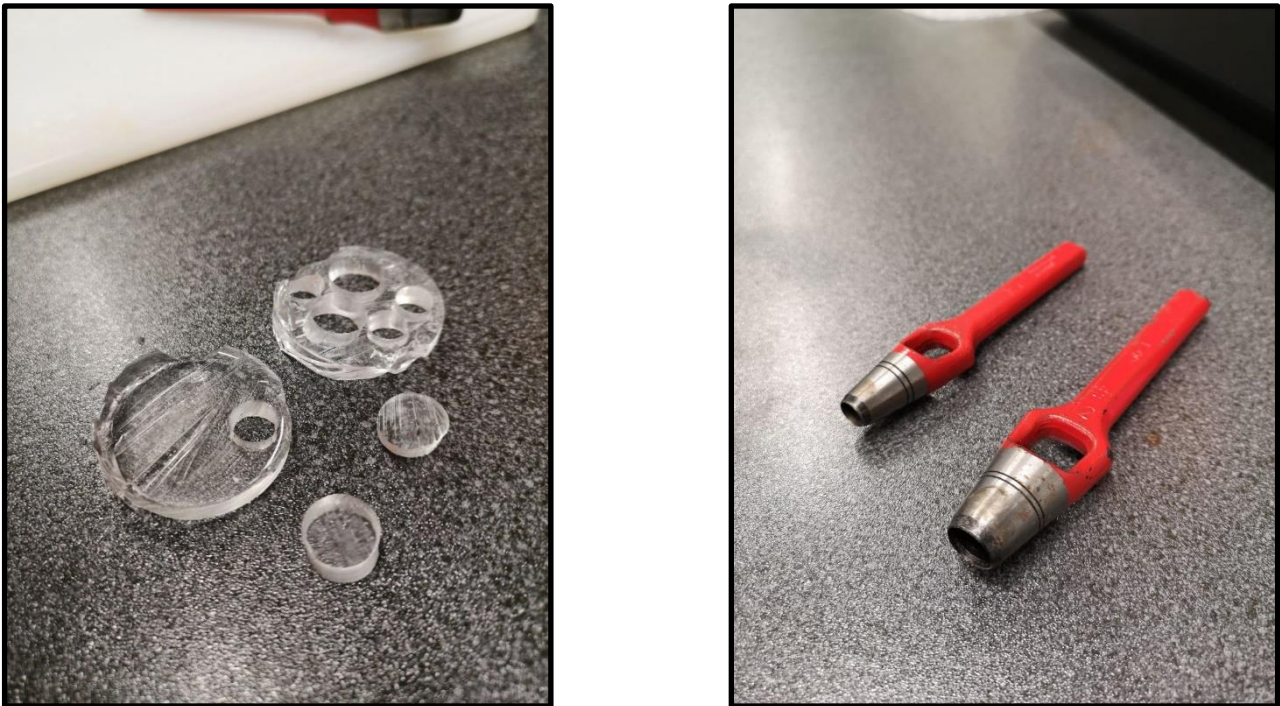


Figure 3.1 *The PDMS caps formed from the larger parts (left) using a set of punchers (right).*

Finally, other tries were made with polyvinyl chloride (PVC) pre-printed caps (Figure 3.2, right), locked in place with polytetrafluorethylene (PTFE) tape, commonly called Teflon in its industrial version (Figure 3.2, left).



Figure 3.2 *The PTFE tape (left) and the PVC caps (right) used.*

Despite being of complex assembly, this kind of approach worked properly, showing a perfect water sealing capacity for one hour. For this test, the chamber was totally filled with cold water and left in horizontal position for one hour (Figure 3.3).

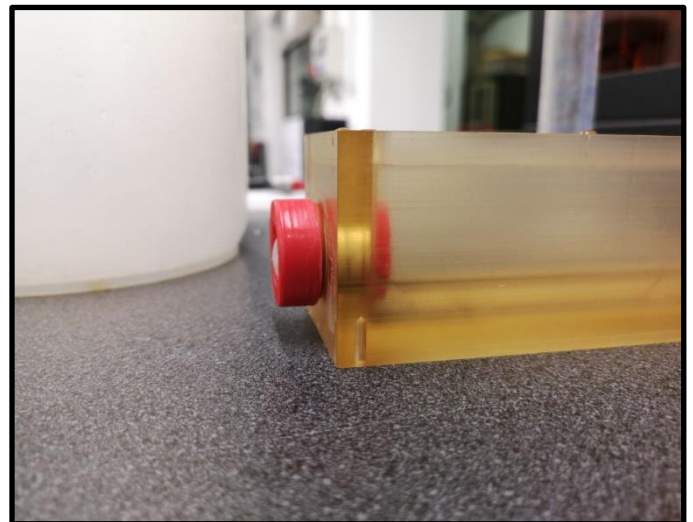
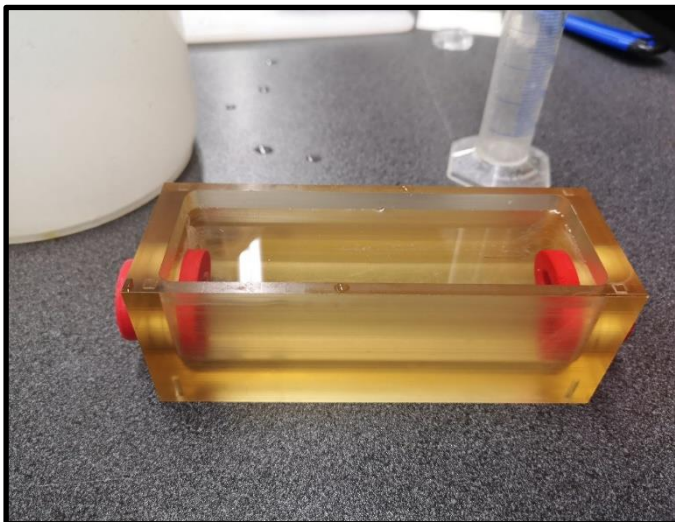


Figure 3.3 *The bioreactor perfusion and assembly inlet were mounted and closed with PVC caps and Teflon tape. The system showed water seal capacity for one hour when filled with cold water.*

3.1.2 Sterilization of the bioreactor components

The second study carried out with the printed objects was to test the capability of keeping sterility of the bioreactor. However, before doing that, it is necessary to sterilize the single components. PLA capability of resisting sterilization processes without compromising its mechanical properties depends on its specific chemical composition³⁴. However, as a first approach, the use of cycles in ethanol baths was decided to test the material reaction. In order to do this, a first test was done on a 3D printed piece which would not have been used on the final device, avoiding compromise of a

useful component. Hence, the test piece underwent a cycle of 24 hours bath in 70% ethanol (EtOH) in distilled water. This was followed by 15 minutes baths in 70%, 80%, 90% and twice in 100% ethanol. At a first observation, the material did not change its shape. Nevertheless, a notable change in the mechanical properties of the object was observed. Indeed the object, which was characterized by a brittle and hard nature, appeared rubbery and soft. However, it was observed that even only one 5 hours cycle in 70% EtOH was sufficient for proper sterilization, with the possibility to also preserve the mechanical properties of the components.

Indeed, sterilization of the chamber and of the 3D printed components was performed together. As for the chamber, it was meticulously rubbed first with 90% and then with 70% EtOH on all its surfaces, both inside and outside, along with the lid. Then, the chamber holes were closed through the same method used for the water sealing test, hence using Teflon tape and PVC caps. Once the chamber holes were closed, 70% EtOH was poured inside the chamber and the 3D printed components were put inside, completely covered by the ethanol (Figure 3.4). This ethanol bath was made for 5 hours, assuring sterilization. All this process was made outside of the sterile hood, also to test the capability of the chamber to keep sterile its inner part, even in a non-sterile environment. Once the 5 hours cycle was concluded, the bioreactor was brought under a sterile hood, the ethanol was removed and its components were disassembled.



Figure 3.4 *The 3D printed components were left in a 70% EtOH bath inside the chamber for 5 hours to provide sterility.*

Given the porous nature of the 3D printed components, it was supposed that ethanol could filter inside the screws closing the holes. For this reason, it was necessary to leave the components to dry

in the sterile hood overnight (Figure 3.5). Once the chamber and the components were sterilized, the sterility maintenance test was performed. This will be described in the following paragraph.

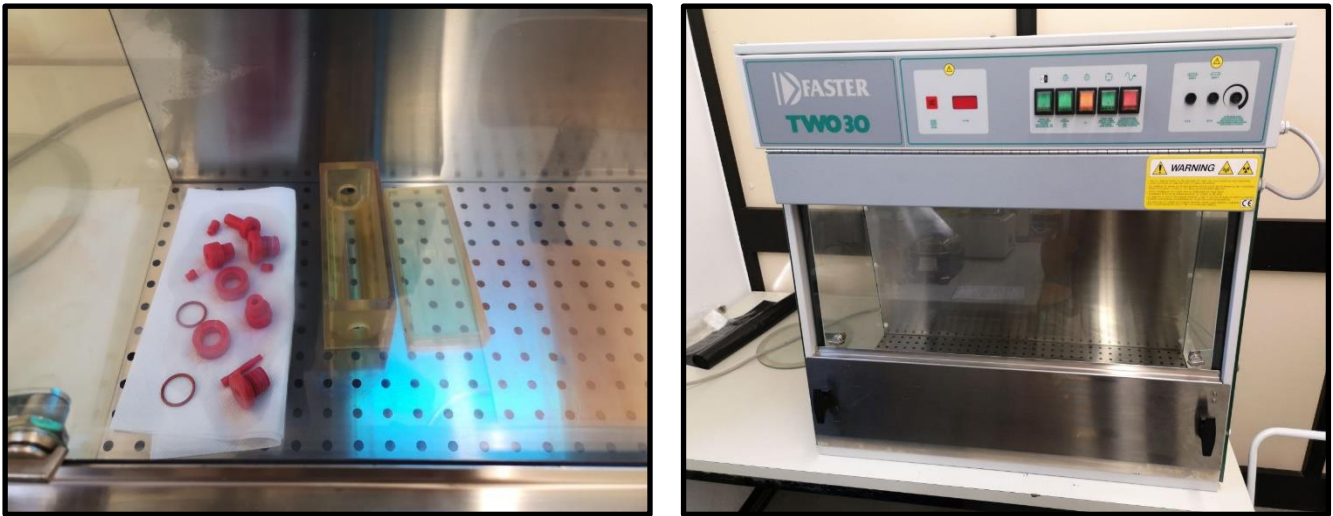


Figure 3.5 *The sterilized 3D printed components and the chamber had to be left to dry in the sterile hood overnight (left). The used sterile hood (right).*

3.1.3 Sterility maintenance of the bioreactor

Once the 3D printed components and the chamber were sterilized, the bioreactor was assembled in a sterile environment. Initially it was thought to use an old cell culture medium to test the sterility maintenance of the system. However, in the laboratory only medium which had been opened for a long time was available, with the risk of being already contaminated. For this reason, phosphate buffer saline (PBS) was instead decided to be used. Hence, 200 ml of PBS were produced. The chamber and the components, now sterilized, were assembled under the sterile hood and PBS was first sterilized and then poured inside the chamber. The system was put in the cell culture incubator for one day (Figure 3.6), assuring an optimal environment in terms of temperature, humidity and gas concentration for pH buffering for the growth of unwanted living microorganisms. The aim was to not observe presence of unwanted bacteria inside the bioreactor. After one day no leakage of liquid was observed and no contamination could be detected by eye (Figure 3.7). The liquid resulted crystalline and unaltered. In Figure 3.7, on the right, it is possible to see small white spots inside the liquid; these are due to the CO₂ gas diffusion inside the liquid due to the physical conditions inside the incubator.



Figure 3.6 The incubator used for the sterility maintenance experiment (left). Note the values of temperature, relative humidity and CO₂ partial pressure. The sterilized PBS-filled bioreactor inside the incubator (right).

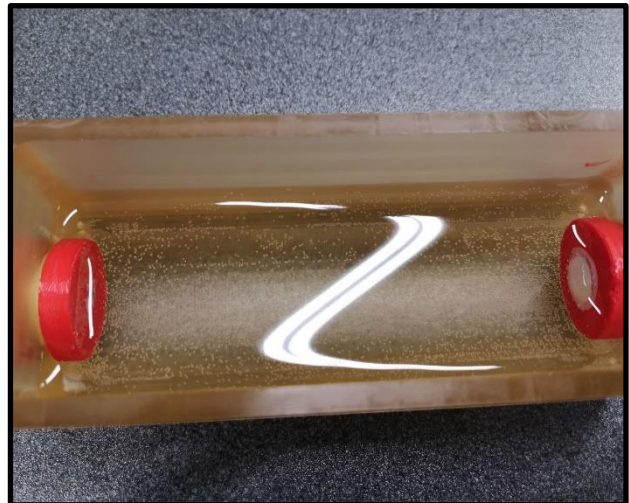


Figure 3.7 The sterilized PBS-filled bioreactor showed no sign of contamination after one day of culture in incubator.

Chapter 4

Conclusions and future developments

In this thesis the procedure behind the production of a versatile bioreactor for tubular constructs of different lengths and diameters has been shown. The main focuses have been on the significance and usefulness of this work, on the choices made to obtain the best final product and on the tests that have been made to evaluate the work.

In this final chapter some considerations on what has been done will be furnished, along with what is required next to go further in this study. Finally, some possible improvements to the presented work will be discussed.

4.1 Conclusions on the system performance

First of all, it must be stated that the system satisfied all the requirements and passed all the tests made. It was possible to develop a closed system, fully sterilizable and mountable in sterile conditions, which showed to be able to isolate what is inside from the outside of the chamber. This, indeed, is one of the main requirements for a bioreactor.

A very relevant test would have been to mount a real scaffold inside the bioreactor for the sterility maintenance test. However, the Covid-19 pandemic restrictions strongly hindered the work of many graduate students' theses work. For this reason, no constructs or tubular scaffolds were available in the laboratory for this test.

Alternative production of the perfusion axis

In addition, it was not possible to produce all the components showed in the thesis. Indeed, the perfusion axis was first 3D printed, but showed a coarse surface, presenting blobs and holes. In addition to this, also the whole structure was visibly weak (Figure 4.1). Due to the possible

accumulation of pathogens and catabolites into these cavities, the 3D printed perfusion axis was not eligible for use in a bioreactor.

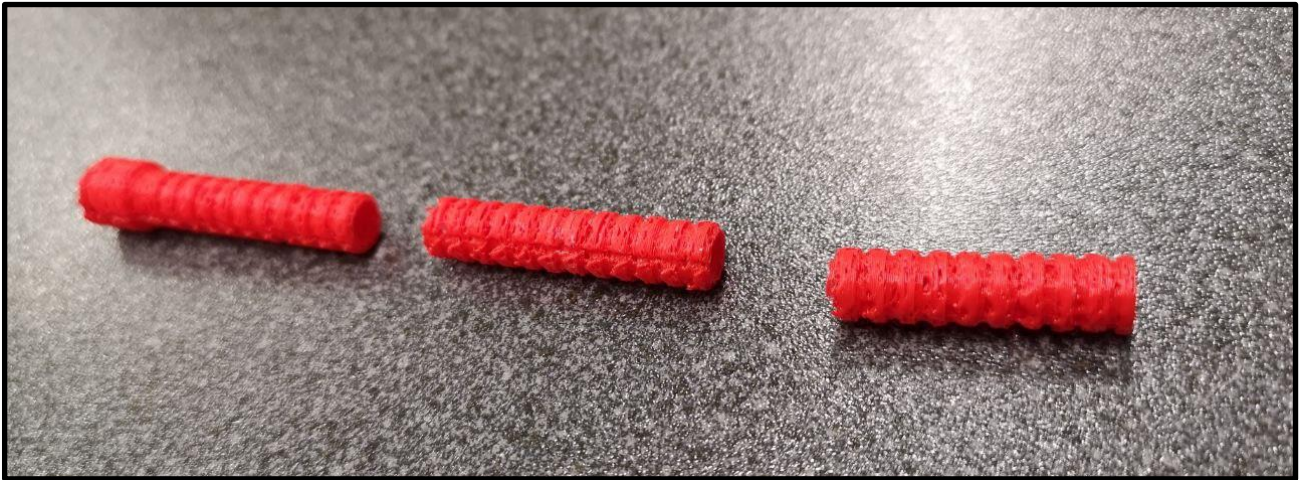


Figure 4.1 *The 3D printed inner perfusion axis did not present a suitable structure for a successful 3D print.*

To face this problem, the dimensions of the perfusion axis, and consequently of all the pieces which interlock with it, had to be increased. However, doing this could have allowed a good print, but would have compromised the usefulness of the whole work, reducing drastically the range of possible diameters for the scaffolds that will be cultured in the system. Indeed, the unsatisfactory quality of this 3D printed piece was not due to an error in its CAD development or in the printing parameters setting. Instead, its dimensions were too small for the 3D printer, which despite presenting a nozzle 0.4 mm wide, could not produce wall with such a small thickness and so small details. To avoid this issue, it was thought to produce only this component in stainless steel through machine tools. Unfortunately, due to the delays caused by the Covid-19 pandemic restrictions, it has not been possible to obtain this component in such material. Nevertheless, a study on how the work would have proceeded has been carried out.

In the case in which the perfusion axis was obtained in stainless steel, it would have been necessary to sterilize it. According to literature though, contaminated stainless steel cannot be sterilized with ethanol, since it has been observed in sterilization of surgical instruments that ethanol fixes proteins and bacteria to the steel surface³⁵. The best way to sterilize stainless steel would be through hot steam, hence this technique would have been used. Regrettably, it has not been possible to produce the component in time for the submission of this thesis. In Figure 4.2 it is present the final bioreactor assembled as much as possible with the produced components. Note that the mobile grip, despite being produced, could not be mounted due to the lack of the inner perfusion axis.

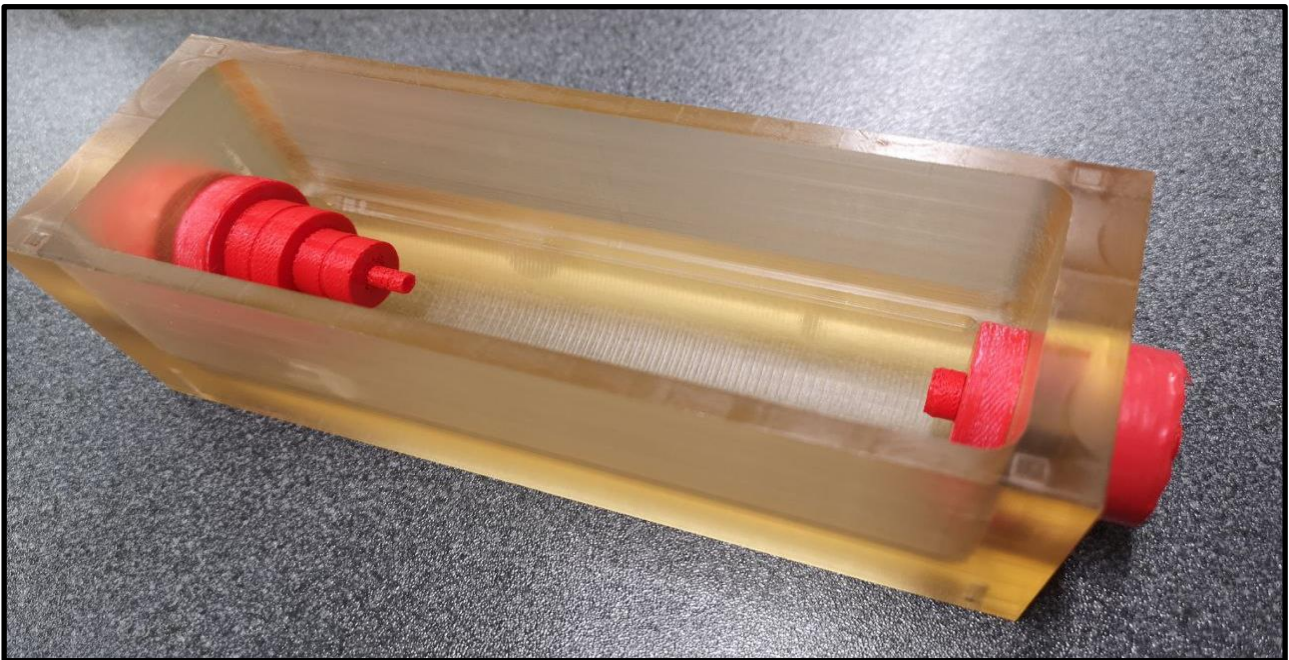
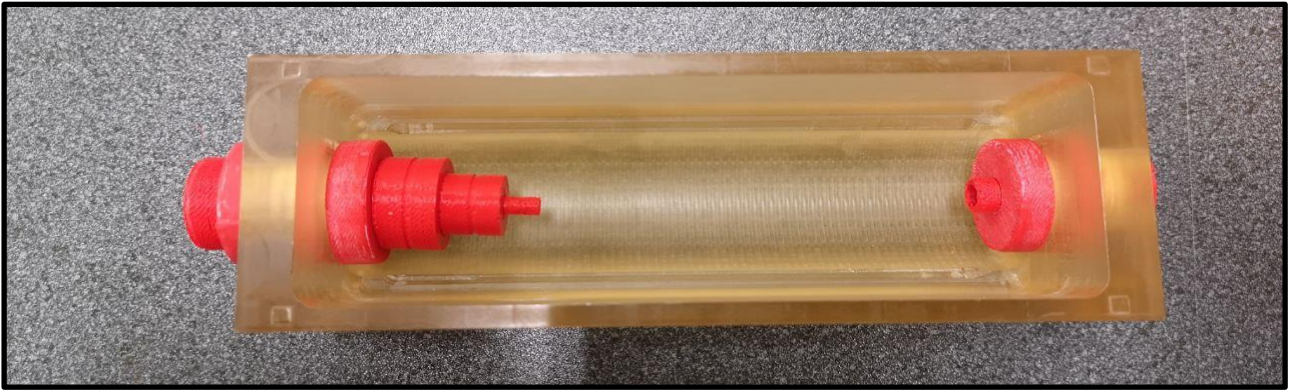


Figure 4.2 *The fully assembled bioreactor from different perspectives. It is possible to appreciate the two inlets fully assembled along with the fixed grip. It was not possible to place the mobile grip due to the absence of the perfusion axis.*

4.2 Future developments and possible improvements

As for the possible improvements to this bioreactor, there would be some changes which could benefit the work. First of all, PLA pieces showed a hard and brittle nature. Despite limitations are due to the material properties, it would be possible to produce a new CAD model, trying to strengthen the fragile parts of the components, which have been easily identified during this work. Indeed, it has been observed rupture of several 3D printed components, often in the same spots (Figure 4.3). The key to improve the mechanical resistance of the components would consist of increasing the surface area of contact between separate parts of the same components, avoiding thin walls.

In addition, a further improvement, but which will require longer printing times, would consist of increasing the *infill percentage* parameter from 40% to 50 or 60%. Moreover, it has been observed, as already said in the previous chapter, that the components presented a certain permeability to water. This feature was expected, of course, due to the nature of the pieces themselves, obtained through deposition of a thin filament. However, increasing the *infill percentage* would surely improve the impermeability of the objects, simplifying tests like the one for water seal.

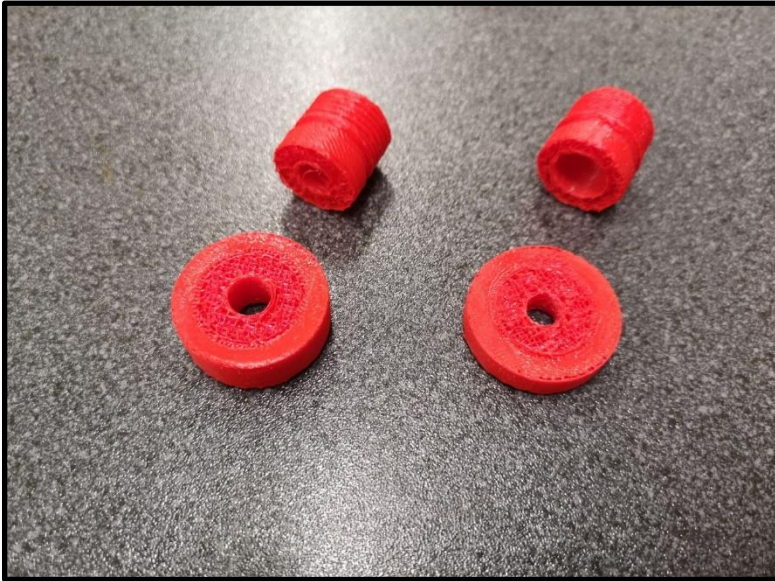


Figure 4.3 *Rupture of the components often happen on the plane of linkage between volumes of different width.*

Another change that is required to improve the quality of the system concerns the cavities left on the components forming the inlets to insert O-rings. As usual, the role of O-rings in bioreactor is to improve the water seal and the sterility maintenance. However, it has been observed that the 3D printed components presented too small cavities for the O-rings. Etching deeper cavities would possibly solve this issue.



Figure 4.4 *The O-rings used to enhance the sterility maintenance and the water seal were too thick to be fully compatible with the etches on the 3D printed rings components.*

Also, it has been quite difficult and time-consuming to find a way to close the holes which were left open in the chamber. Indeed, these holes are open according to the model itself, as they should be closed by the perfusion system on one side and by the three-way stopcock on the other side. Of course, during the initial phases of development, these systems are not complete yet, hence it would

be useful to think a way to close these holes more simply than using Teflon tape and PVC caps, as it was shown in the previous chapters. It would be easy to develop two 3D printed caps which perfectly fits the 8- and 12-mm holes. These pieces would require a very high *infill percentage* to prevent liquid leakage.

Bibliography

1. Prasongchean W, Ferretti P. Autologous stem cells for personalised medicine. *New Biotechnology*. 2012;29(6):641-650. doi:10.1016/j.nbt.2012.04.002
2. Kolios G, Moodley Y. Introduction to stem cells and regenerative medicine. *Respiration*. 2012;85(1):3-10. doi:10.1159/000345615
3. Biswas A, Hutchins R. Embryonic stem cells. *Stem Cells and Development*. 2007;16(2):213-221. doi:10.1089/scd.2006.0081
4. Hollister SJ. Porous scaffold design for tissue engineering. *Nature Materials*. 2005;4(7):518-524. doi:10.1038/nmat1421
5. Ahmed S, Chauhan VM, Ghaemmaghami AM, Aylott JW. New generation of bioreactors that advance extracellular matrix modelling and tissue engineering. *Biotechnology Letters*. 2019;41(1). doi:10.1007/s10529-018-2611-7
6. Paschos NK, Brown WE, Eswaramoorthy R, Hu JC, Athanasiou KA. Advances in tissue engineering through stem cell-based co-culture. *Journal of Tissue Engineering and Regenerative Medicine*. 2015;9(5):488-503. doi:10.1002/term.1870
7. Brand-Saberi BEM, Schäfer T. Trachea: Anatomy and physiology. *Thoracic Surgery Clinics*. 2014;24(1):1-5. doi:10.1016/j.thorsurg.2013.09.004
8. Tennant M, McGeachie JK. BLOOD VESSEL STRUCTURE AND FUNCTION: A BRIEF UPDATE ON RECENT ADVANCES. *Australian and New Zealand Journal of Surgery*. 1990;60(10):747-753. doi:10.1111/j.1445-2197.1990.tb07468.x
9. Patti MG, Gantert W, Way LW. Surgery of the esophagus: Anatomy and physiology. *Surgical Clinics of North America*. 1997;77(5):959-970. doi:10.1016/S0039-6109(05)70600-9
10. Canda AE, Turna B, Cinar GM, Nazli O. Physiology and pharmacology of the human ureter: Basis for current and future treatments. *Urologia Internationalis*. 2007;78(4):289-298. doi:10.1159/000100830
11. Levin DE, Dreyfuss JM, Grikscheit TC. Tissue-engineered small intestine. *Expert Review of*

Medical Devices. 2011;8(6):673-675. doi:10.1586/erd.11.56

12. Grillo HC. Tracheal replacement: A critical review. *Annals of Thoracic Surgery*. 2002;73(6):1995-2004. doi:10.1016/S0003-4975(02)03564-6
13. Baiguera S, Jungebluth P, Burns A, et al. Tissue engineered human tracheas for in vivo implantation. *Biomaterials*. 2010;31(34):8931-8938. doi:10.1016/j.biomaterials.2010.08.005
14. Bancroft GN, Sikavitsas VI, Mikos AG. Design of a flow perfusion bioreactor system for bone tissue-engineering applications. *Tissue Engineering*. 2003;9(3):549-554. doi:10.1089/107632703322066723
15. Richards DJ, Tan Y, Jia J, Yao H, Mei Y. 3D Printing for Tissue Engineering. *Israel Journal of Chemistry*. 2013;53(9-10):n/a-n/a. doi:10.1002/ijch.201300086
16. Chen CS, Mrksich M, Huang S, Whitesides GM, Ingber DE. Geometric control of cell life and death. *Science*. 1997;276(5317):1425-1428. doi:10.1126/science.276.5317.1425
17. Lin H, Lozito TP, Alexander PG, Gottardi R, Tuan RS. Stem cell-based microphysiological osteochondral system to model tissue response to interleukin-1B. *Molecular Pharmaceutics*. 2014;11(7):2203-2212. doi:10.1021/mp500136b
18. Wang YI, Abaci HE, Shuler ML. Microfluidic blood-brain barrier model provides in vivo-like barrier properties for drug permeability screening. *Biotechnology and Bioengineering*. 2017;114(1):184-194. doi:10.1002/bit.26045
19. Vunjak-Novakovic G, Martin I, Obradovic B, et al. Bioreactor cultivation conditions modulate the composition and mechanical properties of tissue-engineered cartilage. *Journal of Orthopaedic Research*. 1999;17(1):130-138. doi:10.1002/jor.1100170119
20. Macchiarini P, Jungebluth P, Go T, et al. Clinical transplantation of a tissue-engineered airway. *The Lancet*. 2008;372(9655):2023-2030. doi:10.1016/S0140-6736(08)61598-6
21. Tan Q, Hillinger S, Van Blitterswijk CA, Weder W. Intra-scaffold continuous medium flow combines chondrocyte seeding and culture systems for tissue engineered trachea construction. *Interactive Cardiovascular and Thoracic Surgery*. 2009;8(1):27-30. doi:10.1510/icvts.2008.179804
22. Lin CH, Hsu S hui, Huang CE, Cheng WT, Su JM. A scaffold-bioreactor system for a tissue-

engineered trachea. *Biomaterials*. 2009;30(25):4117-4126.

doi:10.1016/j.biomaterials.2009.04.028

23. Haykal S, Salna M, Marcus P, Hassanabad MF. Double-Chamber Rotating Bioreactor for Dynamic Perfusion Cell Seeding of Large-Segment Tracheal Allografts: Comparison to Conventional Static Methods Neoadjuvant treatment for early lung cancer View project Lung transplantation View project. Published online 2014. doi:10.1089/ten.TEC.2013.0627
24. Niklason LE, Gao J, Abbott WM, et al. Functional arteries grown in vitro. *Science*. 1999;284(5413):489-493. doi:10.1126/science.284.5413.489
25. The molecular origins of life : assembling pieces of the puzzle : Brack, A. (André) : Free Download, Borrow, and Streaming : Internet Archive. Accessed March 22, 2021. <https://archive.org/details/molecularorigins0000brac/page/1/mode/2up>
26. 3D Design | SOLIDWORKS – Dassault Systèmes. Accessed March 4, 2021. <https://www.3ds.com/products-services/solidworks/>
27. AutoCAD for Mac & Windows | 2D/3D CAD Software | Autodesk. Accessed March 4, 2021. <https://www.autodesk.com/products/autocad/overview?support=ADVANCED>
28. Rhino - Rhinoceros 3D. Accessed March 4, 2021. <https://www.rhino3d.com/>
29. Slic3r - Open source 3D printing toolbox. Accessed March 4, 2021. <https://slic3r.org/>
30. Ultimaker Cura: Powerful, easy-to-use 3D printing software. Accessed March 4, 2021. <https://ultimaker.com/software/ultimaker-cura>
31. Netfabb | Additive Manufacturing and Design Software | Autodesk. Accessed March 4, 2021. <https://www.autodesk.com/products/netfabb/overview?plc=F360NFP&term=1-YEAR&support=ADVANCED&quantity=1>
32. Gungor-Ozkerim PS, Inci I, Zhang YS, Khademhosseini A, Dokmeci MR. Bioinks for 3D bioprinting: An overview. *Biomaterials Science*. 2018;6(5):915-946. doi:10.1039/c7bm00765e
33. Daly AC, Critchley SE, Rencsok EM, Kelly DJ. A comparison of different bioinks for 3D bioprinting of fibrocartilage and hyaline cartilage. *Biofabrication*. 2016;8(4). doi:10.1088/1758-5090/8/4/045002

34. Zhao Y, Zhu B, Wang Y, Liu C, Shen C. Effect of different sterilization methods on the properties of commercial biodegradable polyesters for single-use, disposable medical devices. *Materials Science and Engineering C*. 2019;105:110041.
doi:10.1016/j.msec.2019.110041
35. Costa D de M, Lopes LK de O, Hu H, Tipple AFV, Vickery K. Alcohol fixation of bacteria to surgical instruments increases cleaning difficulty and may contribute to sterilization inefficacy. *American Journal of Infection Control*. 2017;45(8):e81-e86.
doi:10.1016/j.ajic.2017.04.286